Coupled Hybrid Electric Aircraft Design and Strategic Airline Planning

Elise Scheers

Technische Universiteit Delft

TU Delft

Coupled Hybrid Electric Aircraft Design and Strategic Airline Planning

by

Elise Scheers

to obtain the degree of Master of Science
at the Delft University of Technology,
to be defended publicly on Monday March 13, 2023.

Student number:	4680847	
Project duration:	April 25, 2022 - March 13, 2023	
Thesis committee:	Dr.ir. M.F.M. Hoogreef	TU Delft, Supervisor
	Ir.P. Proesmans	TU Delft, Supervisor
	Dr.ir. B.F. Lopes Dos Santos	TU Delft, Chair
	Dr.ir F. Oliviero	TU Delft, Examiner

TU Delft

Acknowledgements

This report marks the end of my educational career at Delft University of Technology, where I completed both my Bachelor and Master in Aerospace Engineering. I dedicated myself to the last part of my study program, this research project, which presents the research done in coupling hybrid-electric aircraft design and strategic airline planning.

First and foremost, I would like to express my gratitude to my thesis supervisors Maurice Hoogreef and Pieter-Jan Proesmans for their invaluable guidance, support and feedback throughout the thesis project. Their expertise and insights have shaped this project to its current shape. I would like to express my gratitude to Bruno Lopes Dos Santos for providing valuable feedback from a different point of view. His suggestions have been immensely valuable in refining and improving the research.

I am deeply grateful to my family for their persistent love and making it possible for me to pursue this education. I would also like to thank my boyfriend for his unwavering support throughout this thesis project. He listened patiently to my concerns and helped me think through potential solutions and outcomes by offering his perspective and expertise.

Lastly, I would like to express my sincere gratitude to Delft University of Technology. The educational experience has been instrumental in shaping my academic and professional journey.

Elise Scheers
Delft, March 2023

Contents

List of Figures

List of Tables

Nomenclature

Abbreviations and Acronyms

ACARE	Advisory Council for Aeronautics Research in Europe
AEO	All Engines Operative
ATR	Average Temperature Response
BHL	Bauhaus Luftfahrt
CAEP	Committee on Aviation Environmental Protection
CENTRELINE	Concept validation study for fuselage wake filing propulsion
CESTOL	Cruise-Efficient Short Takeoff and Landing
DLR	German Aerospace Center
DOC	Direct Operating Cost
DRAGON	Distributed fans Research Aircraft with electric Generators
ECO – 150	Environmentally Conscious 150
EI	Emission Index
EIS	Entry into service
ESAero	Empirical Systems Aerospace
FHAachen	Aachen University of Applied Sciences
FM	Fuel mass
GA	General Aviation
IATA	International Air Transportation Association
ICAO	International Civil Aviation Organization
IFR	Instrumental Flight Rules
MINLP	Mixed-Integer Nonlinear-Programming
NASA	National Aeronautics and Space Administration
NLR	Netherlands Aerospace Center
NOVAIR	Novel Aircraft Configurations and scaled Flight Testing Instrumentation
OEI	One Engine Inoperative
PAX	Passenger Capacity
PSO	Public Service Obligation
SOC	State-of-Charge
SOS	System-of-systems

$SRIA$	Strategic Research and Innovation Agenda
$STARC-ABL$	Single-aisle Turboelectric Aircraft with an Aft Boundary-Layer propulsor
$SUGAR$	Sustainable Ultra Green Aircraft Research
$TeDP$	Trailing edge Distributed Propulsion
$TLAR$	Top-level Aircraft Requirement
TOP	Take-Off Parameter
$TUDelft$	Delft University of Technology
$VTOL$	Vertical Take-off and Landing
$XDSM$	Extended Design Structure Matrix

Roman Symbols

A	Aspect ratio [−]
B	Number of propeller blades [−]
b	Span [m]
c	Climb rate [m/s]
C_D	Drag coefficient [−]
C_L	Lift coefficient [−]
d	Diameter [m]
DOH	Degree of Hybridization [−]
E	Energy [Wh]
e	Oswald efficiency factor [−]
e	Specific energy [Wh/kg]
g	Gravitational acceleration [m/s^2]
h	Altitude [m]
h	Height [m]
H_e	Degree of Hybridization of Energy [−]
H_p	Degree of Hybridization of Power [−]
L/D	Lift over drag ratio [−]
l	Length [m]
M	Mach number [−]
m	Mass [kg]
P	Power [W]
R	Range [m]
R	Redesign Cycle [−]
S	Distance [m]

S	Distance [m]
S	Wing Area [m^2]
SP	Specific power [W/kg]
t/c	Thickness-to-chord ratio [−]
T	Thrust [N]
V	Velocity [m/s]
V	Volume [m^3]
W/P	Power loading [N/W]
W/S	Wing loading [N/m^2]
W	Weight [N]
w	Width [m]

Chemical Formulas

C_xH_y	Hydrocarbons
CH_4	Methane
CO	Carbon Monoxide
CO_2	Carbon Dioxide
H_2O	Water Vapour
N_2	Nitrogen
NO_x	Nitrogen Oxides
O_2	Oxygen
O_3	Ozone
SO_2	Sulphur oxides

Greek Symbols

η	Efficiency [−]
Λ	Sweep angle [deg]
λ	Taper ratio [−]
Φ	Supplied power split [−]
ϕ	Shaft power ratio [−]
ρ	density [kg/m^3]
ξ	Throttle [−]

Subscripts

BAT	Battery
$comb$	Combustion
$components$	Components of the hybrid-electric powertrain

$conv$	Conventional
$convert$	Converters
ec	Engine Control
el	Electrical
EM	Electric Motor
eng	Engine
ess	Engine Starting System
F	Fuel
fs	Fuel System
GB	Gearbox
GT	Gas turbine
kin	Kinetic
L	Landing
OE	Operational empty
P	Propeller
p	Propulsive
pc	Propeller Control
PL	Payload
$PMAD$	Power Management And Distribution system
pot	Potential
$prop$	Propulsion System
PT	Powertrain
S	Shaft
s	Stall
TO	Take-off
tot	total
VT	Horizontal Tail
VT	Vertical Tail

Introduction

The air transportation sector is rapidly growing, increasing the need for reducing aviation's impact on climate. Several aviation emission targets have been set up to limit the climate impact of aircraft. In the United States, guidelines and performance goals for emissions and noise level reductions are established by the environmentally responsible $N+i$ goals [1]. In Europe, targets are established by the European comission in cooporation with the Advisory Council of Aviation Research (ACARE) through the Flightpath 2050 plan [12]. Despite the fact that propulsion systems are becoming more efficient, the improvements are reaching a plateau. It is expected that the technological advancements alone will fall short of meeting these climate targets [74]. This has steered the research towards the introduction of innovative technologies and electrification of the propulsion system. It is believed that electrified aircraft can offer the technological rupture required to meet the aggressive climate targets [65]. Furthermore, the aviation climate impact is not only a function of these novel technologies but also of how these aircraft are operated within the airline route networks. The aircraft allocation and routes should be such that resources are utilized efficiently.

Previous work by *Zuijderwijk* [98] presents a study on how regional airlines can strategically adapt to fleet replacement by electrified aircraft and presents a methodology to couple strategic airline planning and electrified aircraft designs. This work however, only considers pre-defined electrified aircraft and makes only minor configuration adaptations without actually considering new aircraft designs. The study presented here will extend on the work from *Zuijderwijk* [98] by adapting hybrid-electric aircraft design for high-level aircraft requirements such as payload capacity, cruise range and required runway length for take-off and landing. Furthermore, this research will integrate climate optimization in the design of new hybrid-electric aircraft by adapting the aircraft operations.

The goal of this project is to develop a methodology for the design of a climate-optimized hybrid-electric regional aircraft fleet by means of coupling hybrid-electric aircraft design with strategic airline planning, while examining the climate-optimal design point. For this, three main research topics were studied: Hybrid-Electric Aircraft Design, Climate-Optimized Aircraft Design and Fleet-and-Network Integrated Aircraft Design, as seen in the Venn diagram in Figure 1.

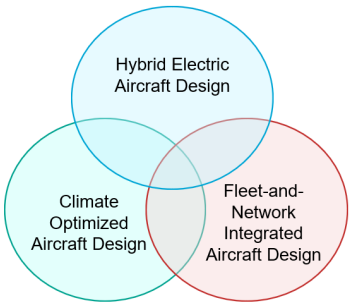

Figure 1: Venn Diagram of research topics

This thesis report is organized as follows: In Part I, the scientific paper is presented. The paper presents the coupled methodology for aircraft design, strategic airline planning and climate optimization analysis. The methodology is tested for the SATA Air Açores airline network, serving 9 islands in the Azores. Various case runs are performed in order to provide answers to the following research question: *"What is the impact of considering airline fleet-and-network allocation integrated with hybrid-electric aircraft design and climate optimization, in terms of airline profitability, expected climate impact and optimal aircraft design?"*. Part II contains the relevant Literature Study that support the research. This part was previously graded under the TU Delft master course 'AE4020'. Lastly, Part III provides some additional work. It contains additional equations and derivations used in the hybrid-electric aircraft design module and the fleet-and-network allocation module.

I

Scientific Paper

Coupled Hybrid Electric Aircraft Design and Strategic Airline Planning

Elise Scheers,*

Delft University of Technology, Delft, The Netherlands

Abstract

With the aviation sector growing each year, the need for a reduced climate impact is becoming increasingly important. Electrification of the propulsion system is believed to offer promising avenues in achieving this reduction. Additionally, airlines operating these aircraft have to adapt their operations and network to optimally utilize these aircraft. This research presents a methodology for the coupled design of a hybrid-electric aircraft fleet with strategic airline planning to optimally serve a specific network. The objective is to maximize the airline profit and minimize the network CO_2 emissions. Aircraft design trade-offs in payload, range and runway length will guide the creation of new aircraft until the optimal aircraft fleet is determined. The methodology is tested in a case study for the regional airline network of SATA Air Açores. The study investigates the impact of introducing new hybrid-electric aircraft designs in the fleet on the creation of new aircraft, the aircraft allocation and the network performance. By directly integrating hybrid-electric aircraft design (having a parallel hybrid architecture) with strategic airline planning, it is possible to reduce the network CO_2 emissions by -11% at the cost of an airline profit decrease of -13%. When including a climate optimization, an additional reduction of network CO_2 emissions is achieved of -27% with a small additional decrease in profit of -1%. Network profitability and climate impact are mainly dictated by the fleet diversity and the assumed technology level of the batteries employed in the aircraft. This research highlights the importance of including climate optimization in the design of new aircraft and the need for more advanced hybrid-electric propulsion architectures (such as distributed propulsion systems) to further contribute to climate impact reduction.

1 Introduction and Literature Review

The demand for air travel is expected to grow annually and the need for limiting the climate impact of aviation is an increased concern. Multiple emission targets have been set up to limit the noise and emissions of aviation. One of these are the environmentally responsible $N+i$ goals from NASA, which illustrate the climate goals for transportation aircraft in the United States [31][1]. In Europe, climate goals are established through the *Flightpath 2050 Strategy* [31][6].

Conventional propulsion systems have become progressively more efficient, it is however believed that these improvements will fall short to meet these climate targets [31]. This has steered the research towards more disruptive technologies, such as electrification of the propulsion system. The advancements in electrical component technology and the potential for configuring the electrical system and airframe for increased synergy, make the field of electrified aircraft promising in providing the technological breakthrough necessary to meet the climate goals [26]. However, the environmental impact of air transportation is not only dependent on these novel aircraft technologies and integrated designs, but also of how these aircraft are operated within the airline route networks [15]. There is a necessity for a tighter coupling between airline strategic planning and aircraft design to allow for optimal resource utilization and reduced climate impact. This can be accomplished through the inclusion of fleet-and-network integrated vehicle design. This paper provides the research into a methodology for coupled design of climate-optimized hybrid-electric aircraft with strategic airline planning.

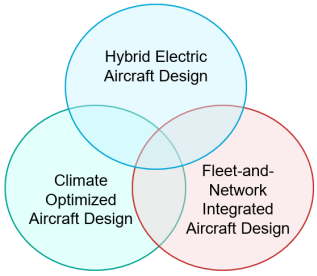

Figure 1: Venn diagram of research topics

*Msc Student, Flight Performance and Propulsion, Faculty of Aerospace Engineering, Delft University of Technology

A literature search was performed on three main research topics: Hybrid-Electric Aircraft Design, Climate-Optimized Aircraft Design and Fleet-and-Network Integrated Aircraft design as seen in the Venn diagram of Figure 1. The challenging climate targets set for the aviation industry have been addressed with the promising approach of electrifying aircraft. Many hybrid-electric aircraft sizing processes make use of retrofitting electrified propulsion systems into existing conventional aircraft. *Pornet et al.* [25] [26] used this approach to derive sizing theorems and design guidelines. In later studies by *Voskuijl et al* [40] and *De Vries et al.* [10], performance equations are adapted and a new Breguet range equation is derived. Furthermore, power control parameters and control laws are introduced by *Voskuijl et al.* [40] and *Zamboni et al.* [42]. The most recent design methods carry out clean-sheet conceptual design of hybrid-electric aircraft. *De Vries* [9] designs a hybrid-electric transport aircraft featuring distributed propulsion. This study considers the aero-propulsive interactions of novel propulsion layouts. The study of *Finger* [11], focuses on the design of hybrid-electric general aviation aircraft with vertical takeoff and landing capabilities. Although designed for different types of aircraft, both design methods are extremely complementary.

Conventional aircraft emit CO_2, H_2O, NO_X and soot particles due to the combustion of kerosene. These emission species have a (in)direct effect on climate and local air quality as they change the atmospheric composition. Literature shows studies have been carried out to directly relate climate impact and aircraft design for conventional aircraft. *Antoine and Kroo* [2] set up a framework for using multidisciplinary design optimization using environmental performance as an optimization objective when conceptually designing aircraft. *Proesmans and Vos* [27] make use of the average temperature response, a more comprehensive climate metric which includes the strong altitude effects of emissions. A turbofan aircraft is designed for several objectives such as minimum fuel mass, minimum direct operating cost and minimum average temperature response. *Thijssen* [35] builds upon this work and implements propeller aircraft into the optimization problem. The study by *Vos, Wortmann and Elmendorp* [39] investigates the effect of fuel type on the optimum cruise altitude for a single-aisle medium-range transport aircraft. It was concluded that the cruise altitude is an important design parameter for LNG-fuelled aircraft if equivalent CO_2 emissions are to be minimized, to a much larger degree than for kerosene-fuelled aircraft. For hybrid-electric aircraft, a limited amount of studies have been carried out to assess the climate impact. *Van Bogaert* [38] investigated the potential fuel burn reduction of a parallel hybrid-electric regional aircraft when compared to the kerosene alternative. *Yin et al.* [41] calculated the potential contrail coverage when flying with hybrid-electric aircraft and modified the Schmidt-Appleman criteria.

The impact of aviation on climate is influenced not only by innovative technologies but also by the aircraft operations in the airline network. Generally, aircraft design and the design of the operational network are determined independently, but there is a necessity to couple the two disciplines. Quite some research has already been performed to integrate conventional aircraft with fleet allocation. Coupling the design of aircraft and the design of the network is considered as a *System-of-Systems (SOS)* problem where there are yet-to-be-determined systems as well as existing systems of which the former should be designed in order to increase the overall *SOS* performance. The resulting statement is a mixed-integer, non-linear programming problem, which are deemed hard to solve. *Crossely et al.* [7] [30] showed a promising approach to solve the problem using a response surface model and decomposition model. *Taylor and Weck* [33] were the first to present the benefits of concurrently optimizing vehicle design an an airline network. The work of *Crossely et al.* was extended by *Mane et al.* [23] through a sequential decomposition approach and traditional MINLP approaches. The work was extended in multiple papers by Mane et al. by incorporating uncertain passenger demand by considering the uncertainty of on-demand fractional aircraft ownership operations [20] [21] [22]. Different objectives have been studied for coupling aircraft design and network allocation. *Govindaraju and Crossley* [13] and *Davendralingam and Crossley* [8] investigated the approach to maximize the airline profit instead of an aircraft specific objective in a profit-motivated fleet allocation problem. *Bower and Kroo* [5] performed a multi-objective aircraft optimization of a single-aisle conceptual aircraft and minimize the CO_2 en NO_X emissions of a fleet in a route network. Govindaraju et al. [14] investigates the trade-off between fleet-level fuel reduction and other fleet-level performance metrics. Alongside, research has been performed by *Jansen and Perez* in a series of successive papers. Aircraft family design and fleet assignment are coupled for minimum operating cost and fuel burn with a fixed deterministic trip demand [15]. Later, uncertain passenger demand was considered [16] and after that, the complexity of the problem was increased by including operations in multiple markets [17] [18]. Regarding hybrid-electric aircraft, the paper of *Zuijderwijk* [43] presents a study on how regional airlines can strategically adapt to fleet replacement by not-yet-designed electrified aircraft. A methodology is presented to couple strategic airline planning and electrified aircraft designs. Impacts on network performance, such as profit, CO_2 emissions and operating routes, as well as chosen aircraft are studied.

From the existing literature, it was observed that earlier research was performed on designing conventional aircraft particularly suited for a certain network by using integrated strategic airline planning and design. The design and operations of electrified aircraft are only considered through the use of pre-defined electrified aircraft and making only minor configuration adaptations without actually considering new aircraft designs. Furthermore, adapting the hybrid-electric aircraft design for high-level aircraft requirements (e.g. payload capacity, cruise range and required runway length for take-off and landing) and its operations (e.g. velocity, altitude and

level of hybridization) for minimizing the climate impact is not thoroughly researched before. This translates in the objective of this research:

> *"This research aims to develop a methodology for the design of a climate-optimized hybrid-electric regional aircraft fleet by means of coupling hybrid-electric aircraft design with strategic airline planning in a fleet-and-network model while examining the climate-optimal design point.*

To achieve this objective, the research question that guides this study is:

> *"What is the impact of considering airline fleet-and-network allocation integrated with hybrid-electric aircraft design and climate optimization, in terms of airline profitability, expected climate impact and optimal aircraft design?"*

2 Methodology

The proposed methodology for coupling climate optimized hybrid-electric aircraft design with strategic airline planning is presented. This coupling methodology is composed of three modules: The Hybrid-Electric Aircraft Design Module, The Climate Optimization Module and The Fleet-and-Network Allocation Module.

2.1 Hybrid-Electric Aircraft Design Module

The Hybrid-Electric Aircraft Design Module is responsible for designing a hybrid-electric aircraft for a set of top level aircraft requirements (TLAR). To directly couple the Aircraft Design Module with the Fleet-and-Network Allocation Module, the module is required to be flexible and computationally inexpensive. Nonetheless, it should be able to capture the discipline interactions and trade-offs of hybrid-electric aircraft design. This is achieved by developing a conceptual aircraft design tool based on analytical and semi-empirical methods. An existing aircraft design tool developed at the Flight Performance and Propulsion department by *Proesmans and Vos* [27] is adapted and extended to implement hybrid-electric propeller aircraft. For this extension, the methodology presented by *De Vries* [9] is studied and a simplified method is implemented for determining the energy required during the mission phases. The adaptations mainly focus on reducing the computational time, as the existing method is fairly computationally expensive. Furthermore, the design method presented in this paper will focus on designing aircraft with a parallel hybrid propulsion architecture and not implement distributed propulsion systems or aero-propulsive interaction effects. It should be noted that, similar to the approach of *De Vries* [9], the hybrid-electric propulsion system is treated as a black-box and the level of fidelity of the hybrid-electric powertrain models are kept to a minimum. The hybrid powertrain is presented in a simplified representation and includes energy sources, nodes, components which transform one type of power into another and the power paths which connect these elements. The batteries and electrical machines with rectifiers and converters are not modelled specifically as they do not change the type of power transmitted. They are solely characterized by a transmission efficiency, a specific energy and specific power value. Other components such as cables and switches are gathered in a power-management and distribution box. The simplified hybrid-electric powertrain architecture is shown in Figure 2, where F is the fuel, GT is the gas turbine, GB is the gearbox, P is the propeller, EM is the electric motor, BAT is the battery and $PMAD$ is the power-management and distribution box.

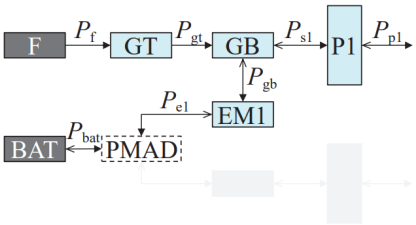

Figure 2: Parallel hybrid powertrain architecture [9]

An Extended Design Structure Matrix (XDSM) in Figure 3 shows the iterative hybrid-electric aircraft design set-up. The aircraft design module is governed by the Initializer and the Synthesizer/Converger.

2.1.1 Initializer

Designing a hybrid-electric aircraft starts by running the Initializer once. The Initializer takes the design mission profile and required payload mass inputs and makes a conventional kerosene aircraft using a Class I weight estimation method with fuel fractions and statistical aerodynamics data from *Roskam* [29].

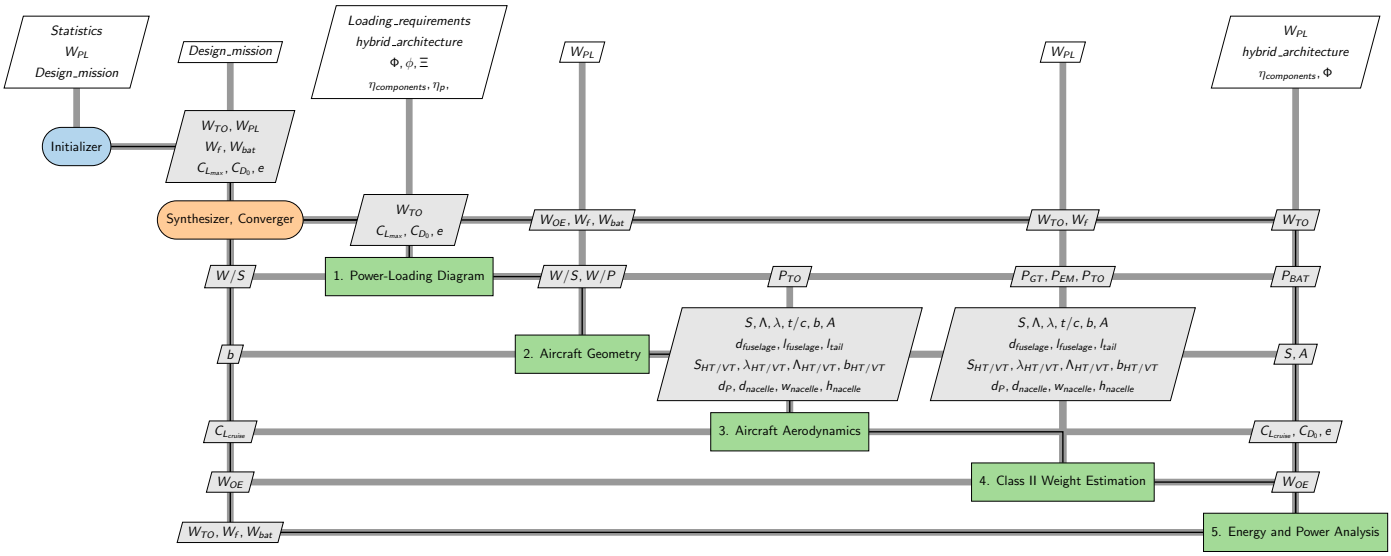

Figure 3: XDSM of Hybrid-Electric Aircraft Design Module

2.1.2 Hybrid-Electric Aircraft Design

The initial weight distribution and aerodynamics from the Initializer are fed to the Aircraft Synthesizer to design a hybrid-electric aircraft. This module iterates over 5 hybrid-electric aircraft design disciplines and updates the initial input values until convergence of the design. The hybrid-electric design disciplines are shown in green in Figure 3 and consist of:

1. Power-loading Diagram
2. Aircraft Geometry
3. Aircraft Aerodynamics
4. Class II Weight Estimation
5. Energy and Power Analysis

2.1.3 Power-loading Diagram

The first discipline sets up the aircraft power-loading diagram for different performance constraints. The power-loading diagram shows the power-loading (W/P) ratio versus the wing loading (W/S) and the constraints limit the feasible design space. An example figure is provided in Figure 4 which shows an aircraft power-loading diagram for loading requirements on stall speed, take-off length, cruise speed and climb gradient in one engine inoperative (OEI). The green colored area shows the feasible design space, the red diamond shows the design point at the maximum feasible W/S and highest feasible W/P.

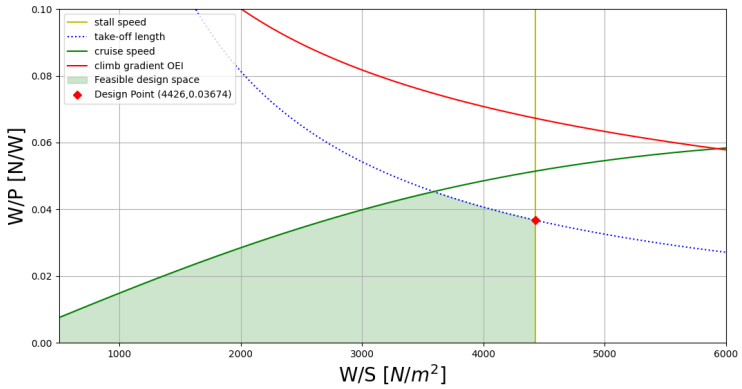

Figure 4: Example Aircraft Power-Loading diagram

For hybrid-electric aircraft, the aircraft power-loading diagram can be split in multiple power-loading diagrams for each component in the powertrain. The powertrain matrix described by *De Vries* [9] is used to deduce the power requirements of the different powertrain components. The matrix is shown in Equation 19 and has the constant powertrain component efficiencies (η) and the aircraft propulsive power (P_p) as an input. The

propulsive power is obtained from the power-loading values of each constraint in the aircraft level power-loading diagram. Additionally, the designer is required to specify three power control parameters:

- The supplied power split ratio; which represents the ratio of amount of power drawn from the electrical energy source with respect to the total amount of power drawn from all energy sources (Equation 1). For parallel hybrid-electric aircraft, this value is between 0 and 1, in case the battery is being discharged.
- The shaft power ratio; which is the ratio of the amount of shaft power produced by the secondary electrical machines with respect to the total shaft power (Equation 2). For parallel architectures, this value is always equal to 0.
- The gas-turbine throttle; which represents the power produced by the gas turbine with respect to the maximum power it can produce and takes a value between 0 and 1 for parallel hybrid-electric architectures (Equation 3).

$$\Phi = \frac{P_{bat}}{P_{bat} + P_f} \qquad (1) \qquad \phi = \frac{P_{s2}}{P_{s2} + P_{s1}} \qquad (2) \qquad \xi_{GT} = \frac{P_{GT}}{P_{GT_{max}}} \qquad (3)$$

The powertrain matrix is applied to all constraint lines in the aircraft power-loading diagram in order to draw the constraint lines for the component-specific power-loading diagrams. For each constraint, the power control parameters have to be defined.

2.1.4 Aircraft Geometry

The aircraft geometry is generated which conceptually sizes the fuselage, main wing, horizontal tail, vertical tail and turboprop of the hybrid-electric aircraft. The sizing equations are obtained from the conventional aircraft sizing methods presented by *Torenbeek* [36]. The turboprop dimensions, including the propeller diameter, length, height and width of the nacelle are obtained from *Thijssen* [35]. The initial sizing of the hybrid-electric aircraft does not differ from the conventional methods, however the aircraft volumetric constraints are considered for placement of the battery. It is preferred to locate the battery in the wing together with the fuel in order to keep the additional mass as close as possible to the center of gravity and thus limit the effects on aircraft stability. The available wing volume is calculated using the formula in *Torenbeek* [36] and depends on the wing surface area, span, thickness-to-chord ratio and taper ratio. The required battery volume and fuel volume are calculated from the specific densities. If the wing volume does not allow for the battery to be stored together with the fuel, the battery will be located in the fuselage compartment under the floor. For this, the cross-sectional area and floor location are determined from conceptual fuselage geometry sizing equations. An example of the fuselage cross-section is provided in Figure 5 and shows the fuselage inner diameter and outer diameter circles. The blue points locate the height of the aisle, the cabin seats and floor location. The green box shows a possible battery placement. Figure 6 provides the top view and side view of the conceptual aircraft outer geometry.

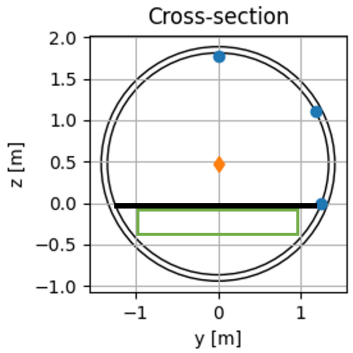

Figure 5: Battery location in fuselage compartment. Blue points: aisle height, cabin seat height, floor location; Green square: possible battery location

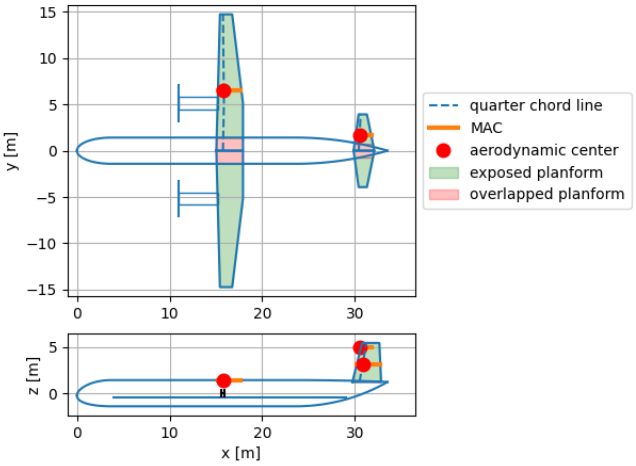

Figure 6: Example of aircraft geometry

2.1.5 Aircraft Aerodynamics

The aircraft geometry is divided into elements: wing section, fuselage section, nacelle section and empennage section. The aerodynamic values of drag coefficient (C_D, C_{D_0}) and Oswald efficiency factor (e) are updated according to the method from *Obert* [24]. The profile drag of all sections is determined and related to the flat plate skin friction coefficient using statistical data. By multiplying the skin friction coefficient with the shape

factor of each element, the drag of the full aircraft can be determined by summing the drag of the different elements. To determine the take-off and landing drag polars, the effect of landing gear and flap settings on the clean zero-lift drag coefficient and oswald efficiency factor are included in the factors ΔC_{D_0} and Δe according to the corrections outlined in *Roskam* [29].

2.1.6 Class II Weight Estimation

After the geometry generation, it is possible to conduct a Class II weight estimation and calculate the operational empty weight of the aircraft by considering the different aircraft systems and structures. The operational empty weight is build up from the airframe weight, hybrid powertrain weight, services and equipment weights and the operational item weights. The airframe of the aircraft is composed of the wing, fuselage, empennage, surface controls, undercarriage, nacelles and pylons. The airframe systems weights are computed from traditional Class II weight estimation methods outlined by *Torenbeek* [36]. The hybrid-electric powertrain weight is not determined from traditional Class II weight estimations but estimated from the (equivalent) specific power values of the gas turbine and electric motor and their respective required powers obtained from the component-level power-loading diagrams. The specific power value for the electric motor is a design input and can be obtained from state-of-the art literature. The specific power of the gas turbine is calculated by first determining the weight of a conventional engine using the relations in *Teeuwen* [34] and is consisting of the engine mass, fuel system mass and propulsion system mass. The propulsion system mass considers the control and starting systems, but not the propeller mass itself. The propeller mass is added separately and is again obtained from the relation presented in *Teeuwen* [34].

2.1.7 Energy and Power Analysis

After determination of the operational empty weight, an energy analysis and a power analysis are performed to estimate the fuel mass and battery mass required to perform the mission. A design mission profile is determined in correspondence to the instrumental flight rules (IFR) reserve fuel requirements and is sketched in Figure 7. The design mission comprises of:

- A harmonic mission; where the cruise range is defined at maximum passenger capacity.
- A diversion mission; of 100 NM range at an altitude of 5000 ft.
- An endurance mission; of 45 minutes at 1500 ft altitude.

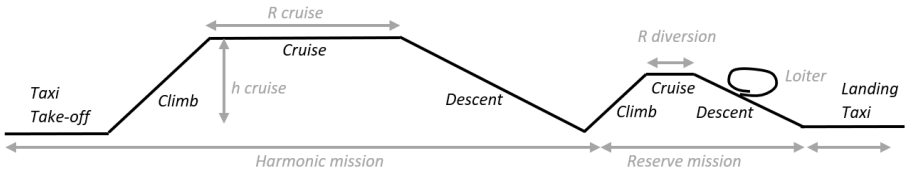

Figure 7: Design mission profile

The energy analysis is simplified when compared to the approach presented by *De Vries* [9], with the goal to reduce the computational time. Instead of a time-stepping approach which divides the mission into several segments, the hybrid range equation derived by *De Vries et al.* [10] is used to calculate the required energy during the cruise phase of the mission. The energy required during the other mission phases is obtained using the conventional fuel fractions, combustion and electrical efficiencies and the power split value. With the specific energy of fuel, the fuel weight is obtained directly. Similarly, the battery weight required for meeting the energy requirements can be obtained from the battery specific energy. To this value, a margin is added to limit the state-of-charge of the battery to avoid reducing its battery cycle life. Nevertheless, for determining the final battery weight, one should check whether it is sized by either energy or power requirements. To size the battery for power, the required battery power is obtained from the powertrain model analysis. When assuming a battery specific power value at pack level, the weight of the battery can be calculated. The highest value of the two will eventually determine the battery weight.

For this computed fuel and battery weight, the maximum take-off weight can be re-calculated from Equation 4, where W_{OE} is the operational empty weight previously obtained from the Class II weight estimation and W_{PL} is the weight of the payload which is an aircraft design input.

$$W_{TO} = W_{OE} + W_{PL} + W_f + W_{bat} \tag{4}$$

2.1.8 Synthesizer/ Converger

The design loop is entered again with this new maximum take-off weight until convergence of the take-off weight is reached within a specified tolerance level. The Synthesizer/Converger is in charge of checking the convergence of the aircraft design. Furthermore, the it evaluates whether the aircraft design adheres to the following additional constraints:

- The determined wing loading is smaller or equal than the one for stall speed: $W/S \leq W/S_{stall}$;
- The lift coefficient during cruise is lower than the buffet onset value: $C_{L_{cruise}} < C_{L_{buffet}}$;
- As narrow-body aircraft are operating on category C airports, the wing span is limited to the maximum wing span of this airport category, being 36 meters [1]: $b \leq 36m$.

2.2 Verification and Validation

The hybrid-electric aircraft design module is verified and validated in a two step procedure. First, the hybrid design tool is used to design a fully-kerosene based Dash 8 Q400 aircraft. After this, the modules particularly implemented to integrate hybrid-electric aircraft are validated by designing a parallel hybrid Dornier 228 aircraft. Both results of the design cycle will be compared to values obtained from literature.

2.2.1 Conventional Dash 8 Q400

To design a conventional aircraft with the hybrid-electric design module, all power split values for all constraints and mission phases are set equal to zero. The energy analysis of hybrid design module is based on the conventional fuel fractions method. It is therefore important to match the fuel fractions with the actual aircraft values. The fuel fractions for the different mission phases are determined as a fraction of the maximum take-off mass using the data listed in the Q400 Fuel Efficiency Manual [4]. Furthermore, the aircraft is designed with the following inputs:

- Aircraft capacity: 80 passengers
- Payload mass: 8480 kg
- Maximum fuel mass: 5300 kg
- Mission
  - Cruise with 500 NM range at 23000 ft altitude and high speed cruise velocity of 182 m/s
  - Diversion of 100 NM at altitude 5000 ft and cruise speed of 182 m/s
  - Loiter of 45 minutes at altitude 1500 ft.
- Aspect ratio 12.8
- Take-off length 1300 m
- Stall speed 47.15 m/s
- Undercarriage stored in the nacelle, high wing configuration, T-tail configuration

The results of the sizing tool are summarized in Table 1. The reference weight distribution values are directly obtained from the Fuel Manual [4]. The reference wing area and span are obtained from the Dash 8 specifications on Airlines Inform Website[2]. The reference wing loading value is simply calculated from the maximum take-off weight and wing area. Similarly, The reference power-loading is obtained from the aircraft maximum take-off weight and take-off power. The Dash 8 Q400 is powered by two Pratt&Whitney PW150A engines, with a nominal take-off power of 4095 kW according to the Certificate Details [37]. The results show a maximum difference with respect to the reference data of 6.2% in the wing area calculation and an average difference in weight prediction of 3.0%, and such the design tool is deemed accurate enough to predict the weight distribution and initial sizing for the conceptual design of conventional aircraft.

[1] https://www.skybrary.aero/articles/icao-aerodrome-reference-code
[2] https://www.airlines-inform.com/commercial-aircraft/dash-8q400.html

Table 1: Validation Results Conventional Dash 8 Q400

Parameter	Result	Reference	Difference
Operational Empty Mass [kg]	18 690	17 819	+4.9%
Maximum Take-off Mass [kg]	30 560	29 574	+3.3%
Payload Mass [kg]	8 490	8 489	+0.0%
Total Fuel mass [kg]	3 380	3 266[3]	+3.5%
fuel mass take-off [kg]	43	42	+2.4%
fuel mass climb [kg]	330	324	+1.9%
fuel mass cruise [kg]	1350	1335	+1.1%
fuel mass descent [kg]	330	318	+3.8%
reserve fuel mass [kg]	1320	1 247[4]	+5.9%
Wing Area [m^2]	67	63.1	+6.2%
Wing Span [m]	29	28.4	+2.1%
Wing loading [N/m^2]	4430	4597	-3.6%
Power loading [N/W]	0.037	0.036	+2.7%

2.2.2 Parallel Hybrid-Electric Dornier 228

A parallel hybrid Dornier 228 is designed with the same inputs as *Finger et al.* [12] to verify and validate the design disciplines related to hybrid-electric aircraft design. The verification procedure will focus on checking the correct usage of the powertrain matrix by comparing the aircraft-level and component-level power-loading diagrams. The battery and fuel weight determination is validated by comparing the results coming from the energy analysis discipline with the results of the hybrid Dornier sizing.

The power-loading diagrams are constructed for the following constraints from *Finger et al.* [12]:

- Cruise speed constraint: cruise velocity 115 m/s at cruise altitude 3000m with η_p of 80%;
- Take-off length constraint: take-off distance 793 m at sea level;
- Stall speed constraint: stall speed 34.6 m/s at sea level;
- Climb rate constraint in all engines operative condition (AEO): climb rate 8 m/s with η_p of 70%;
- Climb rate constraint in one engine inoperative condition (OEI): 2m/s climb rate with η_p of 65%.

It should be noted that adjustments had to be made to the aerodynamic data as listed in the reference paper, as the paper makes use of a two term drag polar (Equation 5), while the aerodynamics module presented in this work makes use of a symmetric drag polar (Equation 6). The symmetric aerodynamic drag values are obtained by matching the drag polar as close as possible to the two term drag polar, however, this causes a slight error in drag estimation for validating the results. The estimated aerodynamic values are:

- Zero-lift drag coefficient $C_{D_0} = 0.025$
- Oswald efficiency factor in clean configuration $e = 0.8$
- Maximum lift coefficient in clean configuration $C_{L_{max}} = 1.7$

$$C_D = C_{D,min} + \frac{(C_L - C_{L,minD})^2}{\pi A e} \quad (5) \qquad C_D = C_{D_0} + \frac{C_L^2}{\pi A e} \quad (6)$$

The aircraft-level, gas turbine and primary electric motor power-loading diagrams are constructed with the inputs as provided above and in the reference paper from *Finger et al.* [12]. The diagrams are shown in Figures 8, 9 and 10 respectively. The results of the design point determination is summarized in Table 2 and shows that the module is able to generate the correct power-loading diagrams and determine the correct design point. There is a slight offset in the power-loading values when compared to the reference, due to the difference in the aerodynamic drag polar.

Table 2: Verification Power-Loading Diagram Results Hybrid Dornier 228

	Result	Reference	Sizing constraint
Aircraft Design Point (W/S, P/W) [$N/m^2, W/N$]	1958, 17.89	1958, 17.85	OEI rate of climb
Gas Turbine Design Point (W/S, P/W) [$N/m^2, W/N$]	1958, 16.78	1958, 16.77	AEO rate of climb
Electric Motor Design Point (W/S, P/W) [$N/m^2, W/N$]	1958, 1.80	1958, 1.78	OEI rate of climb
Gas Turbine Mass [kg]	318	317	/
Electric Motor Mass [kg]	19.0	18.9	/

[3]Calculated from maximum take-off mass and zero-fuel mass.
[4]Calculated by subtracting total fuel mass with the fuel mass of the different mission phases.

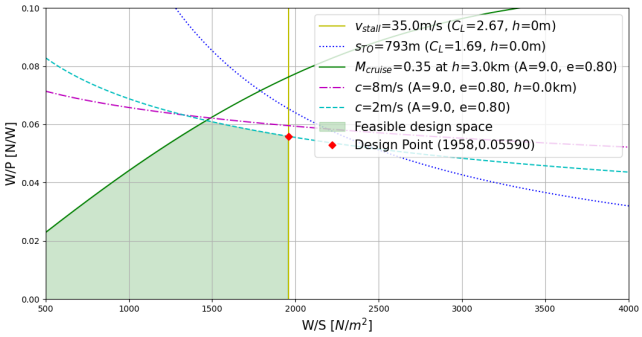

Figure 8: Aircraft-level power-loading diagram

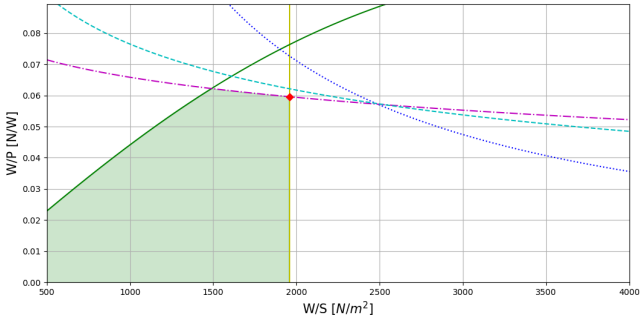

Figure 9: Gas Turbine power-loading diagram

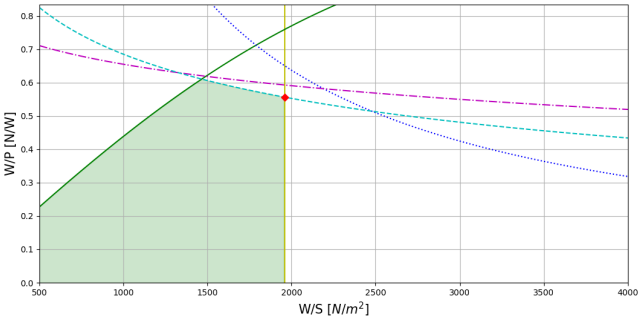

Figure 10: Electric Motor power-loading diagram

Additionally, also the energy analysis module is validated. This by comparing the fuel mass and energy mass required to perform an aircraft mission with the following characteristics:

- Cruise with 396 km range at 3000 m altitude and cruise speed 115 m/s;
- Diversion of 270 km at altitude 1000 m and 85 m/s;
- Endurance of 30 minutes at 450 m altitude.

The results of the energy analysis are summarized in Table 3 and show a maximum difference of 3.5% in the weight prediction of the fuel weight.

Table 3: Validation Energy Analysis Results Hybrid Dornier 228

Parameter	**Result**	**Reference** [12]	**Difference**
Fuel mass [**kg**]	498	481	+3.5%
Battery mass [**kg**]	117	115	+1.7%

2.3 Climate Optimization Module

The second module used in the coupling strategy is the Climate Optimization Module, which is responsible for optimizing the hybrid-electric aircraft for minimal climate impact. The effects of the operational cruise velocity, cruise altitude and cruise power split are investigated through a design space exploration study. The best operational conditions will be looked for that minimize the climate. Climate impact is measured by the amount of total CO_2 emissions, as the conceptual nature of the design tool allows to quantify these emissions and *Thijssen* [35] shows that for low altitude operations of propeller aircraft, the climate impact is governed by the CO_2 emissions and short-lived emissions dependent on fuel burn. The total CO_2 emissions are the sum of the CO_2 emissions coming from burning fuel in-flight, the production of kerosene on-ground and the electricity production on-ground. In addition to kerosene and electricity production, also battery production causes CO_2 emissions. This contribution was neglected as life cycle assessment studies show dominance of the operational phase [32]. Furthermore, there is a large uncertainty in assessing life-cycle emissions for battery production due to the variety of methods and materials used in manufacturing. The order of magnitude can vary from 56 to 494 kg CO_2/kWh [19]. The CO_2 emission indices for fuel burn, fuel production and electricity production are shown in Table 4. The electricity production assumes renewable energy sources.

The design space exploration study is carried out by first exploring the full design space using a Latin Hybercube Sampling method (LHS) with the aim of narrowing it down to only the feasible designs. With the LHS method, each parameter is sampled between an upper limit and lower limit in an independent way.

This causes the method to not consider any dependencies between the variables. To capture the interaction effects between multiple parameters, a full factorial sampling method is implemented afterwards. This allows for characterizing the main effects and interactions of the design parameters on the total CO_2 emissions. The outcome data of the full-factorial sampling is interpolated using a 4D interpolation scheme and the optimum combination of the parameters are determined.

Table 4: CO_2 emission indices for several operations [32]

EI_kerosene_inflight	**EI_kerosene_onground**	**EI_electricity_onground**
3.155 kg CO_2/ kg fuel	478.22 g CO_2/kg fuel	30.01 g $CO2$/ kWh electricity

It should be acknowledged that due to the conceptual nature of the hybrid-electric design tool, the CO_2 optimization module may not be able to fully capture the real-life trends of optimum aircraft operational conditions. In order to allow for the use of higher-fidelity optimization algorithms, a detailed climate impact analysis of the aircraft would require a time-stepping mission analysis where the aircraft states (such as: altitude, distance, velocity, fuel flow, fuel mass etc.) are known at all times of the mission. This was outside of the scope of the current research and therefore the results of this study should be considered as preliminary indications of possible outcomes, rather than as conclusive evidence. It is acknowledged that further research and optimization efforts are necessary to improve the accuracy of the results. However, the methodology presented here can be used as a starting point for understanding general trends and guide future work.

2.4 Fleet-and-Network Allocation Module

The last module is the Fleet-and-Network Allocation Module. This module is required to simultaneously develop the network and allocate the fleet choice while accounting for hybrid-electric aircraft operations. The fleet-and-network model used is an existing model developed by *Zuijderwijk* [43] which employs a constrained, linear programming problem. The main difference with general fleet-and-network models is the integration of the battery charging operations. As not every airport in the network has a charging facility, the airline network is defined in routes instead of single flights. The module does not take into consideration the operational planning, flight scheduling, maintenance and crew planning. The fleet-and-network model has the objective to maximize the airline profit by assigning passengers to flights and flights to aircraft. The results of the Fleet-and-Network Allocation Module presents the network performance (revenue, cost, profit, emissions) and the network development (flights, flight frequencies, passenger flows, fleet choice). For more information on the set-up of the Fleet-and-Network Allocation Module, the reader is referred to the research of *Zuijderwijk* [43].

2.5 Network and Aircraft Performance

For the integration of aircraft design with fleet-and-network allocation, different aircraft designs will be proposed to the airline fleet. The performance of each aircraft in the network is evaluated by evaluating the network performance. The optimal aircraft fleet is chosen in order to maximize the network objective. This section outlines the parameters used to measure network and aircraft performance.

2.5.1 Network Performance

The network objective is maximized by determining the values of the model decision variables:

- The amount of aircraft needed from a certain aircraft type k.
  Formulation: ac_k, where $k \in \mathbf{K}$: set of aircraft types
- The frequency of an aircraft type k on a route r in a given period.
  Formulation: z_k^r, where $k \in \mathbf{K}$: set of aircraft types and $r \in \mathbf{R}$: set of routes
- The number of passengers traveling from demand origin airport a to demand destination airport b on a route r in a given period.
  Formulation: $x_{a,b}^r$, where $a,b \in \mathbf{N}$: set of airport and $r \in \mathbf{R}$: set of routes
- The number of transfer passengers travelling from demand origin airport a to demand destination airport b on a route r followed by a transfer route m in a given period.
  Formulation: $w_{a,b}^{r,m}$, where $a,b \in \mathbf{N}$: set of airport and $r,m \in \mathbf{R}$: set of routes

Generally, the objective of an airline is to maximize profit and is therefore the main performance indicator of the network. Profit is defined similar as *Zuijderwijk* [43] and is the airline revenue subtracted by the costs. The revenue is determined from the yield between an airport pair per passenger-kilometer ($yield_{a,b}$) multiplied with

the route distances ($dist_{a,b}$) and amount of passengers or transfer passengers ($x^r_{a,b}$ or $w^{r,m}_{a,b}$). The revenue is corrected with a stop factor (SF) and a transfer factor (TF), which accounts for a decrease in revenue whenever a passenger travelling from origin to destination has to undergo an additional stop or has to transfer between subsequent flights. The total cost consists of the total ownership ($cost\_ownership$), which is dependent on the amount of aircraft of a certain type (ac_k), and the operating cost ($cost\_operating$), which is dependent on the frequency of aircraft use (z^r_k).

Apart from profit, also the total network emissions will count as an important performance indicator. The total emissions are calculated as the sum of the aircraft emissions of a certain aircraft type on a route ($emissions^r_k$) times the frequency of that aircraft on the route (z^r_k), for a given period of time.

2.5.2 Aircraft Performance

Each aircraft in the airline fleet is characterized by the following design parameters: aircraft capacity, maximum mission range, required runway length, operating cruise speed, operating cruise altitude and operating cruise power split. The performance of each aircraft is measured by the performance indicators: fuel and battery energy capacity, CO_2 emissions, operating times and aircraft costs.

Fuel and battery energy capacity
An aircraft is designed for a harmonic mission, consisting of a climb-and-descent cycle and a cruise phase. The climb-and-descent cycle consists of the taxi, takeoff, climb, descent and landing phase. The cruise phase is executed over a given range value (R_cruise). Each aircraft is characterized by the following parameters:

- The amount of fuel and battery energy required for a climb-and-descent cycle: $fuel\_climb\_descent_k$ and $energy\_climb\_descent_k$;
- The amount of fuel and battery energy required per flown kilometer in cruise: $fuel\_km_k$ and $energy\_km_k$;
- The maximum amount of fuel and battery energy required to fly the harmonic mission: max_fuel_k and max_energy_k.
  Calculating the maximum fuel and battery energy is straightforward en given by Equations 7 and 8.

$$max\_fuel_k = fuel\_km_k \cdot R\_cruise_k + fuel\_climb\_descent_k \tag{7}$$

$$max\_energy_k = energy\_km_k \cdot R\_cruise_k + energy\_climb\_descent_k \tag{8}$$

An aircraft operating between an origin airport a and destination airport b can do this either by a direct flight, or by having an additional stop at another airport c. The two corresponding route profiles are visualized in Figure 11 and Figure 12 sequentially. To calculate the amount of fuel and battery energy required to fly a certain mission, Equations 9 and 10 are used, where $R\_cruise\_route^r$ is the cruise distance flown for the route and $route\_stops^r$ are the stops on that route.

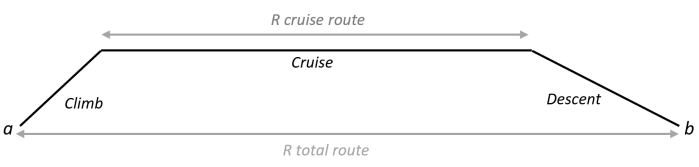

Figure 11: Route profile for a 1-stop mission

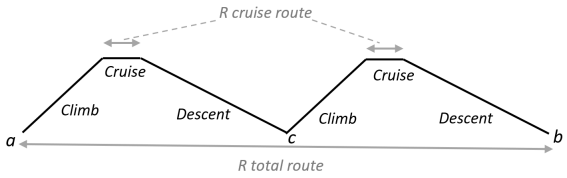

Figure 12: Route profile for a 2-stop mission

$$fuel^r_k = fuel\_km_k \cdot R\_cruise\_route^r + fuel\_climb\_descent_k \cdot route\_stops^r \tag{9}$$

$$energy^r_k = energy\_km_k \cdot R\_cruise\_route^r + energy\_climb\_descent_k \cdot route\_stops^r \tag{10}$$

To determine whether a certain aircraft type can fly a given route, the fuel and battery energy required to fly the route should be lower or equal to the maximum defined by the aircraft **and** the runway length required by the aircraft to take-off and land should be smaller or equal to the minimal runway length on the route. The resulting statements are listed in Equation 11.

$$fuel^r_k \leq max\_fuel_k \quad and \quad energy^r_k \leq max\_energy_k \quad and \quad min\_runway^r \geq runway_k \tag{11}$$

CO_2 emissions
Equations 9 and 10 indicate the amount of fuel and battery energy required to fly a certain route r with aircraft type k. From this, it is possible to estimate the CO_2 emissions of this aircraft on the particular route as the CO_2 emissions are directly related to the amount of fuel and battery energy required through the emission indices. The emission indices used are those shown in Table 4 for in-flight fuel burn, on-ground kerosene production and on-ground electricity production. The emission calculation is given in Equation 12.

$$\begin{aligned} emissions_k^r = \quad & EI\_kerosene\_inflight \cdot fuel_k^r \; + \\ & EI\_kerosene\_onground \cdot fuel_k^r \; + \\ & EI\_electricity\_onground \cdot energy_k^r \end{aligned} \tag{12}$$

Operating times
Another set of performance parameters is the operational times required to operate an aircraft at the airport. The charging operations of hybrid-electric aircraft have an influence on the turnaround time and the turnaround cost. Hybrid-electric aircraft are assumed to be recharged using a Battery Swapping Station which swaps the empty batteries for charged ones. The study of *Zuijderwijk* [43] provides time estimations for the minimum time between landing and take-off from each airport and is composed of the landing-and-takeoff time, the turn-around time and the refueling or recharging time.

Costs
Also the cost estimations were directly taken from *Zuijderwijk* [43]. The total costs of an aircraft considers both the ownership costs and the operating costs and are estimated using a linear cost equations depending on the number of seats.

2.6 Coupling Strategy

The design of a hybrid-electric aircraft fleet for a particular airline network which contributes to a lower climate impact, is achieved by integrating the three modules. Figure 13 graphically shows the coupling strategy of the three modules marked with their corresponding colors: hybrid-electric aircraft design , climate optimization and fleet-and-network allocation. The three modules are used sequentially one after another and multiple iterations on aircraft design and strategic airline planning are performed to come up with the fleet choice that best suit the given network. The coupling strategy makes use of the aircraft inputs and performance indicators and are shown between the curly brackets in Figure 13. To check how well aircraft are performing within the network and determine whether new aircraft designs are required, the performance indicators of the network will be compared in each iteration.

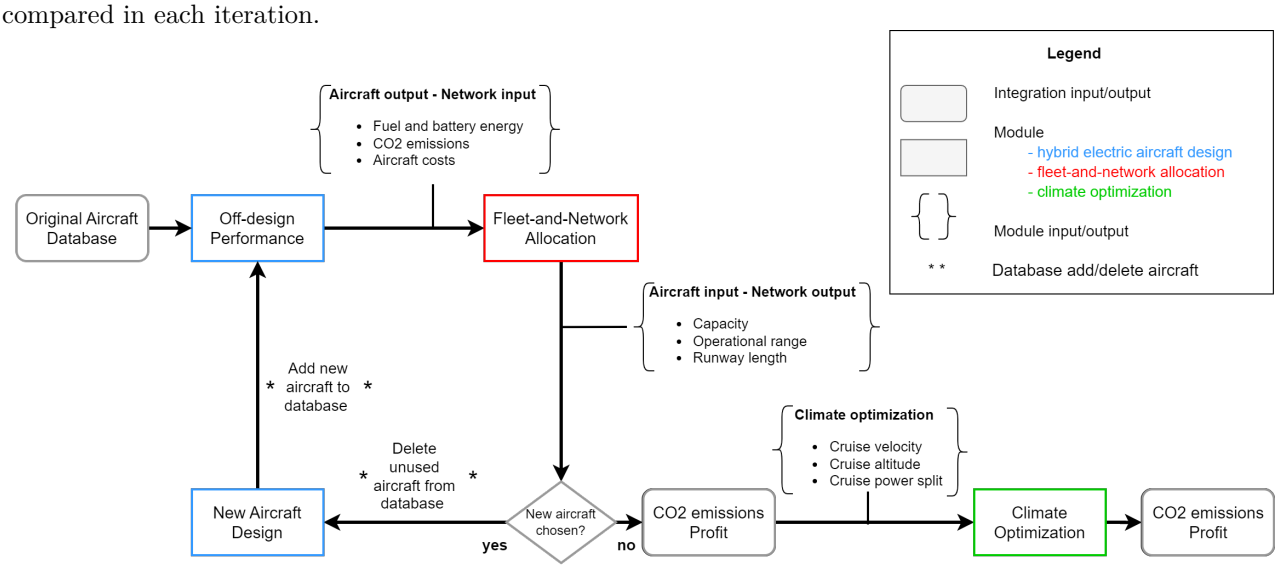

Figure 13: Coupling strategy workflow

The strategy first requires a set of input aircraft, referred to as the original aircraft fleet. These aircraft and their respective performance indicators, are stored in an aircraft database. Adaptations will be made to the design inputs of these aircraft in order to come up with a newly designed set of aircraft. The network performance is directly related to the aircraft operating in the airline network. The aircraft operations are largely defined by the amount of passengers an aircraft can carry over a route distance between two or more airports and the possible airports the aircraft can operate at. The latter is currently limited by the minimum runway length

of an airport pair. It is therefore most interesting to find the best combinations of capacity-range-runway to optimally serve the network. In each design iteration loop, changes will be made to the existing aircraft in terms of required aircraft capacity, maximum operating range and required runway length. The strategy to do so is threefold consisting of (1) an off-design performance investigation, (2) a fleet-and-network allocation and (3) new aircraft design propositions.

2.6.1 Off-design Performance

In this study, aircraft are designed for a harmonic mission, with the range defined at maximum payload capacity. The aircraft design at this point is hereafter referred to as the 'on-design' aircraft. It is investigated whether operating an aircraft outside of its design point would have a beneficial influence on the network performance. In the off-design performance investigations, trade-offs will be made for existing aircraft designs without changing the aircraft design itself. These trade-offs are captured by a payload-range trade-off and a payload-runway trade-off.

Payload vs. Range

In the context of strategic airline planning, the payload-range trade-off is an important consideration. For conventional kerosene aircraft, it is possible to decrease the payload mass in order to take more fuel and such increase the aircraft range. The larger the aircraft range, the more routes in the network can be flown. However, when decreasing the payload mass, the frequency of certain routes might need to increase in order to meet the desired passenger demand, which in terms increases the cost of flying the aircraft. This payload-range trade-off is captured by the well-known Breguet range equation and for the sake of completeness shown in Equation 13, where the sum of the operational empty weight, payload weight and fuel weight ($W_{OE} + W_{PL} + W_f$) equals the take-off weight $[N]$, η_{GT} is the gas turbine efficiency [-], η_P the propeller efficiency [-], L/D the aerodynamic efficiency [-] and e_f the fuel specific energy $[J/kg]$. Originally, this equation was established for kerosene-aircraft and clearly shows the logarithmic dependency of range on fuel weight.

$$R = \eta_{GT} \cdot \eta_P \cdot (\frac{L}{D}) \cdot (\frac{e_f}{g}) \cdot ln \left[\frac{W_{OE} + W_{PL} + W_f}{W_{OE} + W_{PL}} \right] \tag{13}$$

For hybrid-electric aircraft however, the payload is not simply traded for fuel, but also battery mass plays an important role. In this case, the range equation can better be expressed as a trade-off between payload mass and aircraft energy. *De Vries et al.* [10] derived this equation for hybrid-electric aircraft. The final expression can be seen in Equation 14, where η_1, η_2 and η_3 are the powertrain branch efficiencies [-] which relate the component efficiencies for various hybrid-electric powertrain architectures. $E_{0,tot}$ is the total energy of fuel and battery carried on-board $[J]$, Φ is the cruise power split value [-] and e_b is the battery specific energy $[J/kg]$. The equation is valid if the supplied power split, flight speed, lift-to-drag ratio and transmission efficiencies are constraint throughout the cruise phase.

$$R = \eta_3 \cdot (\frac{e_f}{g}) \cdot (\frac{L}{D}) \cdot (\eta_1 + \eta_2 \frac{\Phi}{1-\Phi}) \cdot ln \left[\frac{W_{OE} + W_{PL} + \frac{g}{e_{bat}} \cdot E_{0,tot} \cdot (\Phi + \frac{e_{bat}}{e_f} \cdot (1-\Phi))}{W_{OE} + W_{PL} + \frac{g}{e_{bat}} \cdot \Phi \cdot E_{0,tot}} \right] \tag{14}$$

Using the hybrid range equation, the payload-range diagram can be constructed to visualize the payload range trade-off, see Figure 14. One can clearly inspect the harmonic range value at the maximum payload mass, after which the payload is decreased and fuel and battery mass is increased until the maximum amount of fuel that can be stored is reached. After this point, both the fuel and battery mass are kept constant and solely payload is traded for extra range. Additionally, the aircraft mass build-up is shown in Figure 15 as this more clearly visualizes the trade-off between payload mass and energy mass.

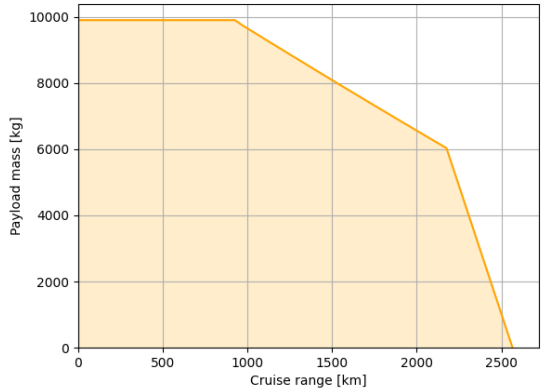

Figure 14: Payload-range (varying battery mass)

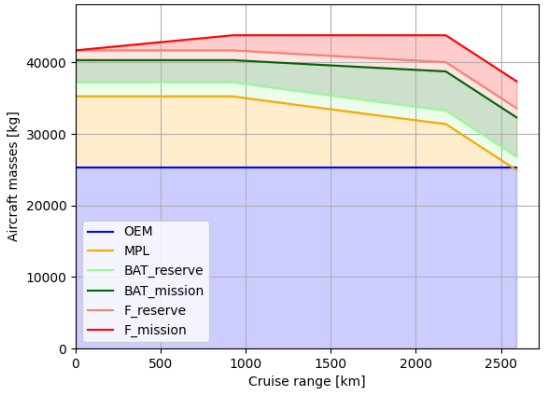

Figure 15: Aircraft masses (varying battery mass)

It is important to note that using this approach, both fuel mass and battery mass are increasing with decreasing payload. From an operational point of view, this is not practical as this would require a different battery for all the different payload-range trade-off configurations. This is why it was decided that during the payload-range trade-off, the battery mass is kept constant at the harmonic design point. However, some additional energy is required at larger ranges which was originally provided by the extra battery mass. This additional energy will therefore be provided by some extra fuel as shown in Equation 15, where m_{bat} is the battery mass from the original payload-range trade-off, $m_{bat_{harm}}$ is the battery mass at the harmonic design point and $m_{bat_{upd}}$ is the final battery mass. Similarly, m_f is the fuel mass from the payload-range trade-off and $m_{f_{upd}}$ is the final fuel mass. This results in a new payload-range trade-off as seen in Figure 16 and Figure 17.

$$\begin{aligned} \Delta m_{bat} &= m_{bat} - m_{bat_{harm}} \\ \Delta m_f &= \frac{e_b}{e_f} \cdot \Delta m_{bat} \end{aligned} \qquad \begin{aligned} m_{bat_{upd}} &= m_{bat_{harm}} \\ m_{f_{upd}} &= m_f + \Delta m_f \end{aligned} \tag{15}$$

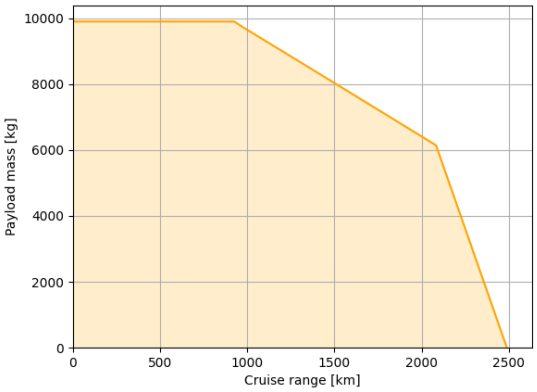

Figure 16: Payload-range (constant battery mass)

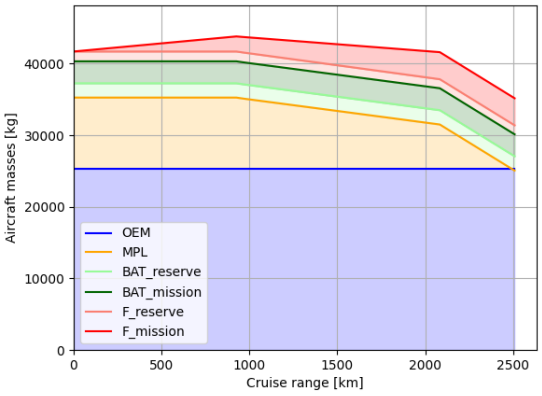

Figure 17: Aircraft masses (constant battery mass)

There are some important consequences when using this approach. First of all, it can be seen that the take-off mass is not constant anymore. The take-off mass is slightly decreasing due to the fact that the additional battery energy required is now delivered by additional fuel which has a much larger specific energy, and therefore less weight. One could also opt to again add more payload and/or more fuel in order to keep the take-off weight constant. This was however not implemented as it was decided that the energy required to fly the mission should not change but the battery energy is simply traded for fuel energy, significantly simplifying the analysis. The decrease in take-off weight will in term cause the aircraft to be able to take off and land from shorter runways. Furthermore, due to the extra fuel and constant battery mass, the power split value is not constant but slightly decreasing with increased range.

For each (new) aircraft in the database, this payload-range trade-off will be made. The payload mass is decreased in steps of 10 passengers until it reaches the specified minimum capacity. For each off-design configuration the aircraft performance parameters are calculated. The combination capacity-range-runway is directly obtained from the trade-off. The performance indicators $fuel/energy\_climb\_descent$, $fuel/energy\_km$ and $max\_fuel/energy$ can be calculated from the aircraft mass build up. The aircraft costs and operating times are assumed to be the same as the original on-design aircraft.

Payload vs. Runway

As mentioned before, an aircraft is only able to fly a certain route when it can take-off and land on the smallest runway length on this route. From this condition, there is again an important trade-off to consider. When decreasing the payload weight, the take-off weight of the aircraft is decreasing and the aircraft can take off and land from smaller runways. Therefore, the aircraft can operate more routes in the network. However, this again means that the frequency of the operation might need to increase in order to meet the passenger demand. In the payload-runway trade-off, the payload is decreased and the required take-off length and landing length are determined for each aircraft configuration.

The required take-off length is estimated using the take-off parameter (TOP) from *Raymer* [28] which can be seen in Equation 16. The take-off weight W_{TO} is varying for each situation as the payload mass is decreased. The wing surface area S, the take-off power P, the lift coefficient in take-off configuration $C_{L_{TO}}$ are all constant and remain the same as the on-design aircraft. The required landing length (S_L) is estimated from the relation between stall speed and landing length from *Roskam* [29]. Equation 17 and 18 shows this relation, and the calculation for the stall speed. To calculate the stall speed, the landing weight W_L is used, which is again different for each configuration due to a decreased payload mass. Also here, the wing surface area S and the maximum lift coefficient in landing configuration $C_{L_{max}}$ are constant and equal to the on-design aircraft.

$$TOP = \frac{W_{TO}}{S} \cdot \frac{W}{P} \cdot \frac{1}{C_{L_{TO}}} \quad (16) \qquad S_L = 0.5847 \cdot V_{S_L}^2 \quad (17) \qquad V_{S_L} = \sqrt{\frac{W_L \cdot 2}{S \cdot \rho \cdot C_{L_{max}}}} \quad (18)$$

The required runway length of an off-design aircraft configuration is then simply the limiting one of the take-off length and the landing length. Similar to the payload-range diagram, a payload-runway diagram can be constructed as seen in Figures 18 and 19 from which the performance parameters of the aircraft are extracted. A kink can be observed in the payload-runway diagram, for which the limiting condition switches from take-off to landing. Also these payload-runway off-design aircraft configurations are added to the aircraft database.

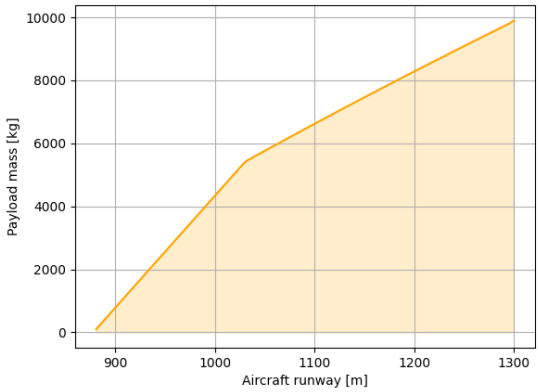

Figure 18: Payload-runway (constant battery mass)

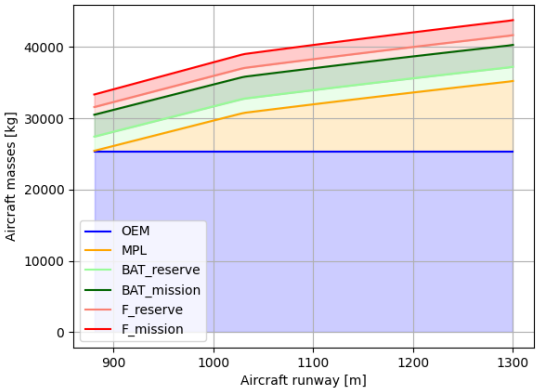

Figure 19: Aircraft masses (constant battery mass)

2.6.2 Fleet-and-Network Allocation

The aircraft, together with their payload-range and payload-runway trade-off configurations, are fed to the Fleet-and-Network Allocation program. The on-design and off-design aircraft configurations are operated in the network such that the airline profit is maximized. With this network allocation output, it is possible to obtain additional information on how the aircraft are operated in the network. For each route in the network, the route distance and minimum airport runway length is known. For each aircraft in the aircraft database, it is possible to plot the routes flown in the payload-range diagram by plotting the operated aircraft capacity and the route distances flown at both its on- and off-design conditions. Each route is represented by a point in the diagram and is accompanied by the minimum runway length of that route. An example figure can be seen in Figure 20. The routes flown with the on-design aircraft are marked with a circle ($\circ$), the routes flown with a payload-range trade-off configuration are marked with a cross ($\times$) and the ones flown with a payload-runway trade-off configuration with a triangle ($\triangle$). It can be observed that there is quite some scattering in terms of the range as some aircraft are operated at lower ranges than what the original aircraft is initially designed for. The payload capacity is lowered in steps of 10 passengers. The network model requires all aircraft configurations to be operated at a certain load factor, which explains the fact that the passenger capacity points are vertically centered at the aircraft configuration capacity. Only when a flight cannot be flown at full capacity, the point will deviate from its vertical position in the graph. From this information on the aircraft operations, new aircraft designs will be generated with a passenger capacity, aircraft range and design runway length which better matches the operations in the network.

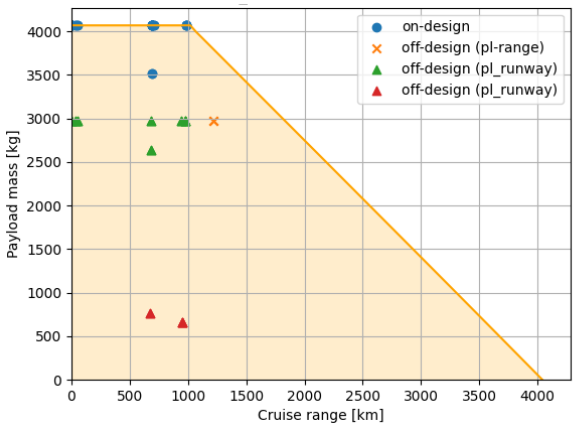

Figure 20: Route operations plotted in payload-range diagram

2.6.3 New Aircraft Design Propositions

The operations of the aircraft in the network will guide the generation of new aircraft designs. The new aircraft designs are based on the ones already in the database, but adaptations are made to the payload-range-runway combination. This is done by two methods: (1) a clustering method and (2) a limit-case operation analysis.

Clustering Method

As could be observed from Figure 20, an aircraft configuration can be operated at ranges smaller or equal than the range for which the aircraft was designed. Often, the operated ranges are grouped in several clusters. New aircraft designs will therefore be generated with (smaller) ranges which better match the route ranges operated at, based on these range clusters. The clustering method is explained through the following example:

When considering the aircraft of Figure 20, a clear range clustering is observed at the payload-runway off-design configuration at payload mass ∼3000 kg, which corresponds to ∼ 30 passengers (▲). For this aircraft configuration, the operated ranges and runway lengths are shown in Table 5. The following step-wise procedure is followed:

Table 5: Distance and runway length for aircraft in Figure 20 at payload 3000 kg

distance [km]	31	51	970	680	680	940
runway length [m]	1655	1595	1342	1268	1270	1342

1. Allocate the route distances to a binary array, where each bin width is defined by a specified 'split' value. E.g. if a split value of 100 km is selected and the maximum route distance is 1100 km, the bins are as showed in the table below as *'Range bins [km]'*. The routes are allocated to a binary array, where *'1'* indicates the aircraft is flying on routes with distances within the range bin width. In the example, the ranges in Table 5 are colored and matched with the binary array allocation in the table below for better visualization.

2. The operational ranges are defined by the maximum range of each range interval.

3. The operational runways are defined by the minimum runway in each interval.

	Range bins [km]	**0-100**	**100-200**	**200-300**	**300-400**	**400-500**	**500-600**	**600-700**	**700-800**	**800-900**	**900-1000**	**1000-1100**
Step 1:	**Binary**	1						1			1	
Step 2:	**Range [km]**	100						700			1000	
Step 3:	**Runway [m]**	1595						1268			1342	

4. The clustering of consecutive intervals into one is defined by a 'threshold' value which specifies the minimum range between two consecutive clusters for which a new aircraft will be designed. E.g. with a threshold value of 400 km, the clustering is as followed:

$$\text{clustered ranges} : [100]\,[700, 1000]$$
$$\text{clustered runways} : [1595]\,[1268, 1342]$$

5. The new aircraft will have a design range equal to the maximum range of each cluster and a design runway length equal to the minimum runway length of each cluster rounded down to 50:

aircraft 1: 30 passengers - 100 km cruise range - 1550 m runway length.
aircraft 2: 30 passengers - 1000 km cruise range - 1250 m runway length.

The clustering method is performed for each configuration, so for each payload capacity the aircraft is operating at. The results of the clustering method are a set of aircraft which are added to the aircraft database.

Limit-case Operations

Using the clustering method, the aircraft operations of the on- and off-design configurations are inspected and clustered together in order to make multiple, smaller aircraft that better fit the network. This does not take into account the design of aircraft with larger passenger capacities and larger operational ranges. Therefore, a limit-case operation analysis is performed in which it is checked whether an aircraft is operating at its limiting conditions of maximum payload and maximum range. The following design strategy is applied to come up with additional aircraft designs:

1. *If* the aircraft operates at its maximum payload *or if* it operates at a payload-runway trade-off condition
   ⇒ increase the payload capacity (+10) for the same aircraft range.

2. *If* the aircraft operates within 5% of the maximum range at a given payload
   ⇒ increase the design range (+ split) for that payload capacity.

3. *If* the aircraft operates within 5% of the harmonic design point
   ⇒ increase both the payload capacity (+10) and the design range (+split) at the same time.

All new aircraft generated from both the clustering method and the limit-case operation analysis, have to adhere to the constraints mentioned in section 2.1.8. Only the designs that have a converged maximum take-off weight within 0.1% with respect to the previous iteration and meet all design constraints, are added to the aircraft database and can be implemented in the next fleet allocation.

2.6.4 Iteration strategy

Looking back at the schematic of the coupling strategy in Figure 13, the first couple of steps have been discussed: the original aircraft database, the off-design performance analysis, the fleet-and-network allocation and the new aircraft design generation. After these steps, the loop is entered again and an iterative procedure takes place. The new aircraft designed after the first loop will again go through an off-design performance analysis and the payload-range and payload-runway trade-off configurations of all of these aircraft designs are added to the aircraft database. After this, another fleet-and-network allocation is performed to see how these new aircraft are operated in the network. Based on the operations, new aircraft are aircraft are proposed and added to the database.

As the aircraft database would be expanding for each iteration, a database clear-up is performed. Only the aircraft chosen in each iteration, together with their payload-range and payload-runway configurations, are kept in the database. Aircraft that are not chosen are removed. The iteration procedure will last until the fleet-and-network allocation does not select any of the newly proposed aircraft designs. At this point, optimal aircraft fleet is known which maximizes the airline profit. An example database for different design iterations is presented in Table 17. The associated time required for the fleet-and-network allocation and new aircraft design creation is shown in Table 18. The time required to obtain a converged aircraft design varies from around 5 seconds for easily converging designs, and can go up till 25 seconds for non-converging designs. Therefore, designing an aircraft is assumed to take about 15 seconds. Similarly, making the off-design aircraft configurations can happen almost instantaneously or can take up to 20 seconds. The assumed time to make the off-design configurations is therefore estimated at 10 seconds. The time required to perform a fleet-and-network allocation is almost independent on the amount of aircraft in the database and always takes about 20 minutes (1200 seconds).

2.6.5 Climate Optimization

The last step of the coupling strategy involves a climate optimization. Currently, the aircraft in the final optimized aircraft fleet are operating at conditions specified by the initial aircraft. However, the operating conditions for each of these aircraft might not be the optimal when considering climate impact. In this last step, all aircraft in the fleet will be optimized individually to minimize the CO_2 emissions over their design mission profile. This will be done through a design space exploration study in which the following parameters will be altered: cruise velocity, cruise altitude and cruise power split, as previously mentioned in section 2.3. The optimized aircraft fleet is then introduced into the network without altering the fleet-and-network allocation. In the climate optimization, it is important to consider that the optimized aircraft can perform the same missions than the non-optimized alternatives, which poses an important constraint on the optimization problem. Finally, the effect of climate optimization on the airline profit and network emissions will be investigated.

3 Case Study

The presented methodology is tested by means of a case study. Similar to the work of *Zuijderwijk* [43], the SATA Air Açores regional airline network is implemented to present the results. The network consists of nine islands in the Azores with one airport located at each island. Not every airport in the network has the possibility for refueling and therefore the current network is operating in routes instead of single flights. This makes it a representative network to implement future (hybrid) electric aircraft operations for which there is not yet a recharging possibility. Public service obligation (PSO) regulations are imposed, posing a requirement on the minimum frquency and capacity of a flight between an airport pair. For more information on the airline network, the reader is referred to the work of *Zuijderwijk* [43].

3.1 Reference Case

In this reference case, the allocation of the existing aircraft in the airline fleet are used to test the validity of the design and allocation module. The network is currently served by two types of conventional turboprop aircraft: the Dash 8 Q400 and Dash 8 Q200. These aircraft are designed using the hybrid-electric design module and the inputs provided in Table 6. The performance parameters of the on-design and off-design payload-range and payload-runway configurations are determined and summarized in Table 13. The cost and time estimations of the aircraft configurations are obtained from the relations presented in *Zuijderwijk* [43].

Table 6: Design Inputs for Kerosene Reference Aircraft

Parameter	**Dash 8 Q400**	**Dash 8 Q200**
Harmonic cruise range [km]	926	1020
Passenger capacity [-]	80	37
Cruise altitude [m]	7010.4	7600
Cruise velocity [m/s]	182	150
Runway length [m]	1300	1000
Aspect ratio [-]	12.8	12.3
Payload mass [kg]	8489	4200
Max fuel [kg]	5300	2500

The network model is run to maximize the airline profit. The average weekly passenger demand and PSO requirements are included as determined in the work of *Zuijderwijk* [43]. The maximum operating time of the aircraft per day, referred to as the block time, is equal to 9.35 hours. Each route in the network has a maximum route size of 2 subsequent flights. Each flight is occupied at 85% of maximum aircraft capacity (load factor 0.85). The effects of having an additional stop or a transfer stop on the airline costs are not included, meaning the stop factor (SF) and transfer factor (TF) are both equal to 1. No climate tax is included in the model. The general fuel cost and battery energy cost are taken from the work of *Zuijderwijk*[43] to enable comparison of the results and are estimated at €0.80 per kg of fuel and €0.1445 per kWh of battery energy. It should be noted that these values are a bit lower than when compared to today's fuel and energy price. The fuel price in Portugal is US$0.68 per liter of fuel[5] which corresponds to €0.85 per kg of fuel. The energy price in Portugal is equal to €0.22 per kWh[6].

3.1.1 Result Fleet and Network Performance

The results of the fleet-and-network allocation show a total fleet size of 5 aircraft is required, 2 times the larger aircraft ($Q400$) and 3 times the smaller aircraft ($Q200$). These results correspond to the results outlined in *Zuijderwijk* [43], who performed a similar fleet allocation for the same airline network. In reality however, the total fleet consists of 6 aircraft with 4 of the type $Q400$ and 2 of the $Q200$ [43]. The difference can be attributed to the simplifications and assumptions made in the model by *Zuijderwijk* [43] and as the study presented here makes use of the same model without altering important parameters such as cost and time estimations, similar results are obtained in the fleet allocation.

From the 2 Q400 aircraft, one is operated at maximum capacity ($Q400_{on}$) and the other is operated at an off-design condition ($Q400_{off}$) where 10 passengers are traded for a lower runway length. The on-design $Q400$ aircraft is operated at routes with small ranges and without an intermediate stop. The aircraft flies on routes with high demand (PDL-TER, PDL-HOR, PDL-PIX, PDL-SMA)[7]. As the aircraft configuration requires a minimum runway length of 1300 m, it can not be operated at the airports GRW, SJZ and CVU. The off-design configuration is operated on routes which can include an additional stop. The highest demand route is not flown. Due to the reduced runway length of this aircraft configuration, the aircraft can now operate from airports GRW and SJZ.

Additionally, 3 Q200 aircraft are needed, of which 2 are operating at maximum passenger capacity ($Q200_{on}$) and 1 is operated at lower passenger capacity and reduced runway length ($Q200_{off}$). The on-design aircraft flies routes with medium ranges and can operate on all airport except CVU. The aircraft flies a lot on the highest demand route, but less or not on the other high-demand routes. For the Q200 aircraft, the passengers are traded in the payload-runway trade-off configuration in order to allow the aircraft to takeoff and land on airport CVU which has a runway length of 761m. To do so, the passenger capacity had to be decreased to 17 passengers. As the passenger capacity is reduced, this aircraft configuration is not flown on the highest demand route. The route distances covered are large because this aircraft configuration is often operated on routes instead of single

[5]https://jet-a1-fuel.com/price/portugal, Visited on 23/02/2023
[6]https://www.costtotravel.com/cost/electricity-in-ponta-delgada-azores, Visited on 23/02/2023
[7]Airport pairs for high demand routes listed from highest demand to lower demand

flights as there is no fueling facility at CVU. The resulting fleet is summarized in Table 7. The routes flown per aircraft configuration are depicted in the left column of Figures 27 to 33. The thickness of the lines represent the frequency of the aircraft on the route, thicker lines means the route is flown more frequent than those with thinner lines.

Table 7: Resulting fleet - Reference case

Aircraft	**Configurations (passengers - total range - runway)**
$Q400$	1x $Q400_{on}$ (80-1135-1300) 1x $Q400_{off}$ (70-1135-1252)
$Q200$	2x $Q200_{on}$ (37-1246-1000) 1x $Q200_{off}$ (17-1246-755)

Due to the conceptual nature of the design and allocation modules; as well as the confidentiality of the SATA Air Açores airline cost/profit results, all network performance results will be compared relatively to this reference case. For validation purposes, the results of this reference case are compared to those obtained in the study of *Zuijderijk* [43]. This comparison is shown in Table 8 and allows to highlight the differences between both aircraft design modules. It can be observed that in both cases, the fleet size is equal to 5 and fleet diversity is equal to 2. The ownership costs are not changed, as the cost estimation of the aircraft was directly taken from the study of *Zuijderwijk* [43]. There is a small change of 8% in the operating cost. The design modules have a significantly different approach in modelling the amount fuel and battery energy required for a route stop. Opposite to the study presented here, the model of *Zuijderwijk* [43] only includes the fuel and battery energy required to perform the take-off and landing phase but does not specifically model the climb and descent phases as it includes those in the cruise phase. The differences in cost predictions in turn cause a slight offset in the airline profit value of 5%. Another remarkable difference can be observed in the total network emissions, where previous work showed much lower emissions (-38%). This difference can again be attributed to the difference in fuel and battery energy modelling, as well as the fact that the study presented here includes the CO_2 emissions for fuel burn in-flight, fuel production on ground and electricity production on ground, while *Zuijderwijk* [43] only includes the former.

Table 8: Comparison of results reference case with *Zuijderwijk* [43]

	Results	**Results *Zuijderwijk***
Fleet size	5	5
Fleet diversity	2	2
Ownership cost	REF	+0%
Operating cost	REF	+8%
Profit	REF	-5%
Emissions	REF	-38%

3.2 Initial hybrid fleet

In order to carry out the full integrated design cycle for a climate optimized aircraft fleet as visualized in Figure 13, the original aircraft database has to be created. In this database, two parallel hybrid-electric aircraft will be implemented which are based on the Q400 and Q200 aircraft with inputs and top-level aircraft requirements listed in Table 15.

The hybrid-electric powertrain properties are established from state-of-the art research goals for the 2035 timeframe and obtained from *De Vries* [9]. The assumptions for the powertrain component properties are listed in Table 14. It should be noted that, even for the 2035 timeframe the powertrain component properties are optimistic. The presented specific energy of the battery at pack level is close to the theoretical limits of lithium-ion batteries at cell level. Therefore, the batteries might require a cell chemistry other than lithium-ion. The specific power for electric motor and converters are obtained from state-of-the art research goals for electrical machines, inverters and rectifiers. The effects of converters are not explicitly modeled but are accounted for by including their weight penalty in the electric motor elements. Furthermore, due to the lack of information for preliminary weight estimation of the cooling and system cables for thermal and power management and distribution, the weights are grouped in the power management and distribution box (PMAD). A total weight penalty of 30% is included and accounted for in the equivalent specific power for the electric motor.

Sizing the hybrid-electric aircraft, again gives the required performance parameters, cost and time estimations. The initial hybrid-electric aircraft will be addressed as 'HE Q400' and 'HE Q200'. The results of the hybrid-electric aircraft sizing configurations are listed in Table 16. With the initial hybrid-electric aircraft database, the fleet-and-network allocation module can be run for the first time.

The CO_2 emissions of the hybrid-electric aircraft are obtained from the emission indices from Table 4 which assumed renewable energy production. The Azores currently generate about 40% of their electricity from renewables such as geothermal energy, wind energy and hydroelectric power[8]. Additionally, Portugal aims to be climate neutral by 2050 and cover 85% of its electricity consumption with renewables by 2030 [3], making this a relevant assumption for this network.

3.2.1 Result Fleet and Network Performance

The results of the fleet allocation show that the total fleet size should increase to 7 aircraft. One additional $HE\ Q400_{on}$ and one additional $HE\ Q200_{on}$ aircraft are required. The main reason for the increase in fleet size compared to the reference case comes from the increase in operating times to operate hybrid-electric aircraft when compared to kerosene aircraft due to the extra time required to swap the battery.

The $HE\ Q400$ aircraft is operated both at its maximum capacity ($HE\ Q400_{on}$) and a configuration where passengers are decreased for an increased range ($HE\ Q400_{off}$). As explained in section 2.6.1, due to the payload-range modelling, the aircraft will have a decreased take-off mass and such also a reduced runway length. The $HE\ Q200$ aircraft is operated at its maximum capacity ($HE\ Q200_{on}$) and a payload-runway trade-off configuration ($HE\ Q200_{off}$). Passengers are traded in order to enable taking off from the CVU airport runway of 761m. The hybrid-electric aircraft has a significant increase in take-off weight when compared to the kerosene alternative, and such the passenger capacity had to be lowered to only 7 passengers.

When compared to the kerosene case, the $HE\ Q400_{on}$ is operated on routes with larger distances and this time also on routes which do have an additional stop. The $HE\ Q400_{off}$ is operating on much lower amount of routes with smaller distances and no additional stops. This off-design configuration only covers the routes which the on-design cannot do (between airports GRW and SJZ). All the other routes are taken up by the on-design aircraft as there is one additional aircraft of this type in the fleet when compared to the reference case.

The $HE\ Q200_{on}$ aircraft covers the same routes as its kerosene alternative, but this time also performs on routes with a larger distance. As there is an additional aircraft of this on-design type in the fleet, it can now take over some of the routes of the off-design configuration ($HE\ Q200_{off}$). The off-design trade-off configuration is operated much less and only covers the routes to CVU. These routes have a long range as there is no charging facility at CVU. The frequency of these routes has increased. Because of the decreased payload, the aircraft has to fly more frequently to meet the demand. The resulting fleet is summarized in Table 9. Also for the initial hybrid aircraft fleet, the routes flown per aircraft configuration are depicted and shown in the right column of Figures 28 to 34. The results of the routes flown can easily be compared for the kerosene and initial hybrid-electric aircraft fleet by comparing the left and right columns.

Table 9: Resulting fleet - Initial hybrid case

Aircraft	**Configurations (passengers - total range - runway)**
$HE\ Q400$	2x $HE\ Q400_{on}$ (80-1109-1300) 1x $HE\ Q400_{off}$ (70-1483-1258)
$HE\ Q200$	3x $HE\ Q200_{on}$ (37-1226-1000) 1x $HE\ Q200_{off}$ (7-1226-731)

The results of fleet composition, airline cost, airline profit and total network emissions are summarized in Table 12 to enable easy comparison between the different case studies. Due to the increased amount of aircraft and increased flight frequency, both the operating cost and ownership cost are increased when compared to the reference situation. The operating cost is increased by +16%, the ownership cost is increased by +42%. These increase in costs in term have a negative effect on the airline profit, which is decreased by -27%. The reduction in emissions from operating hybrid-electric aircraft is offset by the increased amount of aircraft and flight frequency, resulting in a zero total network emission reduction.

3.3 Redesigned hybrid fleet

With the information from running the fleet-and-network model with the initial aircraft database, new hybrid-electric aircraft can be designed. In each design iteration, a lot of new aircraft designs are proposed to the network, but only a limited amount are actually performing better than the ones already in the database.

3.3.1 Result Fleet and Network Performance

In Figure 21 an attempt was made to visualize the chosen airline fleet. Each aircraft type is represented by a name, color and their payload-range-runway combination. When one aircraft is operated at multiple

[8]https://clean-energy-islands.ec.europa.eu/countries/portugal/azores

configurations (on-design and off-design), the aircraft are shown in the same color and connected through a vertical line. The amount of aircraft needed from a certain type or configuration is denoted by the number in the upper right corner. When an aircraft goes through a redesign, a new aircraft is generated and the name gets an additional term R_x where x denotes the amount of redesign cycles it has gone through. A redesign cycle is marked with a red arrow. Whenever an aircraft is chosen without the need of a redesign, it is marked with a green arrow. The figure is accompanied by the results listed in Table 10, which shows information about the fleet choice and network performance for each design cycle. When considering the design cycle in Figure 21 and the results in Table 10 the following can be observed:

- Run 0: This run represents the fleet choice as listed in Table 9, consisting of the initial $HE\ Q400$ and $HE\ Q200$ aircraft with their chosen off-design trade-off configurations. There are only two types of aircraft in the fleet and therefore the aircraft are required to operate at off-design conditions in order to perform the required operations, which are currently limited by the runway length requirements. The total fleet size is equal to 7.
- Run 1: In this run, the original $HE\ Q400_{on}$ aircraft is chosen without a redesign. Additionally, 4 newly designed aircraft are part of the fleet. The total fleet size is reduced to 6 aircraft. The fleet diversity is significantly increased to 5. This makes it possible to better allocate the various types of aircraft in the network as they are particularly designed to serve a certain set of routes. All aircraft in the fleet are now operated at their on-design condition and thus no payload-range or payload-runway trade-off had to be made. This translates into an increase in profit of +14% and decrease in emissions of -8% with respect to the previous run.
- Run 2: In this run, two aircraft from the previous run are chosen without a redesign. Furthermore, 4 newly designed aircraft are added to the fleet, which are second redesign aircraft, denoted by R_2. The fleet size remains at 6 while the fleet diversity increases to 6, meaning there is one aircraft of each type. Again, all aircraft are operated at their on-design configuration. The profit in this run is not increasing, however, the emissions are decreased by -3% with respect to the previous run. The fleet in this second run represents the final hybrid-electric airline fleet as no new aircraft were selected in a third run. The final chosen aircraft fleet consists of the following aircraft, represented by their payload-range-runway combinations:
  1. *On_design* 80-1109-1300
  2. *On_design* 70-809-1250
  3. *On_design* 70-309-1550
  4. *On_design* 37-1126-1250
  5. *On_design* 7-1126-750
  6. *On_design* 17-826-750

The complete aircraft database for each design run is provided in Table 17, which shows the newly designed aircraft added in each run (+) and the aircraft that are deleted after the run (-). The database table is complementary the the redesign cycle schematic of Figure 21 and chosen aircraft are marked with the same colors. Furthermore, the time estimations required to perform the full fleet design is presented in Table 18 and took about 2 hours in total.

The aircraft in the final fleet, with their performance indicators, are shown in Table 19. The allocation of the different aircraft on the routes are shown in Figures 36 to 41.

Table 10: Network results for hybrid-electric fleet redesign cycle, profit and emissions are compared to reference case

	Run 0	**Run 1**	**Run 2**
Fleet size	7	6	6
Fleet diversity	2	5	6
Profit	-27%	-13%	-13%
Emissions	+0%	-8%	-11%

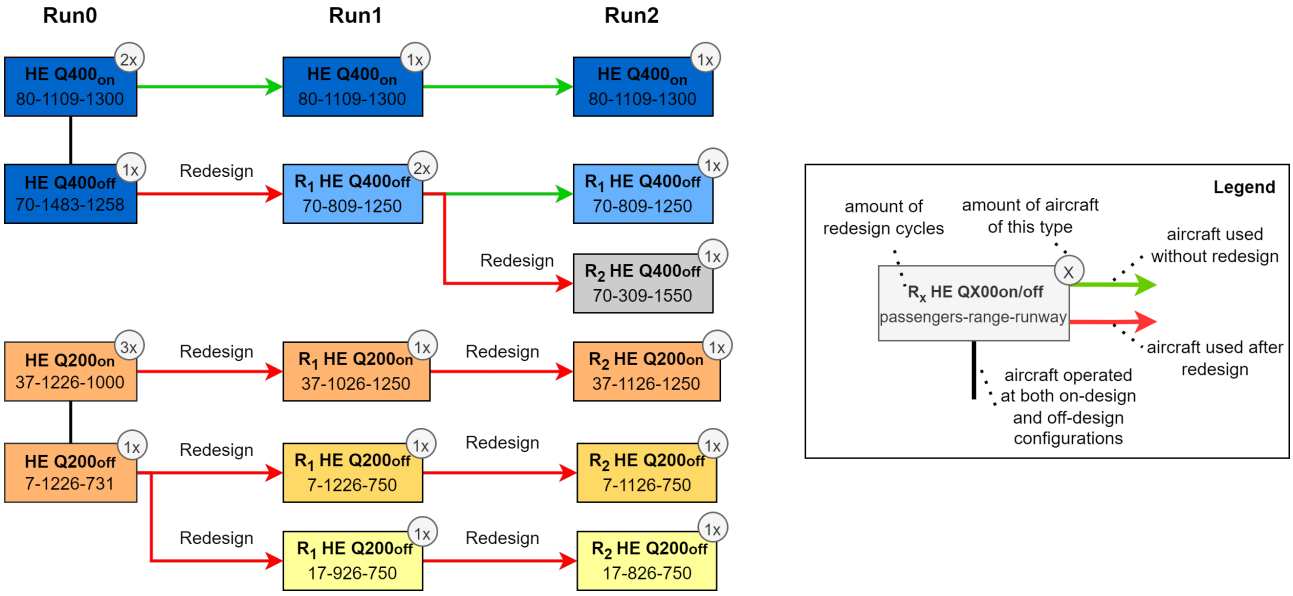

Figure 21: Schematic of aircraft redesign cycle

The resulting network performance of the final hybrid-electric fleet is again summarized in Table 12. Compared to the initial hybrid case, in which hybrid-electric aircraft were allocated without redesigning the fleet, a significant decrease in ownership cost (-32%) can be observed. This, one one hard, is due to the decreased fleet size. On the other hand, it is because the fleet consists of smaller aircraft and the costs are a function of the number of aircraft seats. This indicates one shortcoming of the method presented: a higher fleet diversity can lead to lower airline costs while in reality a more standardized fleet is accompanied by lower costs of operations and maintenance. Apart from that, the higher fleet diversity allows the aircraft to be allocated more efficiently in the network and thus lowers the total network emissions by -11%. When comparing the final hybrid-electric fleet with the reference kerosene fleet, a total decrease in emissions of -11% can be obtained at the cost of a decrease in profit of -13%.

Also the hybrid-electric redesign case is compared to the results of *Zuijderwijk* [43] for validation purposes and highlighting the differences in the outcomes. From Table 11 it can be observed that the operating cost and ownership cost are less than listed in *Zuijderwijk* [43], which can be attributed to the reduced fleet size and increased fleet diversity. The emissions are significantly higher, for which there are multiple causes. As mentioned before, there is a fundamental different approach for modelling the climb and descent phases. In the study presented here, it was observed that due to the higher weight of hybrid-electric aircraft, the decrease in fuel due to the hybridization during climb and descent is offset by the increase in aircraft weight. The conceptual aircraft design tool is however quite conservative in this sense and might over-stress the influence of these phases. Furthermore, the study presented here includes the CO_2 emissions from kerosene and electricity production. Additionally, the work of *Zuijderwijk* [43] made use of more advanced battery systems with higher specific energy densities. On top of that, it makes use of hybrid-electric aircraft designs with more advanced technology which benefit from the increased synergy between propulsion system and airframe by using distributed propulsion. The results show the importance of assumed aircraft technology level and the benefit of fully making use of the aero-propulsive interactions of novel propulsion systems.

Table 11: Comparison of results hybrid-electric design case with *Zuijderwijk* [43]

	Results	**Results *Zuijderwijk***
Fleet size	6	7
Fleet diversity	6	5
Ownership cost	REF	+13%
Operating cost	REF	+3%
Profit	REF	-6%
Emissions	REF	-75%

3.4 Climate-Optimized hybrid fleet

Now that the final hybrid-electric aircraft fleet is known, the climate optimization model can be run. For each aircraft, the cruise altitude, velocity and power split will be varied in order to obtain operating conditions that

are minimizing the CO_2 emissions. First, the design space is explored using a LHS method. The altitude and velocity are varied between ±30% of the original aircraft parameters. The variation is bounded in order to limit the effects on the network model profit. Velocity has a direct effect on the operating cost, as it has an effect on the operational time. Both velocity and altitude have an indirect effect on profit through the operating costs, as these are dependent on the fuel and electricity costs required to perform a certain mission. In case more advanced fleet-and-network models would be used in which both horizontal and vertical routes are explored, altitude might also have a direct influence on network profit. The power split value in cruise is bounded between 0 and 0.5. During the LHS method, 100 points were tested and the feasible designs are those having a proper convergence, adhere to the aircraft design constraints and are able to perform the same missions as the original aircraft. The LHS method has narrowed down the large design space to a feasible design space. After this, a full factorial sampling method is applied in which the aircraft parameters are varied using a 6x6x6 parameter variation. To give the reader an idea about the computational time to perform the aircraft fleet design cycle and the climate optimization, a time-estimate for the full design run is provided in Table 18. This shows that optimizing one aircraft for climate takes about 1 hour and 20 minutes for the assumed amount of points tested in the design space exploration.

3.4.1 Result Fleet and Network Performance

The optimized aircraft are sized and the results can be seen in Table 20. A trend can be seen in the optimized aircraft operations. All aircraft are operated at lower altitudes and velocities. For aircraft with high passenger capacity and large ranges, the power split value remains practically unchanged. When lowering the capacity, the aircraft is less heavy and benefits from a larger degree of hybridization. The power split is highest when both the aircraft capacity and cruise range are small.

The aircraft are introduced in the fleet-and-network model, without altering the fleet allocation. The results on the network performance are once more summarized in Table 12. It can be seen that with respect to the non-optimized aircraft in the design case, the ownership cost remains unchanged as the same amount of respective aircraft types are used. There is a change in operating cost of +1%, of which the cause is twofold. A cost increase is expected as the operational time of the aircraft is increased due to the decreased cruise speed. However, this increase in cost is offset by a decrease in fuel and energy cost from optimizing the aircraft for minimal climate impact which implies minimizing the fuel and battery energy required. The emissions are decreased largely with -27%. Compared to the kerosene allocation, the total emissions can be reduced by -38% at the cost of a profit decrease of -14%.

3.4.2 Effect on Design Point

Part of the research goal was to investigate the effect of climate optimization on the aircraft design point (W/S and W/P). When the aircraft is optimized, the constraint line for the cruise speed in the power-loading diagram will be altered, which might affect the chosen design point. It was observed that all of the non-optimized aircraft were originally sized by the take-off length constraint and the stall speed constraint. As these constraint lines do not change for the optimized aircraft, there was no effect on the chosen design point. There was one exception: the *On_design* 7-1126-750 aircraft in the database. The non-optimized aircraft is sized by the cruise speed constraint, while the optimized aircraft is sized by the take-off length constraint. Therefore, this aircraft will be used to demonstrate the effects of climate optimization on the aircraft design point.

Figure 22 shows the aircraft power-loading diagram with the cruise speed constraint before optimization, after optimization (combined effect of Φ, V and h) and the effect of the individual parameters. One can see that on the aircraft-level, there is no effect of the power split value, as this simply changes the power ratio between battery and fuel. Therefore, this effect is more relevant to be discussed in the component-level power-loading diagrams. For the aircraft, lowering the cruise altitude only has an effect at larger wing-loading values, which increases the power-loading slightly. The lower cruise velocity has the largest effect and increases the power-loading value at all wing-loading values. This results in an increase of the feasible design space, with larger power-loading values when compared to the non-optimized aircraft. While the limiting constraint switches from cruise-speed (non-optimized) to take-off length (optimized), the value of the design point is changed only minimally. In case lower wing-loading values would be feasible, which can for example be attained by the use of distributed propulsion, more notable changes in the design point are expected.

To explain the effect of the power split value on the design point, the gas turbine power-loading diagram and electric motor power-loading diagram are depicted in Figure 23 and Figure 24 respectively. Increasing the power split value results in a higher degree of hybridization and such, the gas turbine requires less power, lowering the power-loading values. The opposite is true for the electric motor, which requires more power and therefore the power-loading is decreased. The effect on the electric motor is more pronounced as the magnitude of the power-loading value is about 8 times bigger. Even though the design point is not changed largely, the climate optimization has a large effect on the fuel and battery mass to perform a mission, as seen in Figure 35

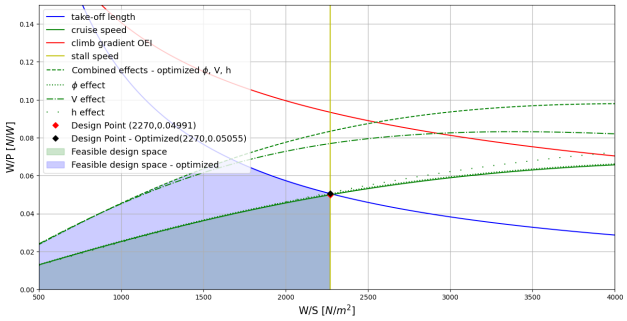

Figure 22: Climate-optimized aircraft-level power-loading diagram

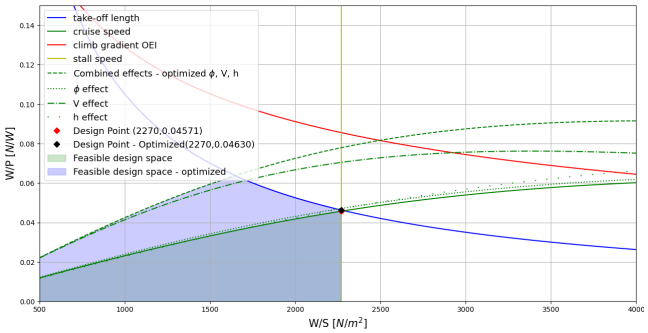

Figure 23: Climate-optimized Gas Turbine power-loading diagram

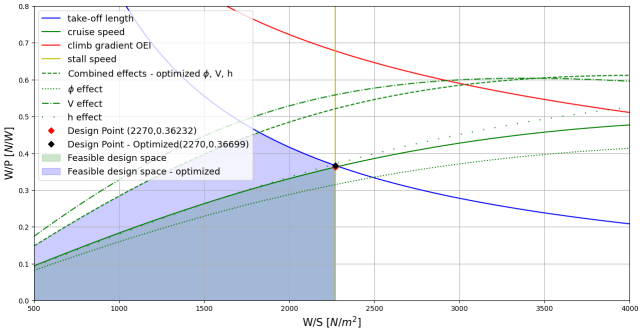

Figure 24: Climate-optimized Electric Motor power-loading diagram

4 Sensitivity Study

When replacing the original SATA Air Açores kerosene fleet with a newly designed hybrid-electric fleet, the network emissions are decreased but profit is increased. The emission reduction presented in this paper, is significantly lower than the one presented in *Zuijderwijk* [43]. This, amongst other reasons, comes from the difference in assumed battery technology level. For this reason, a sensitivity study is performed in which the battery specific energy value is changed from 500 Wh/kg for the design case, to 700 and 1000 Wh/kg in the sensitivity study. The results are visualized in Figure 25, which shows the total network emissions versus profit value for the different design cases. The figure also shows the cases discussed before: A. Kerosene fleet (section 3.1), B. Initial Hybrid-electric fleet (section 3.2), C. Designed hybrid-electric fleet (section 3.3) and D. Climate-Optimized hybrid-electric fleet (section 3.4). Increasing the battery specific energy from 500 Wh/kg to 700 Wh/kg and to 1000 Wh/kg, has a beneficial effect on the profit and the network emissions. The effect on the emissions is larger than the effect on airline profit. However, in terms of profit, the kerosene fleet remains the most attractive for the airline. In terms of emissions, the largest emission decrease is still achieved by a climate optimization. Figure 25 also shows the fleet diversity and the amount of aircraft needed from a certain type. The final fleet composition is color coded and are in-line with the colors in Figures 42b and 42c, which show the fleet composition for each design run. It can be observed that by changing the battery technology level, there is only a limited effect on the final fleet composition.

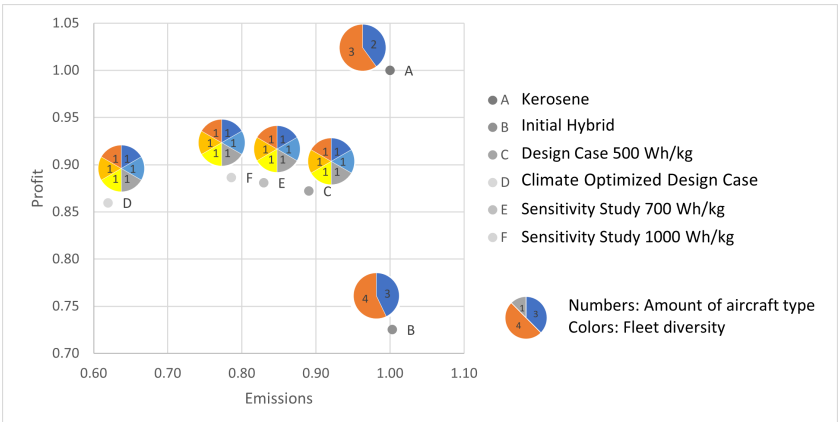

Figure 25: Network profit and emissions for technology level sensitivity study

The decrease in emissions with respect to the kerosene fleet is not only coming from the fact that the aircraft are operated in a hybrid fashion but can also be attributed to an increase in fleet diversity. Therefore, a sensitivity study is performed in which the fleet diversity is fixed, but all aircraft can be operated at unlimited amount of off-design configurations (trade payload for increased range or reduced runway length). The results are shown in Figure 26. When limiting the fleet diversity to 2 types of aircraft in a newly designed hybrid-electric aircraft fleet (G), it is possible to increase the airline profit with respect to the initial hybrid-electric fleet consisting of 2 aircraft (B), however at the cost of slightly increased emissions. When increasing the fleet diversity to 3, 4 and $infinite$, profit is increasing and emissions are decreasing. Again, in terms of profit, the most attractive fleet is still the original kerosene fleet and for emissions, the climate-optimized fleet. Figure 26 also shows the fleet diversity and size, color coded similarly to the fleet compositions in the redesign cycles of Figures 42d, 42e and 42f. It can be observed that when only 2 aircraft types are allowed, the aircraft will be performing at both on- and off-design conditions. Aircraft operating at an on-design condition can take more passengers, but sometimes it is required to operate off-design in order to lower the required runway length and be able to operate from more airports. When the fleet diversity is increased more than 2, none of the aircraft will trade passengers for a decreased runway length, as the new aircraft are particularly designed to take as much passengers as possible, while still enabling taking off from smaller runways. Loosening the maximum fleet diversity constraint will also result in more different aircraft types as the aircraft can be allocated more efficiently. If there is no limit on the maximum fleet diversity, a total of 6 different aircraft is chosen to operate in the network.

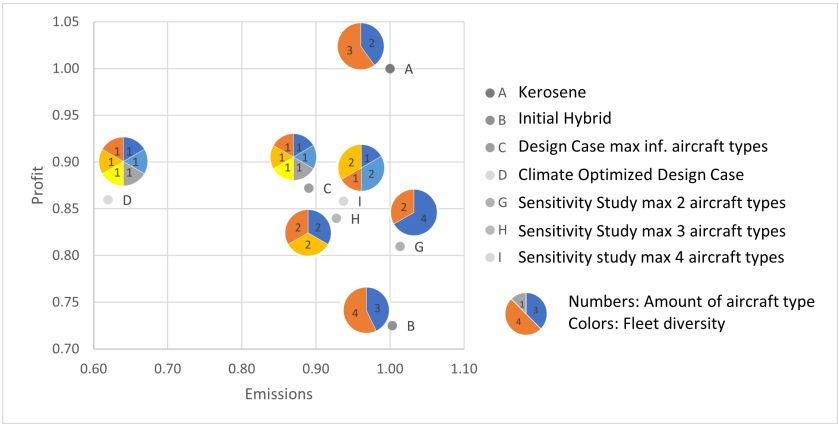

Figure 26: Network profit and emissions for maximum fleet diversity sensitivity study

5 Conclusions

The goal of this research was to develop a methodology for the design of a climate-optimized hybrid-electric regional aircraft fleet, by integrating hybrid-electric aircraft design with strategic airline planning while examining the climate-optimal design point. For this, two important trade-offs were considered: payload can be exchanged for extended aircraft range or reduced runway length. Information on the fleet allocation guides the design process of new hybrid-electric aircraft that better fit the network operations. In order to reduce the total network CO_2 emissions, the operations of the aircraft in the final fleet are modified as part of a climate optimization study. The designed methodology is tested by performing the fleet-and-network allocation for SATA Air Açores airline. Multiple case studies are conducted to provide answers to the research question:

"What is the impact of considering airline fleet-and-network allocation integrated with hybrid-electric aircraft design and climate optimization, in terms of airline profitability, expected climate impact and optimal aircraft design?".

An overview of the results of the case studies in terms of airline costs, profit, total network emissions and fleet composition is provided in Table 12.

Table 12: Overview of network performance for all case studies

Case Description	Operating cost	Ownership cost	Revenue	Profit	Emissions	Fleet size	Fleet diversity
A. Kerosene	ref	ref	ref	ref	ref	5	2
B. Initial hybrid	+16%	+42%	-1%	-27%	+0%	7	2
C. Design Case no max diversity, 500 Wh/kg	+8%	+10%	-3%	-13%	-11%	6	6
D. Climate optimized design case	+9%	+10%	-3%	-14%	-38%	6	6
E. Sensitivity study - technology no max diversity, 700 Wh/kg	+7%	+10%	-3%	-12%	-17%	6	6
F. Sensitivity study - technology no max diversity, 1000 Wh/kg	+7%	+10%	-3%	-11%	-21%	6	6
G. Sensitivity study - diversity 2 max diversity, 500 Wh/kg	+13%	+18%	-0%	-19%	+1%	6	2
H. Sensitivity study - diversity 3 max diversity, 500 Wh/kg	+11%	+12%	-2%	-16%	-7%	6	3
I. Sensitivity study - diversity 4 max diversity, 500 Wh/kg	+9%	+12%	-3%	-14%	-6%	6	4

Replacing the current kerosene fleet with a hybrid-electric fleet has a negative effect on the airline costs and profit in all cases. Even though the aircraft cost estimations for hybrid-electric aircraft and kerosene aircraft are based on the same linear relationships with respect to aircraft seats, the airline costs are increased when operating hybrid-electric aircraft. This is mainly due to the increased operating time of hybrid-electric aircraft as the turnaround time now also includes the time required to swap the battery. The effect of increased turnaround time is twofold: first it causes an increase in the operating cost, secondly it requires the fleet to operate with an increased amount of aircraft to perform the network operations. The increase in fleet size in its turn largely increases the ownership costs. Furthermore, the hybrid-electric alternatives have an increased aircraft weight. In order to take-off/land from the same runway length, the aircraft can take less payload thus increases the flight frequency of the aircraft to achieve the same passenger demand. Having to fly more often also negatively influences the aircraft costs. This leads to the fact that in terms of airline profitability, operating the kerosene fleet is the most profitable option for the airline.

The design case (case C.) however demonstrates the potential to decrease the network emissions with respect to the current kerosene fleet by -11% when the hybrid-electric fleet is designed particularly for the specified network. Apart from operating the aircraft in a hybrid fashion, the decrease in emissions can be attributed to the higher fleet diversity. With a more diverse fleet, airlines can assign aircraft that are a better fit for specific routes, resulting in lower total emissions. For example, limiting the aircraft fleet diversity to 3 types (case H.) results in only -7% emissions decrease with respect to the kerosene fleet.

Furthermore, battery technology levels have a notable effect on the total network emissions. Increasing the battery specific energy shows an expected beneficial effect on emissions. Higher battery specific energies result in less heavy batteries, this has an effect on the amount of fuel and battery energy required and such directly influences the emissions. When changing the battery specific energy from 500 Wh/kg in the design case (C.), to 1000 Wh/kg (F.), the emissions can be decreased with -21% with respect to the kerosene reference.

The largest emission decrease is obtained using a climate optimization of the final hybrid-electric aircraft fleet (case D.). Emissions can be reduced with -38% with respect to the kerosene fleet, which is more than the reductions obtained by changing the aircraft payload-range-runway combinations and re-allocation of the aircraft.

6 Discussion and Recommendations

Previous work by *Zuijderwijk* [43], which makes use of the same fleet-and-network allocation model, showed a much higher decrease in emissions when replacing the kerosene fleet with a hybrid-electric fleet. This work makes use of advanced hybrid-electric aircraft designs with more advanced technology levels. This shows the importance of fully making use of the benefit from the aero-propulsive interactions of novel propulsion systems

by inclusion of distributed propulsion. It is therefore recommended to extend the hybrid-electric aircraft design tool with these advanced propulsion systems to better evaluate the possibilities of hybrid-electric aircraft for reducing the climate impact.

Additionally, the results of this study highlight the importance of altering the aircraft operational parameters (such as cruise altitude, velocity and power split) in a climate optimization study. The climate optimization module is currently limited by the conceptual design nature of the hybrid-electric aircraft design tool. The tool is able to conceptually design and size aircraft, but does not entirely capture the effects of operating conditions, such as altitude and velocity effects. The hybrid-electric aircraft design module would benefit from a more detailed mission analysis, including a numerical calculation scheme in which the flight mechanics states are calculated using a time-stepping approach. Also a detailed turboprop parameter performance analysis would be suggested to better estimate specific fuel consumption values, thrust and power in cruise and take-off conditions, engine parameters and efficiencies. With the use of a propeller engine performance analysis and an aircraft design mission analysis, it would be possible to more accurately capture the effects of climate-optimized aircraft design and evaluate other relevant emissions such as NO_X, H_2O and soot.

Furthermore, the climate optimization is currently performed outside of the hybrid-electric fleet design loop. For future work it is recommended to integrate the climate optimization with fleet design to directly include the effects of aircraft parameters on fleet-and-network allocation and network performance (operating times, costs, profit, etc.). It would be possible to do this with a gradient-based optimization algorithm, however, as many aircraft designs are evaluated in each design loop, this could become too computationally expensive. Alternatives would be to investigate whether it is possible to include some sort of climate surrogate model to predict the climate optimization outcomes. The author of this paper is not familiar with surrogate modelling and can therefore not guide in further recommendations for integrating these models in the current coupling strategy. Or else, one could make use of a design logic to define the aircraft parameters related to climate impact minimization. In the work presented, design logics are outlined to couple aircraft design and fleet-and-network allocation directly for range, passenger capacity and runway length. Similarly, the climate optimization and aircraft design could be coupled. One can for example look at possible ways to ensure the aircraft is operated at well-suited aerodynamic and operational conditions that minimize the fuel burn, as fuel burn plays an important role for the total CO_2 emissions.

Lastly, a recommendation is made for the aircraft passenger trade-off configurations. Currently, the network model receives possible aircraft configurations which trade passengers for increased range or reduced runway length, in steps of 10 passengers. These discrete aircraft configurations are gathered in a large database and fed to the model, meaning the current methodology is limiting flexibility for payload trade-offs. A recommendation would be to directly integrate the payload-range and payload-runway trade-off in the network model to enable investigating trade-off with smaller passenger steps. A direct integration is possible as the payload-range and payload-runway trade-offs have a linear relation, which is required by the linear programming model used in the network model.

References

[1] N. Aeronautics. Nasa aeronautics: Strategic implementation plan: 2019 update, 2019.

[2] N. E. Antoine and I. M. Kroo. Framework for aircraft conceptual design and environmental performance studies. *AIAA journal*, 43(10):2100–2109, 2005.

[3] A. P. R. E. Association. Renewable electricity in the portuguese energy system until 2050. Technical report, Technical report, 2018.

[4] Bombardier. Fuel efficiency manual q400 nextgen. Technical report, 2013.

[5] G. Bower and I. Kroo. Multi-objective aircraft optimization for minimum cost and emissions over specific route networks. In *The 26th Congress of ICAS and 8th AIAA ATIO*, page 8905, 2008.

[6] E. Commission, D.-G. for Mobility, Transport, D.-G. for Research, and Innovation. *Flightpath 2050 : Europes vision for aviation : maintaining global leadership and serving societys needs*. Publications Office, 2011.

[7] W. Crossley, M. Mane, and A. Nusawardhana. Variable resource allocation using multidisciplinary optimization: Initial investigations for system of systems. In *10th AIAA/ISSMO multidisciplinary analysis and optimization conference*, page 4605, 2004.

[8] N. Davendralingam and W. Crossley. Robust approach for concurrent aircraft design and airline network design. *Journal of Aircraft*, 51(6):1773–1783, 2014.

[9] R. de Vries. Hybrid-electric aircraft with over-the-wing distributed propulsion: Aerodynamic performance and conceptual design. 2022.

[10] R. De Vries, M. F. Hoogreef, and R. Vos. Range equation for hybrid-electric aircraft with constant power split. *Journal of Aircraft*, 57(3):552–557, 2020.

[11] D. F. Finger. *Methodology for multidisciplinary aircraft design under consideration of hybrid-electric propulsion technology*. PhD thesis, RMIT University, 2020.

[12] D. F. Finger, R. de Vries, R. Vos, C. Braun, and C. Bil. A comparison of hybrid-electric aircraft sizing methods. In *AIAA Scitech 2020 Forum*, page 1006, 2020.

[13] P. Govindaraju and W. A. Crossley. Profit motivated airline fleet allocation and concurrent aircraft design for multiple airlines. In *2013 Aviation Technology, Integration, and Operations Conference*, page 4391, 2013.

[14] P. Govindaraju, N. Davendralingam, and W. A. Crossley. A concurrent aircraft design and fleet assignment approach to mitigate environmental impact through fuel burn reduction under operational uncertainty. *Journal of Aerospace Operations*, 4(4):163–184, 2017.

[15] P. Jansen and R. Perez. Coupled optimization of aircraft family design and fleet assignment for minimum cost and fuel burn. In *12th AIAA Aviation Technology, Integration, and Operations (ATIO) Conference and 14th AIAA/ISSMO Multidisciplinary Analysis and Optimization Conference*, page 5495, 2012.

[16] P. W. Jansen and R. E. Perez. Coupled optimization of aircraft design and fleet allocation with uncertain passenger demand. In *2013 Aviation Technology, Integration, and Operations Conference*, page 4392, 2013.

[17] P. W. Jansen and R. E. Perez. Robust coupled optimization of aircraft design and fleet allocation for multiple markets. In *AIAA/3AF Aircraft Noise and Emissions Reduction Symposium*, page 2735, 2014.

[18] P. W. Jansen and R. E. Perez. Coupled optimization of aircraft families and fleet allocation for multiple markets. *Journal of Aircraft*, 53(5):1485–1504, 2016.

[19] N. Lutsey and D. Hall. Effects of battery manufacturing on electric vehicle life-cycle greenhouse gas emissions, 02 2018.

[20] M. Mane and W. Crossley. Concurrent aircraft design and resource allocation under uncertainty for on-demand air transportation. In *The 26th Congress of ICAS and 8th AIAA ATIO*, page 8903, 2008.

[21] M. Mane and W. Crossley. Concurrent aircraft design and trip assignment under uncertainty: Fractional operations. In *9th AIAA Aviation Technology, Integration, and Operations Conference (ATIO) and Aircraft Noise and Emissions Reduction Symposium (ANERS)*, page 7007, 2009.

[22] M. Mane and W. A. Crossley. Allocation and design of aircraft for on-demand air transportation with uncertain operations. *Journal of aircraft*, 49(1):141–150, 2012.

[23] M. Mane, W. A. Crossley, and Nusawardhana. System-of-systems inspired aircraft sizing and airline resource allocation via decomposition. *Journal of aircraft*, 44(4):1222–1235, 2007.

[24] E. Obert. Drag polars of nineteen jet transport aircraft at mach numbers m= 0.40-0.60 (unpublished). Technical report, Technical report, 2013.

[25] C. Pornet, C. Gologan, P. C. Vratny, A. Seitz, O. Schmitz, A. T. Isikveren, and M. Hornung. Methodology for sizing and performance assessment of hybrid energy aircraft. *Journal of Aircraft*, 52(1):341–352, 2015.

[26] C. Pornet and A. T. Isikveren. Conceptual design of hybrid-electric transport aircraft. *Progress in Aerospace Sciences*, 79:114–135, 2015.

[27] P.-J. Proesmans and R. Vos. Airplane design optimization for minimal global warming impact. In *AIAA Scitech 2021 Forum*, page 1297, 2021.

[28] D. Raymer. *Aircraft design: a conceptual approach*. American Institute of Aeronautics and Astronautics, Inc., 2012.

[29] J. Roskam. *Airplane design*. DARcorporation, 1985.

[30] S. Roy, W. A. Crossley, K. T. Moore, J. S. Gray, and J. R. Martins. Next generation aircraft design considering airline operations and economics. In *2018 AIAA/ASCE/AHS/ASC Structures, Structural Dynamics, and Materials Conference*, page 1647, 2018.

[31] S. Sahoo, X. Zhao, and K. Kyprianidis. A review of concepts, benefits, and challenges for future electrical propulsion-based aircraft. *Aerospace*, 7(4):44, 2020.

[32] A. E. Scholz, J. Michelmann, and M. Hornung. Design, operational and environmental assessment of a hybrid-electric aircraft. In *AIAA Scitech 2021 Forum*, page 0259, 2021.

[33] C. Taylor and O. L. De Weck. Coupled vehicle design and network flow optimization for air transportation systems. *Journal of Aircraft*, 44(5):1479–1486, 2007.

[34] Y. Teeuwen. Propeller design for conceptual turboprop aircraft. 2017.

[35] R. Thijssen. Propeller aircraft design optimization for reduced climate impact. 2022.

[36] E. Torenbeek. *Synthesis of subsonic airplane design: an introduction to the preliminary design of subsonic general aviation and transport aircraft, with emphasis on layout, aerodynamic design, propulsion and performance*. Springer Science & Business Media, 2013.

[37] Transport Canada. *Type Certificate Data Sheet - PW150A*, 08 2000. Issue No. 3.

[38] J. Van Bogaert. Assessment of potential fuel saving benefits of hybrid-electric regional aircraft. 2015.

[39] R. Vos, A. Wortmann, and R. Elmendorp. The optimal cruise altitude of lng-fuelled turbofan aircraft. *Journal of Aerospace Operations*, 4(4):207–222, 2017.

[40] M. Voskuijl, J. Van Bogaert, and A. G. Rao. Analysis and design of hybrid electric regional turboprop aircraft. *CEAS Aeronautical Journal*, 9(1):15–25, 2018.

[41] F. Yin, V. Grewe, and K. Gierens. Impact of hybrid-electric aircraft on contrail coverage. *Aerospace*, 7(10):147, 2020.

[42] J. Zamboni, R. Vos, M. Emeneth, and A. Schneegans. A method for the conceptual design of hybrid electric aircraft. In *AIAA Scitech 2019 Forum*, page 1587, 2019.

[43] N. Zuijderwijk. Study to the adaptation of electrified aircraft by regional airliner. 2022.

Appendices

A Hybrid-Electric Powertrain matrix

Equation 19 shows the powertrain matrix described by *De Vries* [9]. It is used to obtain the power requirements for the different components in the hybrid-electric powertrain in case both the gas turbine and battery are providing power to the propeller.

$$\begin{bmatrix} -\eta_{GT} & 1 & 0 & 0 & 0 & 0 & 0 & 0 & 0 & 0 \\ 0 & -\eta_{GB} & 1 & 1 & 0 & 0 & 0 & 0 & 0 & 0 \\ 0 & 0 & 0 & -\eta_{P1} & 0 & 0 & 0 & 0 & 1 & 0 \\ 0 & 0 & -\eta_{EM1} & 0 & 1 & 0 & 0 & 0 & 0 & 0 \\ 0 & 0 & 0 & 0 & -\eta_{PMAD} & -\eta_{PMAD} & 1 & 0 & 0 & 0 \\ 0 & 0 & 0 & 0 & 0 & 0 & -\eta_{EM2} & 1 & 0 & 0 \\ 0 & 0 & 0 & 0 & 0 & 0 & 0 & -\eta_{P2} & 0 & 1 \\ \Phi & 0 & 0 & 0 & 0 & (\Phi - 1) & 0 & 0 & 0 & 0 \\ 0 & 0 & 0 & \phi & 0 & 0 & 0 & (\phi - 1) & 0 & 0 \\ 0 & 0 & 0 & 0 & 0 & 0 & 0 & 0 & 1 & 1 \end{bmatrix} \begin{bmatrix} P_f \\ P_{gt} \\ P_{gb} \\ P_{s1} \\ P_{e1} \\ P_{bat} \\ P_{e2} \\ P_{s2} \\ P_{p1} \\ P_{p2} \end{bmatrix} = \begin{bmatrix} 0 \\ 0 \\ 0 \\ 0 \\ 0 \\ 0 \\ 0 \\ 0 \\ 0 \\ P_p \end{bmatrix} \tag{19}$$

B Kerosene Fleet

Table 13 shows the design results of the kerosene Q400 and Q200 aircraft, together with the off-design aircraft configurations.

Table 13: Kerosene Q400 and Q200 design results

Aircraft name: Q400	**Seats [-]**	**Cruise Range [km]**	**Total Range [km]**	**Speed [km/h]**	**Altitude [m]**	**Runway length [m]**	**Φ cruise [-]**	**max_ energy [kWh]**	**max_ fuel [kg]**	**energy_ stop [kWh]**	**energy_ km [kWh/km]**	**fuel_ stop [kg]**	**fuel_ km [kg/km]**
On_design-80-1135-1300	80	926	1135	655.2	7010.4	1300	0	0	2056	0	0	703	1.46
Off_design-70-1932-1301	70	1723	1932	655.2	7010.4	1301	0	0	3160	0	0	690	1.43
Off_design-60-2633-1293	60	2424	2633	655.2	7010.4	1293	0	0	4083	0	0	679	1.40
Off_design-50-2732-1248	50	2523	2732	655.2	7010.4	1248	0	0	4083	0	0	679	1.35
Off_design-40-2831-1203	40	2622	2831	655.2	7010.4	1203	0	0	4083	0	0	679	1.30
Off_design-30-2930-1158	30	2721	2930	655.2	7010.4	1158	0	0	4083	0	0	679	1.25
Off_design-20-3029-1113	20	2820	3029	655.2	7010.4	1113	0	0	4083	0	0	679	1.21
Off_design-10-3129-1067	10	2920	3129	655.2	7010.4	1067	0	0	4083	0	0	679	1.17
Off_design-70-1135-1252	70	926	1135	655.2	7010.4	1252	0	0	2003	0	0	679	1.43
Off_design-60-1135-1203	60	926	1135	655.2	7010.4	1203	0	0	1954	0	0	652	1.41
Off_design-50-1135-1154	50	926	1135	655.2	7010.4	1154	0	0	1905	0	0	625	1.38
Off_design-40-1135-1105	40	926	1135	655.2	7010.4	1105	0	0	1856	0	0	598	1.36
Off_design-30-1135-1056	30	926	1135	655.2	7010.4	1056	0	0	1808	0	0	571	1.34
Off_design-20-1135-1007	20	926	1135	655.2	7010.4	1007	0	0	1759	0	0	544	1.31
Off_design-10-1135-957	10	926	1135	655.2	7010.4	957	0	0	1709	0	0	517	1.29
Aircraft name: Q200	**Seats [-]**	**Cruise Range [km]**	**Total Range [km]**	**Speed [km/h]**	**Altitude [m]**	**Runway length [m]**	**Φ cruise [-]**	**max_ energy [kWh]**	**max_ fuel [kg]**	**energy_ stop [kWh]**	**energy_ km [kWh/km]**	**fuel_ stop [kg]**	**fuel_ km [kg/km]**
On_design-37-1246-1000	37	1020	1246	540	7600	1000	0	0	1105	0	0	384	0.71
Off_design-27-2441-952	27	2215	2441	540	7600	952	0	0	1857	0	0	374	0.67
Off_design-17-2644-819	17	2418	2644	540	7600	819	0	0	1857	0	0	374	0.61
Off_design-7-2847-744	7	2621	2847	540	7600	744	0	0	1857	0	0	374	0.57
Off_design-27-1246-855	27	1020	1246	540	7600	855	0	0	1047	0	0	355	0.68
Off_design-17-1246-755	17	1020	1246	540	7600	755	0	0	990	0	0	326	0.65
Off_design-7-1246-688	7	1020	1246	540	7600	688	0	0	936	0	0	297	0.63

C Initial Hybrid Fleet

All hybrid-electric aircraft are designed with powertrain component properties for the 2035 timeframe. The values for state-of-the art battery, electric motor and converter performance are taken from *De Vries* [9] and summarized in Table 14.

Table 14: Powertrain component properties (partly from *De Vries* [9])

Parameter	**Symbol**	**Value**
Battery specific energy at pack level	e_{bat}	500 Wh/kg
Battery specific power at pack level	SP_{bat}	1 000 W/kg
Battery specific density at pack level	ρ_{bat}	1 000 Wh/l
Battery State-of-Charge margin	SOC	20%
Electric motor specific power	SP_{EM}	13 000 W/kg
Converters specific power	$SP_{convert}$	19 000 W/kg
PMAD weight penalty	/	30%
Equivalent Electric Motor specific power	$SP_{EM,eq}$	5940 W/kg
Gas turbine efficiency	η_{GT}	40%
Power management and distribution box efficiency	η_{PMAD}	99%
Gearbox efficiency	η_{GB}	96%
Propeller efficiency	η_P	85%
Battery efficiency	η_{BAT}	100%
Degree of Hybridization- power split in all mission phases	$DOH - \Phi$	10% - 0.0485
Gas turbine throttle in all mission phases	ξ_{GT}	100%

The hybrid-electric $HE\ Q400$ and $HE\ Q200$ aircraft are designed with the top-level aircraft requirements listed in Table 15. The initial hybrid-electric aircraft fleet sizing results are shown in Table 16.

Table 15: TLAR for $HE\ Q400$ and $HE\ Q200$

Parameter	**HE Q400**	**HE Q200**
Capacity		
Passengers [-]	80	37
Mass per passenger [kg][1]	110	110
Design Mission		
Cruise range [km]	900	1000
Cruise altitude [m]	7010.4	7600
Cruise velocity [m/s]	182	150
Diversion range [km][1]	185.2	185.2
Diversion altitude [m][1]	1524	1524
Diversion velocity [m/s]	182	150
Loiter time [s][1]	2700	2700
Loiter altitude [m][1]	457.2	457.2
Mission hybrid power control parameters		
Supplied power split (all phases) [-][1]	0.0485	0.0485
Shaft power split (all phases) [-][1]	0	0
Turbine Throttle (all phases) [-][1]	1	1
Aircraft configuration/geometry		
Undercarriage configuration[1]	In nacelle	In nacelle
Wing configuration[1]	High wing	High wing
Horizontal tail configuration[1]	T-tail	T-tail
Aspect ratio[1]	12.5	12.5
Loading requirements		
Cruise speed requirement: velocity [m/s] Cruise speed requirement: altitude [m]	182 7010.4	150 7600
Stall speed requirement: velocity [m/s]	47	41
Take-off length requirement: distance [m]	1300	1000
Climb gradient OEI [%][1]	2.4	2.4

[1]Parameter the same for all hybrid-electric aircraft.

Table 16: Hybrid-electric $HE\ Q400$ and $HE\ Q200$ design results

Aircraft name: HE Q400	**Seats [-]**	**Cruise Range [km]**	**Total Range [km]**	**Speed [km/h]**	**Altitude [m]**	**Runway length [m]**	**Φ cruise [-]**	**max_ energy [kWh]**	**max_ fuel [kg]**	**energy_ stop [kWh]**	**energy_ km [kWh/km]**	**fuel_ stop [kg]**	**fuel_ km [kg/km]**
On_design-80-1109-1300	80	900	1109	655.2	7010.4	1300	0.0485	1361	1869	527	0.93	724	1.27
Off_design-70-1483-1258	70	1274	1483	655.2	7010.4	1258	0.0485	1361	2359	527	0.65	708	1.30
Off_design-60-1852-1216	60	1643	1852	655.2	7010.4	1216	0.0485	1361	2848	527	0.51	691	1.31
Off_design-50-2220-1175	50	2011	2220	655.2	7010.4	1175	0.0485	1361	3337	527	0.41	674	1.32
Off_design-40-2589-1134	40	2380	2589	655.2	7010.4	1134	0.0485	1361	3827	527	0.35	658	1.33
Off_design-30-2958-1094	30	2749	2958	655.2	7010.4	1094	0.0485	1361	4317	527	0.30	641	1.34
Off_design-20-3327-1054	20	3118	3327	655.2	7010.4	1054	0.0485	1361	4807	527	0.27	624	1.34
Off_design-10-3695-1023	10	3486	3695	655.2	7010.4	1023	0.0485	1361	5295	527	0.24	608	1.34
Off_design-70-1109-1224	70	900	1109	655.2	7010.4	1224	0.0485	1361	1830	527	0.93	704	1.25
Off_design-60-1109-1150	60	900	1109	655.2	7010.4	1150	0.0485	1361	1792	527	0.93	682	1.23
Off_design-50-1109-1075	50	900	1109	655.2	7010.4	1075	0.0485	1361	1753	527	0.93	660	1.21
Off_design-40-1109-1018	40	900	1109	655.2	7010.4	1018	0.0485	1361	1715	527	0.93	638	1.20
Off_design-30-1109-983	30	900	1109	655.2	7010.4	983	0.0485	1361	1676	527	0.93	616	1.18
Off_design-20-1109-949	20	900	1109	655.2	7010.4	949	0.0485	1361	1639	527	0.93	595	1.16
Off_design-10-1109-914	10	900	1109	655.2	7010.4	914	0.0485	1361	1600	527	0.93	573	1.14
Aircraft name: HE Q200	**Seats [-]**	**Cruise Range [km]**	**Total Range [km]**	**Speed [km/h]**	**Altitude [m]**	**Runway length [m]**	**Φ cruise [-]**	**max_ energy [kWh]**	**max_ fuel [kg]**	**energy_ stop [kWh]**	**energy_ km [kWh/km]**	**fuel_ stop [kg]**	**fuel_ km [kg/km]**
On_design-37-1226-1000	37	1000	1226	540	7600	1000	0.0485	692	950	272	0.42	374	0.58
Off_design-27-2053-938	27	1827	2053	540	7600	938	0.0485	692	1439	272	0.23	357	0.59
Off_design-17-2884-875	17	2658	2884	540	7600	875	0.0485	692	1929	272	0.16	340	0.60
Off_design-7-3714-814	7	3488	3714	540	7600	814	0.0485	692	2418	272	0.12	323	0.60
Off_design-27-1226-887	27	1000	1226	540	7600	887	0.0485	692	908	272	0.42	353	0.56
Off_design-17-1226-784	17	1000	1226	540	7600	784	0.0485	692	865	272	0.42	330	0.54
Off_design-7-1226-731	7	1000	1226	540	7600	731	0.0485	692	824	272	0.42	308	0.52

D Allocation Kerosene Fleet (left) and Initial Hybrid Fleet (right)

Figures 27 to 34 show the fleet allocation in the SATA Air Açores airline network for the kerosene fleet of the reference case study (current situation) and the initial hybrid fleet where the kerosene fleet is replaced with hybrid-electric alternatives without a redesign of the fleet.

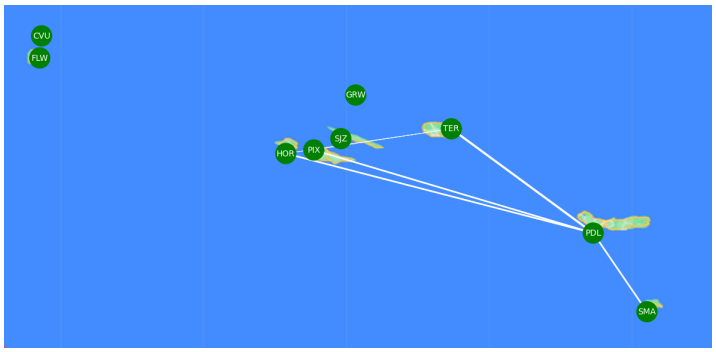

Figure 27: *Q*400 *On_design* 80-1135-1300
min 97 km, max 278 km

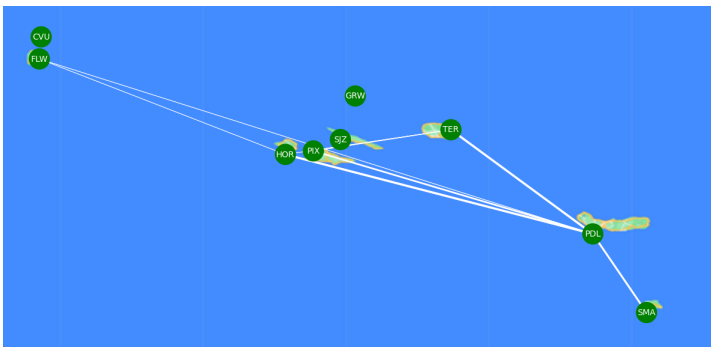

Figure 28: *HE Q*400 *On_design* 80-1109-1300
min 97 km, max 744 km

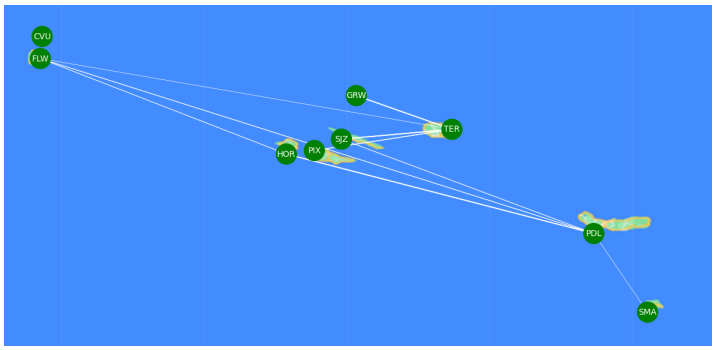

Figure 29: *Q*400 *Off_design* 70-1135-1252
min 97 km, max 868 km

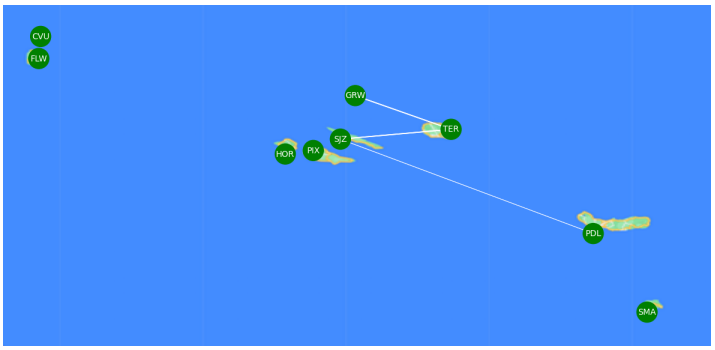

Figure 30: *HE Q*400 *Off_design* 70-1483-1258
min 178 km, max 234 km

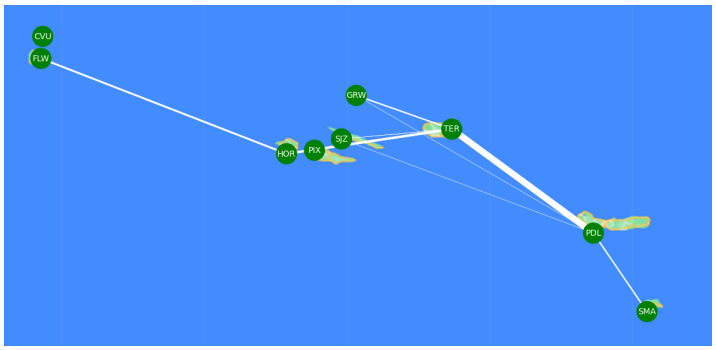

Figure 31: *Q*200 *On_design* 37-1246-1000
min 97 km, max 468 km

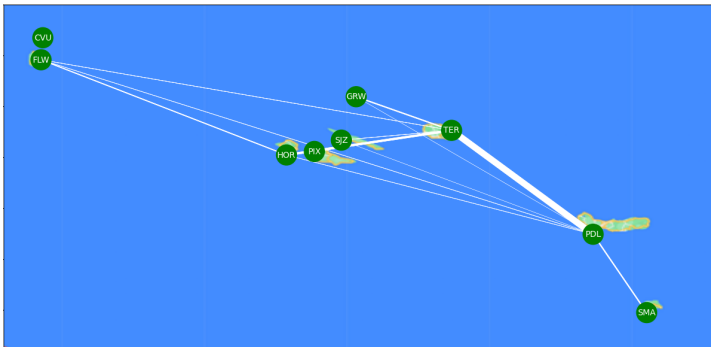

Figure 32: *HE Q*200 *On_design* 37-1226-1000
min 97 km, max 744 km

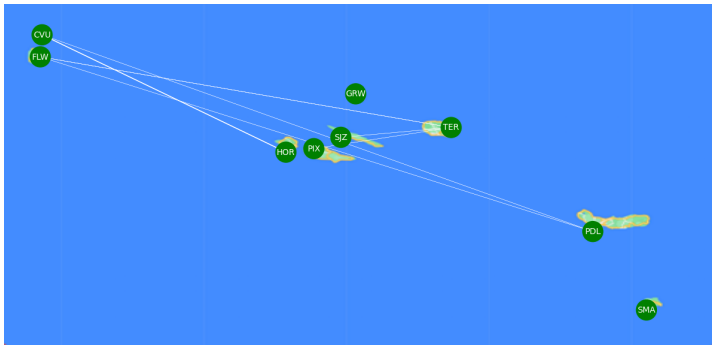

Figure 33: *Q*200 *Off_design* 17-1246-755
min 120 km, max 868 km

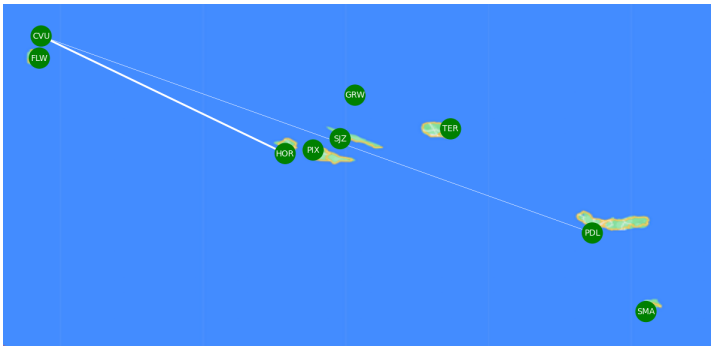

Figure 34: *HE Q*200 *Off_design* 7-1226-731, min 488
km, max 762 km

E Final Hybrid Fleet and Climate Optimization

Table 17 shows an example of the database evolution after each design run. The example presents the database for the design case in section 3.3, consisting of three runs. This table is complementary to the redesign cycle schematic of Figure 21.

- For run 0, the database consists of two different aircraft types: $HE\ Q400$ and $HE\ Q200$. The $HE\ Q400$ aircraft includes its on-design configuration and 14 off-design configurations. The $HE\ Q200$ aircraft includes its on-design configuration and 6 off-design configurations. This results in a total database length of 22 aircraft configurations. The chosen configurations to operate in the network are marked in the respective colors of Figure 21.
- The database of the second run consists of all the chosen aircraft from the previous run. From each chosen configuration of the previous run, several new redesign aircraft are made and denoted with an additional term R_1. These aircraft are added to the database and shown with a *'+'*. There are now a total of 18 different aircraft types in the database, operated at a total of 156 different configurations. Again, the chosen aircraft in this fleet-allocation run are marked with the respective colors of Figure 21.
- In the third run, the chosen aircraft from the previous two runs are kept in the database. These consist of the initial aircraft and the first redesign aircraft R_1. The aircraft that are not used are removed and denoted with a *'-'*. Some aircraft go through a second redesign cycle and are shown with an additional R_2 term. Also these aircraft are added to the database with a *'+'*. The database now includes 26 aircraft types, at 206 aircraft configurations. There were no new aircraft chosen in a third fleet allocation run and therefore the fleet in run 2 is the final optimized fleet and the chosen aircraft are color coded similarly to Figure 21.

Table 17: Example of database evolution for the hybrid-electric fleet design case

Run 0: Database		**Run 1: Database**		**Run 2: Database**
Total aircraft types: 2		**Total aircraft types: 18**		**Total aircraft types: 26**
Total aircraft configs: 22		**Total aircraft configs: 156**		**Total aircraft configs: 206**
*HE Q*400		*HE Q*400		*HE Q*400
80-1109-1300 + 14 **off-design**		**80-1109-1300** + 14 off-design		**80-1109-1300** + 14 off-design
*HE Q*200		*HE Q*200		
37-1226-1000 + 6 **off-design**		37-1226-1000 + 6 off-design	-	
		R_1 *HE* $Q400_{on}$		R_1 *HE* $Q400_{on}$
	+	80-309-1550 + 14 off-design		80-309-1550 + 14 off-design
	+	90-309-1550 + 16 off-design		90-309-1550 + 16 off-design
	+	80-1209-1300 + 14 off-design		80-1209-1300 + 14 off-design
		R_1 *HE* $Q400_{off}$		R_1 *HE* $Q400_{off}$
	+	**70-809-1250** + 12 off-design		**70-809-1250** + 12 off-design
		R_1 *HE* $Q200_{on}$		R_1 *HE* $Q200_{on}$
	+	37-326-1550 + 6 off-design	-	
	+	**37-1026-1250** + 6 off-design		37-1026-1250 + 6 off-design
	+	37-1226-1300 + 6 off-design	-	
	+	47-326-1550 + 8 off-design	-	
	+	47-1026-1250 + 8 off-design	-	
	+	47-1226-1300 + 8 off-design	-	
	+	37-1226-1300 + 8 off-design	-	
	+	47-1326-1300 + 8 off-design	-	
		R_1 *HE* $Q200_{off}$		R_1 *HE* $Q200_{off}$
	+	7-926-750	-	
	+	**7-1226-750**		7-1226-750
	+	**17-926-750** + 2 off-design		17-926-750 + 2 off-design
	+	17-1326-750 + 2 -off design	-	
				R_2 *HE* $Q400_{off}$
			+	**70-309-1550** + 12 off-design
			+	80-809-1250 + 14 off-design
			+	70-909-1250 + 12 off-design
			+	80-909-1250 + 14 off-design
				R_2 *HE* $Q200_{on}$
			+	37-326-1550 + 6 off-design
			+	37-1026-1250 + 6 off-design
			+	47-326-1550 + 8 off-design
			+	**37-1126-1250** + 6 off-design
			+	47-1126-1250 + 8 off-design
				R_2 *HE* $Q200_{off}$
			+	**7-1126-750**
			+	7-326-1550
			+	7-826-1250
			+	17-826-1250 + 2 off-design
			+	17-1126-750 + 2 off-design
			+	17-326-1550 + 2 off-design
			+	**17-826-750** + 2 off-design
			+	27-326-1550 + 4 off-design
			+	27-826-750 + 4 off-design

Table 18 provides the time estimations to perform the full fleet design cycle (section 3.3) and the climate optimization of the final aircraft in the fleet (section 3.4). Making a convergent aircraft design is assumed to take 15 seconds. Adding the off-design performance configurations takes another 10 seconds. The initial aircraft database consists of 2 aircraft: $HE\ Q400$ and $HE\ Q200$, for which the aircraft are designed and the off-design performance configurations are added. The fleet allocation is run with this initial database and takes approximately 20 minutes, or 1200 seconds. In the aircraft redesign run 0, 20 new aircraft are proposed. The converging designs are added to the database. In run 1, 28 aircraft are proposed and in run 2, 33 aircraft are proposed. Run 3 is the last fleet-and-network allocation run, as no new aircraft are chosen and therefore no new aircraft need to be designed. The total time to design the final fleet is estimated at around 2 hours.

The time required to run the climate optimization module is strongly dependent on the number of points chosen for the design space exploration study. In this study, first 100 points were chosen for the LHS method, meaning 100 different aircraft designs were made to limit the feasible design space. After this, a 6x6x6 parameter variation was executed in a Full Factorial Sampling, thus 216 aircraft designs were made to estimate the climate performance. The design space exploration study therefore takes a total of 4740 seconds, or 1 hour and 20 minutes per aircraft. Because the final hybrid-electric aircraft fleet consists of 6 different aircraft types that need to be climate-optimized, the total climate optimization takes around 8 hours.

Table 18: Time estimation for design cycle and climate optimization (4 cores)

Fleet Design			
	Number of aircraft	**Time per aircraft**	**Total time**
Initial aircraft database + off-design	2	15 s 10 s	50 s
Fleet allocation Run 0	/	/	1200 s
New aircraft design Run 0 + off-design	20	15 s 10 s	500 s
Fleet allocation Run 1	/	/	1200 s
New aircraft design Run 1 + off-design	28	15 s 10 s	700 s
Fleet allocation Run 2	/	/	1200 s
New aircraft design Run 2 + off-desgin	33	15 s 10 s	825 s
Fleet Allocation Run 3	/	/	1200 s
Total time for fleet design			=6875 s =115 min = 2 hour

Climate optimization			
	Number of points	**Time per point**	**Total time**
LHS	100	15 s	1500 s
Full Factorial	6x6x6 = 216	15 s	3240
	Number of aircraft	**Time per aircraft**	**Total time**
Climate optimization	6	1500 s + 3240 s = 4740 s	28440 s
Total time for climate optimization			= 28440 s = 470 min = 8 hour

Total time fleet design cycle + climate optimization for design case run	**= 10 hour**

Table 19 provides an overview of the final hybrid-electric airline fleet coming from a full redesign. Table 20 shows the same fleet after the climate optimization.

Table 19: Final Hybrid-electric aircraft fleet

Aircraft name	**Seats [-]**	**Cruise Range [km]**	**Total Range [km]**	**Speed [km/h]**	**Altitude [m]**	**Runway length [m]**	**Φ cruise [-]**	**max_ energy [kWh]**	**max_ fuel [kg]**	**energy_ stop [kWh]**	**energy_ km [kWh/km]**	**fuel_ stop [kg]**	**fuel_ km [kg/km]**
On_design-80-1109-1300	80	900	1109	655.2	7010.4	1300	0.0485	1361	1869	527	0.93	724	1.27
On_design-70-809-1250	70	600	809	655.2	7010.4	1250	0.0485	932	1281	443	0.82	608	1.12
On_design-70-309-1550	70	100	309	655.2	7010.4	1550	0.0485	451	619	380	0.71	523	0.97
On_design-7-1126-750	7	900	1126	540	7600	750	0.0485	341	468	124	0.24	170	0.33
On_design-17-826-750	17	600	826	540	7600	750	0.0485	370	508	177	0.32	244	0.44
On_design-37-1126-1250	37	900	1126	540	7600	1250	0.0485	592	813	248	0.38	341	0.52

Table 20: Climate optimized Final Hybrid-electric aircraft fleet

Aircraft name	**Seats [-]**	**Cruise Range [km]**	**Total Range [km]**	**Speed [km/h]**	**Altitude [m]**	**Runway length [m]**	**Φ cruise [-]**	**max_ energy [kWh]**	**max_ fuel [kg]**	**energy_ stop [kWh]**	**energy_ km [kWh/km]**	**fuel_ stop [kg]**	**fuel_ km [kg/km]**
On_design-80-1109-1300	80	958	1109	501	5066	1300	0.0476	998	1388	338	0.69	464	0.97
On_design-70-809-1250	70	663	809	487	4907	1250	0.0636	806	928	282	0.79	388	0.82
On_design-70-309-1550	70	163	309	487	4907	1550	0.0810	397	461	250	0.90	344	0.72
On_design-7-1126-750	7	952	1126	432	5856	750	0.0570	316	386	90	0.24	123	0.28
On_design-17-826-750	17	668	826	432	5320	750	0.0575	341	418	119	0.33	163	0.38
On_design-37-1126-1250	37	968	1126	432	5320	1250	0.0619	630	723	174	0.47	239	0.50

Climate optimization has a significant influence on the fuel mass and battery mass required to perform a mission. Figure 35 shows the mass distribution for the *On_design* 7-1126-75 aircraft of the final hybrid-electric fleet before and after climate optimization.

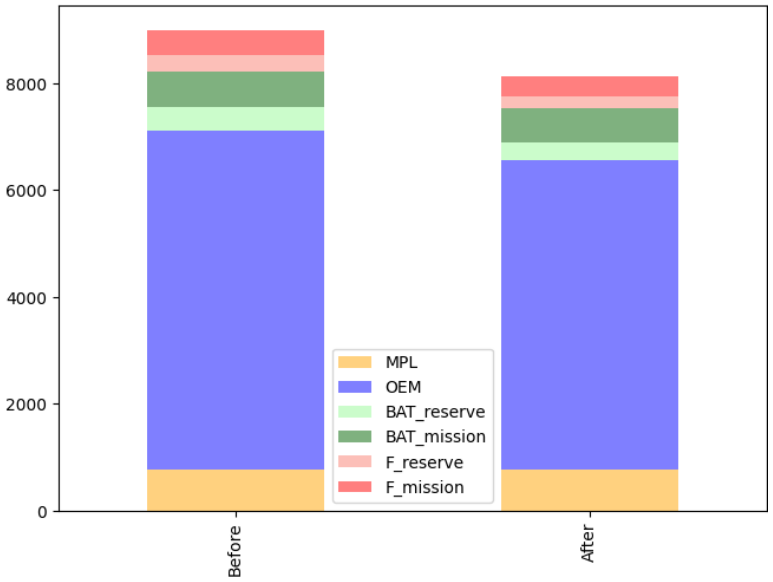

Figure 35: Effect of climate optimization on mass distribution for aircraft *On_design* 7-1126-750. Left = Before optimization, Right = After optimization.

F Allocation Final Hybrid-Electric Fleet

Figure 36 to Figure 41 present the allocation of the aircraft in the final hybrid-electric fleet for the SATA Air Açores network.

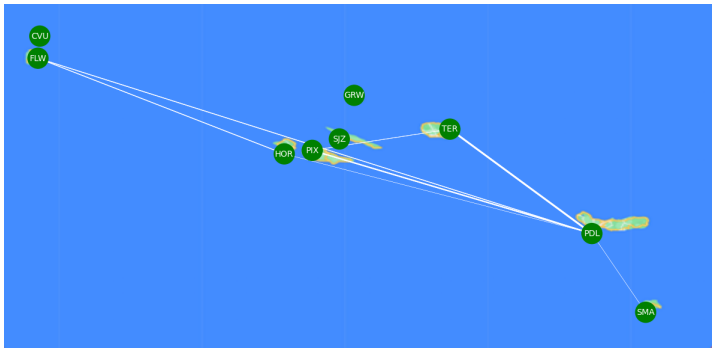

Figure 36: *On_design* 80-1109-1300
min 120 km, max 744 km

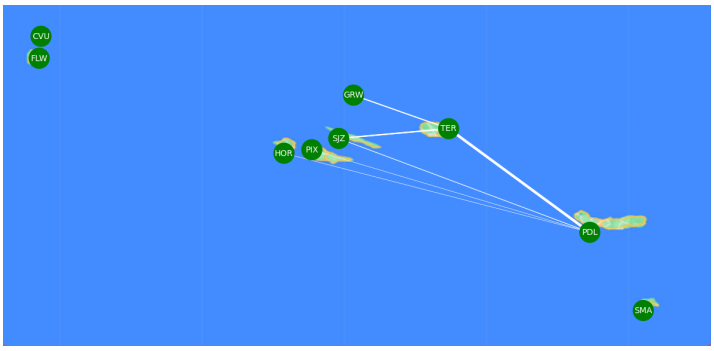

Figure 37: *On_design* 70-809-1250
min 166 km, max 335 km

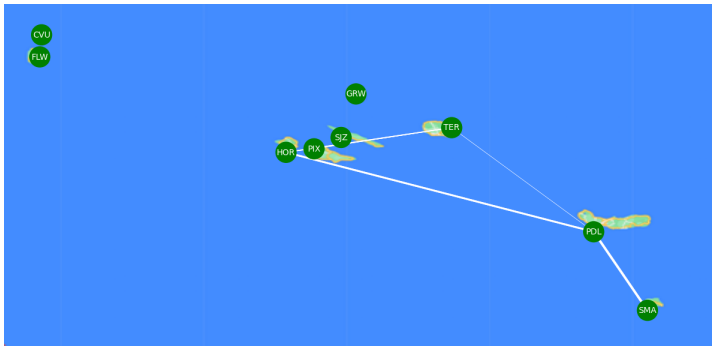

Figure 38: *On_design* 70-309-1550
min 97 km, max 166 km

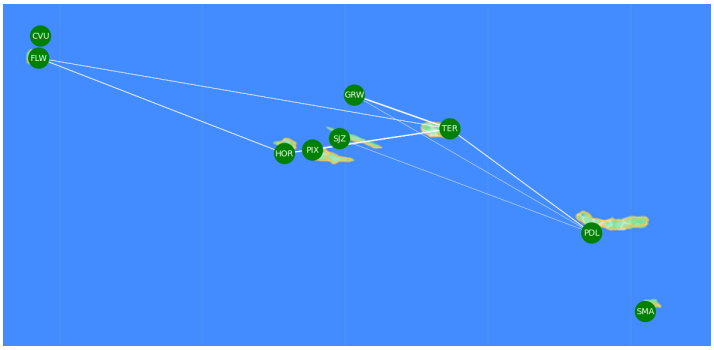

Figure 39: *On_design* 37-1126-1250
min 120 km, max 592 km

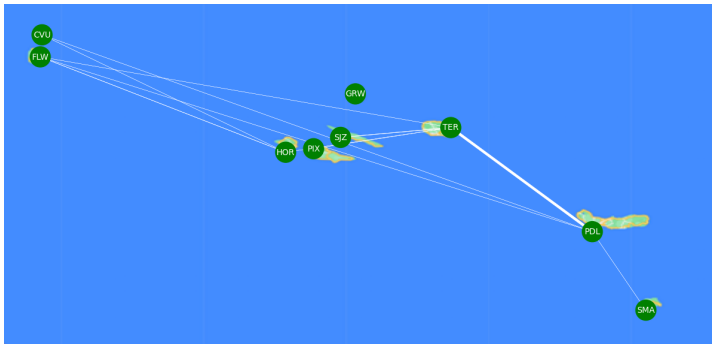

Figure 40: *On_design* 7-1126-750
min 144 km, max 762 km

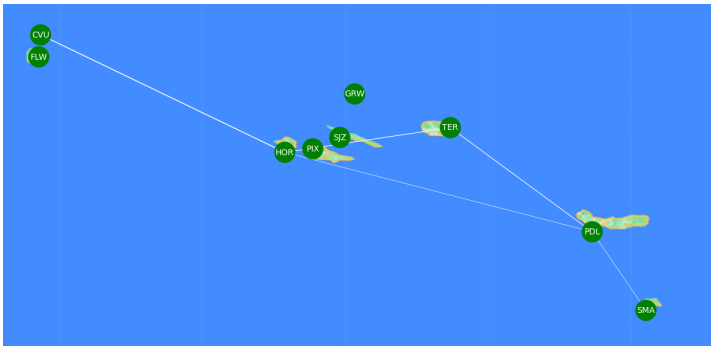

Figure 41: *On_design* 17-826-750
min 97 km, max 488 km

G Sensitivity Study Redesign Cycles

In this part, the aircraft redesign cycles are presented for the different sensitivity study design cases. Figure 42a presents the legend for all figures. Figures 42b and 42c show the chosen fleet for the battery technology sensitivity study. Figures 42d, 42e and 42f show the redesign cycles for the maximum fleet diversity sensitivity study case runs.

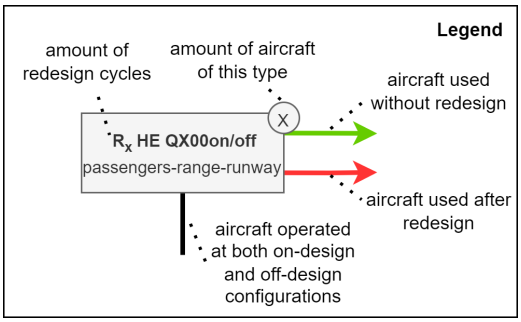

(a) Legend

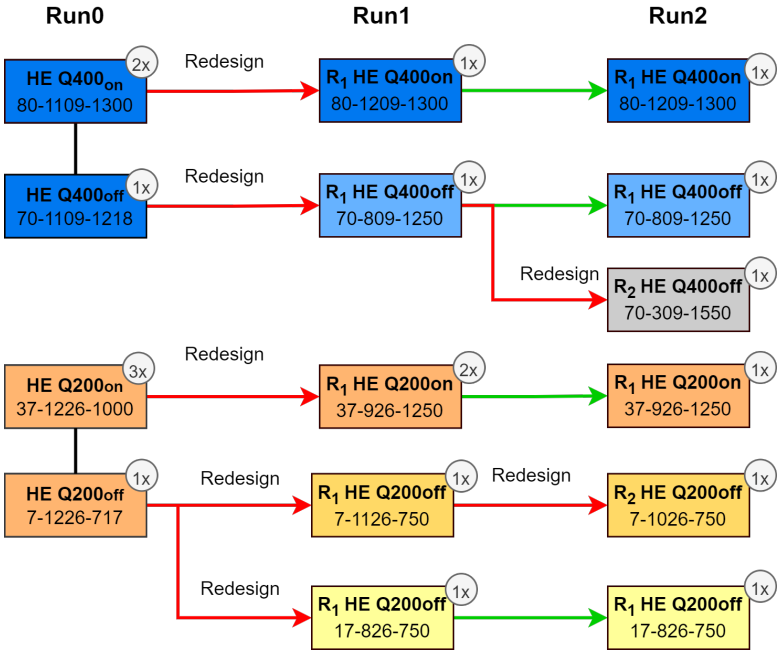

(b) Technology sensitivity study - Battery specific energy $700 Wh/kg$

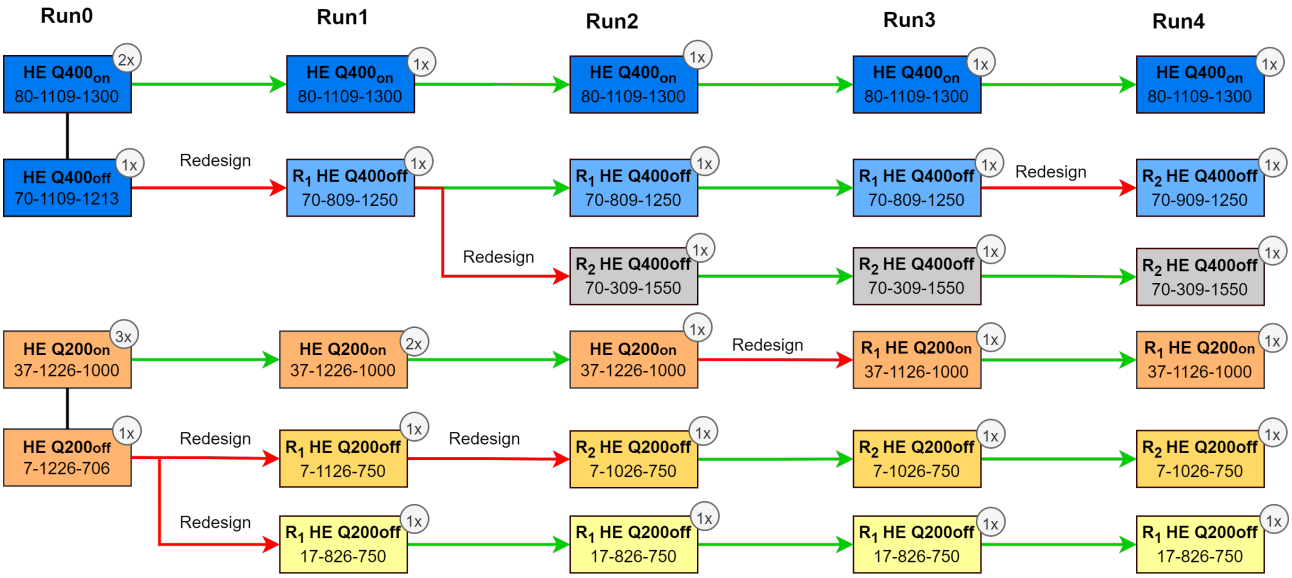

(c) Technology sensitivity study - Battery specific energy $1000 Wh/kg$

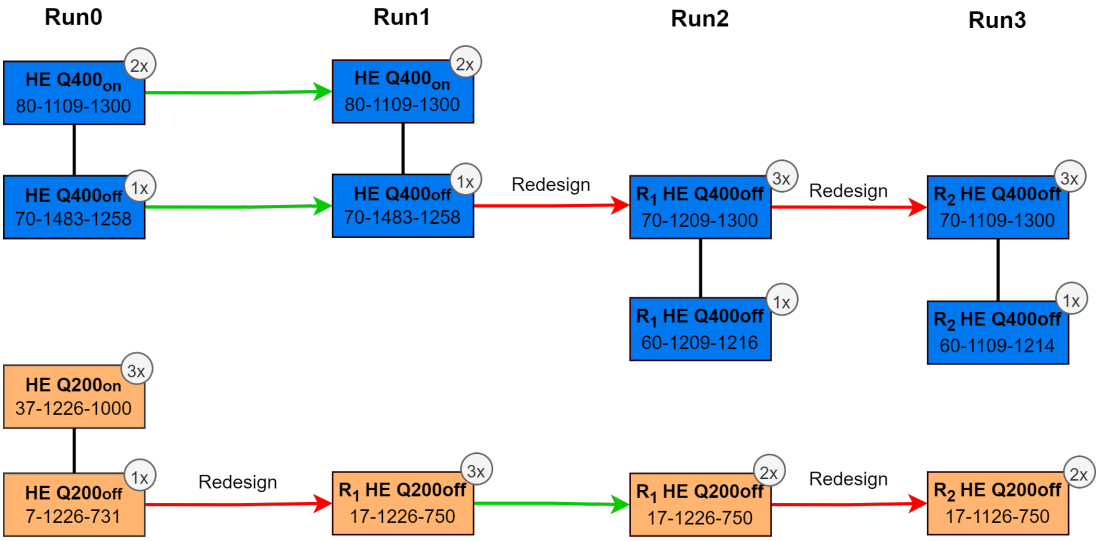

(d) Fleet diversity sensitivity study - maximum diversity of 2

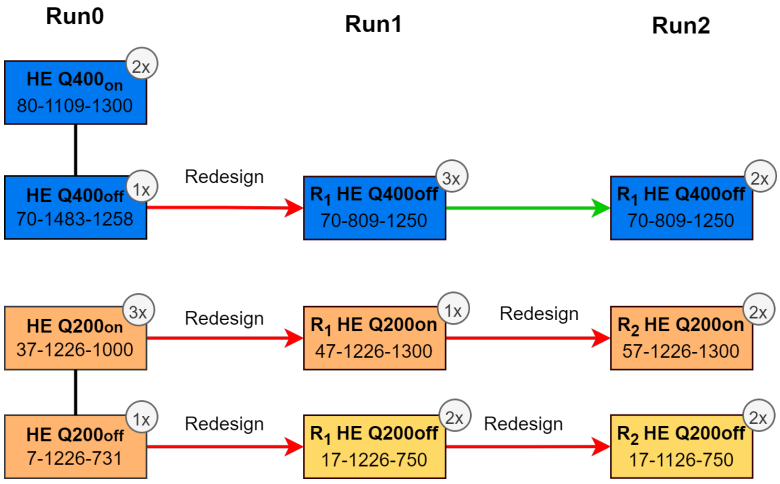

(e) Fleet diversity sensitivity study - maximum diversity of 3

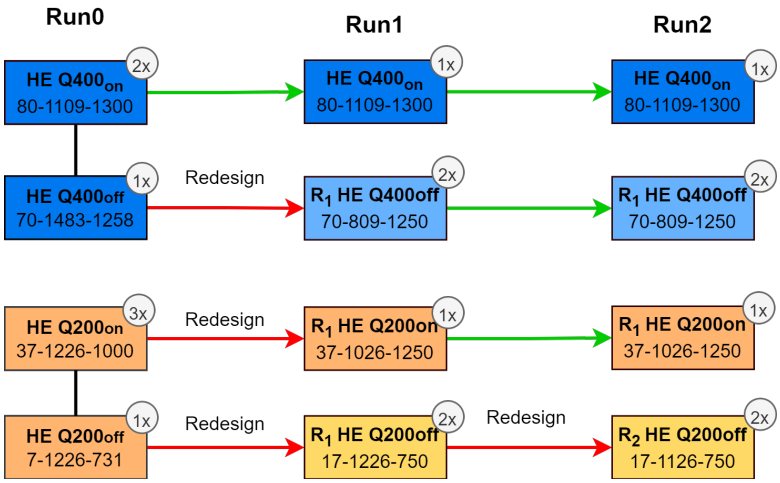

(f) Fleet diversity sensitivity study - maximum diversity of 4

Figure 42: Schematic of aircraft redesign cycles. Each aircraft type is represented by a name, color and their payload-range-runway combination. When one aircraft is operated at multiple configurations (on-design and off-design), the aircraft are shown in the same color and connected through a vertical line. The amount of aircraft needed from a certain type or configuration is denoted by the number in the upper right corner. When an aircraft goes through a redesign, a new aircraft is generated and the name gets an additional term R_x where x denotes the amount of redesign cycles it has gone through. A redesign cycle is marked with a red arrow. Whenever an aircraft is chosen without the need of a redesign, it is marked with a green arrow.

II

Literature Study
previously graded under AE4020

1

Summary

Air traffic is rapidly growing and increases the importance of limiting the impact of aviation on climate. Several aviation climate goals have been set up to limit the noise and emissions for aviation. One of these are the NASA $N+i$ goals, which illustrate the climate targets for transportation aircraft in the United States. In Europe, the aviation noise and emission goals are established through the Flightpath 2050 strategy. Other targets are set up by the International Civil Aviation Organization and the Air Transport Association for emission reductions and a net carbon neutral growth. The progressive development in propulsion technology has made conventional propulsion systems more efficient. It is however believed that these improvements will not be enough to meet the climate goals. This has steered the research towards more disruptive technologies. Electrification of the propulsion system is offering promising avenues in providing the technological rupture and hence meeting the climate targets. Various entities, such as NASA, Boeing, ESAero, Bauhaus Luftfahrt, Airbus, TU Delft and ONERA, have conducted studies on hybrid electric aircraft concepts. All of these consist of conceptual design studies as electrified, manned, fixed-wing aircraft have not yet been achieved for a capacity larger than 4. Apart from the novel aircraft technologies, climate impact is governed by how these aircraft are operated in the airline route network. Aircraft should be allocation in the airline network to ensure optimal use of resources. For this reason, three main research topics are investigated: hybrid electric aircraft design, climate optimized aircraft design and fleet-and-network integrated aircraft design.

Many studies have been performed on methods for the design of hybrid electric aircraft. The first studies focused on retrofitting electrified propulsion systems in existing conventional aircraft in order to come up with sizing principles. In later studies, performance equations are adapted and a new Breguet range equation was derived. Furthermore, power control parameters and control laws are introduced into the design of the hybrid electric propulsion system. The most recent design methods make it possible to carry out clean-sheet conceptual design of hybrid electric aircraft. These methods make use of point-performance analysis through the use of power loading diagrams, a time-stepping mission analysis and a modified Class I mass estimation. Literature on climate optimized aircraft design showed that a lot of research has been conducted on limiting the climate impact of conventional aircraft. Various studies investigate the impact of operational measures, such as changing the flight altitude and including horizontal route deviations. Moreover, studies have been performed to directly limit climate impact in the aircraft design by using multidisciplinary design optimization while considering an environmental performance objective. For hybrid electric aircraft, studies are carried out for the climate impact assessment and compared to conventional aircraft. To provide a tighter coupling between aircraft design and airline operational planning, literature is reviewed on fleet-and-network integrated design. Coupling the design of aircraft in a transportation network leads to a mixed-integer non-linear programming problem, which are difficult to solve. Studies have been performed to solve the problem using a decomposition approach, similar to a multidisciplinary design optimization. Different objectives have been studied, such as airline profit optimization, minimizing operating cost and minimizing emissions.

For the thesis work, the three research topics will be combined. The objective of the thesis work is to develop a methodology for the design of a climate optimized hybrid electric regional aircraft fleet by means of integrating the aircraft design in a fleet-and-network model while considering the climate-optimal design point. To do so, a method will be developed to conceptually design a parallel hybrid electric aircraft. This aircraft will be optimized for minimal climate impact by minimizing the CO_2 emissions from both the kerosene

burned in the mission and battery electricity production. This aircraft design model is integrated into a fleet-and-network model in an iterative approach to maximize network performance. The performance is measured in terms of airline profit or fleet CO_2 emissions. Adaptations will be made to the current aircraft in the fleet and the effects on the airline network performance are investigated. If the climate impact from the airline fleet is lowered with a minimal decrease in profit, airlines are encouraged to add hybrid electric aircraft to their operating fleet in order to lower the environmental impact of flying.

2

Introduction

While the aviation sector is growing every year, the need for a reduced climate impact is becoming increasingly important. Passenger air traffic is rapidly growing. Before the COVID-19 pandemic, Boeing raised a forecast for airplane demand with a yearly average global growth rate of 4.7% during the years 2017-2036 [4]. Similarly, Airbus estimated a global air traffic growth of 4.3% annually in the years 2019-2038 [32]. These numbers have later been adapted for more recent studies which consider the impact of the global pandemic on the air traffic demand. The Boeing commercial outlook now predicts a 4% traffic growth annually between 2021-2040 [5] and Airbus reconnects to a 3.9% annual growth [2]. It will still take some time for the aviation sector to fully recover from the effects of the COVID-19 pandemic. According to the *International Air Transport Association* (IATA) a full recovery of air traffic to the pre-pandemic situation is predicted around the year 2024 [37]. A recent forecast from *Bain & Company* estimates a return to pre-crisis levels only until the second quarter of 2025 [13]. However, in all situations, a growing air transportation traffic demand is foreseen.

With this expected annual growth in air traffic demand, the environmental impact of aviation is becoming a rising concern. The aircraft exhaust comprises of carbon dioxides (CO_2), water vapour (H_2O), nitrogen (N_2), oxygen (O_2), hydrocarbons (C_xH_y), carbon monoxides (CO), nitrogen oxides (NO_x), sulphur oxides (SO_2) and soot particles. Global aviation, including both passenger and freight on domestic and international routes, accounts for 1.9% of the global anthropogenic non-CO_2 greenhouse gas emissions of the year 2016[1]. The CO_2 emissions alone account for 2.5% of emissions of the year 2018[1] [49] . Several aviation emission goals are established to limit the aviation climate impact [1] [12] [61] [38].

While propulsion systems are becoming more and more efficient and conventional aircraft technology is evolving in favor of climate impact reduction, the prospects are starting to reach a plateau and are expected to fall short of achieving the climate targets. This has steered the research towards the introduction of innovative technologies and more disruptive propulsion systems such as boundary layer ingestion and distributed propulsion [65] [74]. In fact, electrification of the propulsion system is offering a promising approach to make aircraft operations less polluting, more efficient and more quiet [74]. Furthermore, the environmental impact of air transportation is not solely a function of these novel technologies and innovative integrated designs, but also of how these aircraft are operated within the airline route networks [43].

Therefore, this research will investigate the design of electrified aircraft integrated in a fleet-and-network model, in order to ensure more efficient resource allocation and a reduced climate impact.

2.1. Literature study objective

This literature study will provide an overview of the existing literature on the design of hybrid electric aircraft. Also current literature on network and vehicle integrated design will be studied as well as climate optimized aircraft design strategies. The three research topics considered are depicted in the Venn diagram in Figure 2.1. The objective of this study is to identify the research gaps in the overlap of the three research topics and to come up with a research objective and research questions to be solved during the thesis work.

[1] The year 2016 and 2018 were given as a reference as these are the last years for which such data is available.

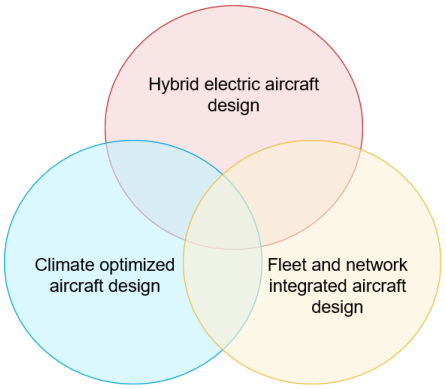

Figure 2.1: Venn Diagram of Research Topics

2.2. Report outline

The report will be structured as follows. First some background information is provided in chapter 3. This will contain the climate goals for aviation, an explanation of the possible hybrid electric aircraft propulsion architectures and lastly, a review of electrified aircraft concepts and prototypes. In chapter 4, a literature review is performed on hybrid electric aircraft design, and the two most promising design methods will be elaborated upon. chapter 5 discusses the available literature on climate optimized aircraft design for both conventional and hybrid electric aircraft. Then, chapter 6 discusses the existing literature on fleet-and-network integrated aircraft design, again considering both kerosene and battery-powered aircraft. From the literature study on the three research topics, clear research gaps should be identified and a research objective can be specified. These are presented in chapter 7. In chapter 8 a preliminary approach is worked out for the thesis work to be performed and a time planning is included. Lastly, chapter 9 draws the relevant conclusions on the research performed.

3

Background

Electrified aircraft grant a promising avenue for reducing the climate impact. This chapter provides the background on climate goals for aviation in section 3.1. Furthermore, a description of possible hybrid electric propulsion system architectures is given in section 3.2. Lastly, the latest and most promising electrified regional aircraft concepts are reviewed in section 3.3.

3.1. Climate goals for aviation

With the growing air transportation sector, the environmental impact of aircraft is becoming an increased concern. Several climate goals for aviation have been established to limit both the noise and emissions.

One of these are the environmentally responsible $N+i$ goals for future subsonic transport aircraft established by the *National Aeronautics and Space Administration* (NASA). These provide guidelines and performance goals regarding emission and noise level reductions for civil transportation aircraft in the United states of America [74]. The $N+i$ nomenclature is used to define the target for three advanced generation aircraft to enter sequentially in targeted time frames, where N refers to current in-service airplanes and i is the generation after N [42]. The targets have been altered throughout the years and a lot of inconsistency is found in literature. Therefore, this paper summarizes NASA's targeted improvements on a system-level according to those found in the Strategic Implementation Plan of 2019 [1]. The metrics are summarized in Table 3.1.

Also in Europe, aviation emission and noise reduction targets are established. This is done by the European commission in cooperation with the *Advisory Council for Aeronautics Research in Europe* (ACARE) through a strategy called *Flightpath 2050* and corresponding S*trategic Research and Innovation Agenda* (SRIA) [74] [12]. The goals target a reduction of 75% of CO_2 emissions per passenger kilometer. From this, 68% reduction is attributed to the improvement of advanced power and propulsion systems and airframe design. The remaining 7% comes from the improvements in air traffic management [65] [41]. Also the European metrics are listed in Table 3.1.

Additionally, the *International Civil Aviation Organization* (ICAO) and the *Air Transport Association* (IATA) have targeted aviation climate action goals. ICAO is an intergovernmental agency of the United Nations, supporting the diplomacy and cooperation between countries when related to air transport techniques and development in order to ensure safe and regulated growth. IATA on the other hand, is a non-governmental organization with key role as board to represent commercial airlines of the world. Both identities have similar goals to reduce emissions by 50% by the year 2050 when compared to the 2005 best in class. Additionally, they aim to achieve a net aviation carbon neutral growth from the year 2020, by introducing a carbon offsetting scheme to hold the aviation emissions at 2020 levels [61] [38] [11]. Furthermore, IATA have sequentially set up more stringent NO_x emission standards by the *Committee on Aviation Environmental Protection* (CAEP).

Table 3.1: Climate targets for aviation

Target metric	NASA N+1	NASA N+2	NASA N+3	Flightpath 2050
Year	2015-2025	2025-2035	Beyond 2035	2050
Noise	- 32 dB[1]	- 42 dB[1]	- 52 dB[1]	- 65%[2]
LTO NO_x emissions	- 75%[3]	-80%[3]	-80%[3]	-
Cruise NO_x emission	-70%[4]	-80% [4]	-80%[4]	-90%[2]
Aircraft Fuel/Energy consumption	-50%[4]	-60%[4]	-80%[4]	-
CO_2 emissions	-	-	-	-75%[2]

[1] Cumulative below Stage 4
[2] Relative to capabilities of typical new aircraft in 2020
[3] Below CAEP 6
[4] Relative to 2005 best in class

3.2. Hybrid electric aircraft design architectures

Multiple propulsion system architecture variations exist for hybrid electric aircraft. This section presents the classification according to the National Academy of Engineering as shown in *De Vries* [17] and lists the most important features of the different architecture options. First, as a reference, the conventional fuel consuming propulsion system is shown in Figure 3.1 under number (1), where F is the fuel, GT is the gas turbine, GB is the gearbox and P is the propulsor.

When considering electrified aircraft, three distinctions can be made. The first propulsion architecture option is making use of the gas turbine to create electrical power without energy storage. These are the turboelectric architectures as seen in numbers (2) and (5) of Figure 3.1. The second group relies on batteries to provide the electrical energy storage, while still making use of fuel. These are the series in (3), parallel in (4) and serial/parallel partial hybrid in (6), also shown in Figure 3.1. The last group, which are the fully electric architectures in (7)(8)(9) of Figure 3.1 are solely powered by batteries. In these electrified architectures the power management and distribution system is depicted as $PMAD$, the battery as BAT and the electric motor as EM.

For the turboelectric (2) and partial turboelectric (5) architectures, the gas turbine is used to generate electricity through the use of an electric generator. The electric motor is driving the propulsor and such the propulsive power is fully electric. All power comes from the fuel, as no additional energy storage (such as batteries) are present. Advantages of this architecture are the decoupling between the gas turbine and the electric motor thrust, enabling a higher performance of the turbomachinery components and flexibility in the design. Furthermore, this architecture works well with novel concepts such as distributed propulsion and boundary layer ingestion. A disadvantage of the propulsion architecture is the lower efficiency due to the losses when converting the mechanical power to electrical power and again from electrical power to propulsive power. The full turboelectric version (2) uses all power from the turboshaft gas turbine to create electrical energy. In the partial turboelectric variant (5), the electric motor provides part of the propulsive power, the rest is generated by a turbofan gas turbine [69].

As part of the battery and fuel powered architectures, the series hybrid architecture in (3) can be observed. This architecture can be considered as a variation of the turboelectric one, where additional propulsive energy is delivered by batteries. Similarly, there is a decoupling between the gas generator and electric motor thrust, resulting in the same advantages as turboelectric architectures. A disadvantage of the series architecture is the higher weight as the electric motor is to provide all propulsive power. In the parallel hybrid electric layout (4), the propulsive power is a mix of conventional gas turbine power and electrical power, where both power sources are mechanically coupled. There is energy storage through the use of batteries. The advantage of this configuration is a weight reduction when compared to the series, due to the propeller power being provided by the two sources. A disadvantage is the fact that the gas turbine is not operating at its optimal conditions, since it is involved in the thrust generation [69].

The last group to consider are the fully electric architectures (7)(8)(9). Here the propulsive power is all-electric and batteries are the only source for propulsive power. The advantages are the high energy efficiency

conversion and the fact that this option is the only potential for zero in-flight emissions. A disadvantage is that aircraft featuring this propulsion architecture rely much on the battery energy density, which is often too low to allow for large mission ranges [69].

One can observe that all of the above mention propulsion system architectures are actually limit cases of the series/parallel partial hybrid one (6). This architecture is a combination of all. It is electrically and mechanically propelled and makes use of batteries for energy storage.

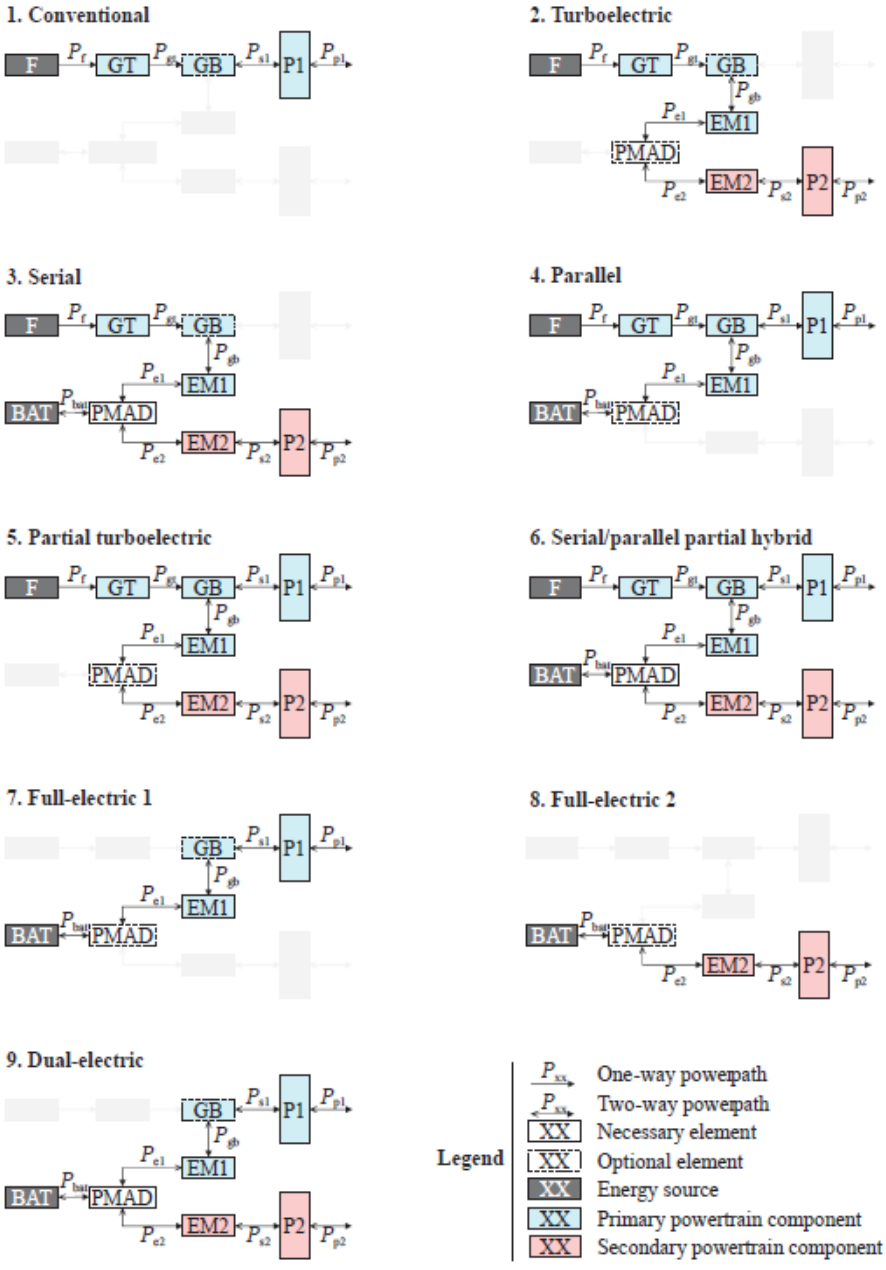

Figure 3.1: Propulsion system architecture classifications from National Academy of Engineering [17]

The above mentioned propulsion architectures can be characterised by two descriptors: degree of hybridization of power (H_p) and degree of hybridization of energy (H_e). The definitions were developed by *Isikveren et al.* [41] and describe the ratios between the conventional and electrical energy sources and power splits in electrified aircraft propulsion systems. The H_p represents the share of maximum installed power of the electrical motor to the total power in the propulsion system as seen in Equation 3.1. The H_e defines the

ratio of energy storage in the electric (battery) energy sources and total energy as seen in Equation 3.2 [74]. If the propulsive power is fully mechanical, H_p is equal to 0. If the propulsive power is fully electrical, H_p is equal to 1. Similarly, if the energy storage is fully kerosene-based, the H_e is 0. If the energy storage is is fully electrical (e.g. from batteries), the H_e is 1. With these parameters, the hybrid electric propulsion systems can be classified as seen in Table 3.2.

$$H_p = \frac{P_{EM}}{P_{tot}} \tag{3.1}$$

$$H_e = \frac{E_{BAT}}{E_{tot}} \tag{3.2}$$

Table 3.2: Hybrid electric aircraft architectures: degree of hybridization

Propulsion architecture	H_p	H_e
Conventional	0	0
Turboelectric	> 0	0
Serial hybrid	1	$0 < H_e < 1$
Parallel hybrid	< 1	$0 < H_e < 1$
Full-electric	1	1

3.3. Electrified aircraft concepts

In order to get a glimpse on the technology advancements of hybrid electric aircraft, the state-of-art hybrid electric aircraft concepts are investigated. For this, the study focused on providing an overview of large and regional commercial aircraft concepts and studies with over 60 seats. The reasons are the large market growth prediction and the significant environmental impact of 14% of total aviation CO_2 emissions that are attributed to this segment [33]. One should note that these aircraft all consist of conceptual design studies as electrified, manned, fixed-wing aircraft have only flown with a maximum capacity of 4 seats. Since the 2000s, an interest was found in conceptual design studies for larger electrified aircraft and started with the NASA-funded industry studies [11]. The first hybrid electric aircraft with more than 50 seats are expected by the year 2032 [69].

NASA sponsored the concept for boosting the promotion of electrified air vehicles through the *Boeing Sustainable Ultra Green Aircraft Research* (SUGAR). The research consists of multiple single-aisle hybrid electric commercial aircraft concepts as seen in Figure 3.2. The airframe features a high span, high aspect ratio and high lift-to-drag truss braced concept. A subset of this exploration is the Boeing SUGAR Volt, which out of many designs was the most promising [74]. The concept features an electrical energy boost design, with parallel hybrid electricity to perform an electrified cruise operation by driving two battery powered motor-assisted turbofans. In Phase 1 of the SUGAR project, this concept was the only one capable of meeting NASA N+3 fuel burn goal of 70%[1] reduction compared to the Free Baseline concept [11] [55]. In Phase 2, a potential fuel burn reduction was estimated between 10.9% and 21.7% with varying degrees of electrification between 1MW and 5.2MW during the cruise phase of the mission [74] [10]. During the second phase of the project, focus was put on implementing advanced technologies applicable to the aircraft expected for the N+4 (2040-2050) time frame. These configurations were assessed under the SUGAR Freeze concept. This concept features two turbofans with liquefied natural gas fired fuel cells in a partial turboelectric propulsion architecture, accompanied by one aft fuselage boundary layer ingestion propulsive fan. This concept showed a fuel burn reduction potential of 64.1% [74] [9].

Another electrified aircraft concept is found in the *Environmentally Conscious 150* (ECO-150) by *Empirical Systems Aerospace* (ESAero) in Figure 3.3. The single aisle narrow body regional airliner has a trailing edge distributed propulsion (TeDP) on a split wing aircraft. The propulsion system is fully turboelectric with 16 electric motor-driven fans embedded in the wing. A very large fuel burn improvement can be achieved of 44% using conventional technology and 59% using superconducting technology when compared to current a

[1] Note that this is not the same as depicted in Table 3.1, as the table shows the updated values of the year 2019, while here the values of 2011 are considered.

single-aisle 737-700 benchmark [23]. When using higher fidelity assessment, this statement is however contradicted and the design showed no fuel burn reduction. However, it was acknowledged that the airplane could be resized for better fuel burn [75]. This shows that the study is not fully converged yet.

The largest transport aircraft ever seriously studied is the NASA N3-X, shown in Figure 3.4. The airframe consists of a blended wing body and is derived from the NASA Boeing CESTOL (*Cruise-efficient Short Takeoff and Landing*) study. Again, a fully turboelectric propulsion concept with TeDP is investigated. The design utilizes 14 electrically powered ducted fans, supplied from two turboshaft driven generators on the wingtips. A 70-72% fuel reduction can be obtained with respect to a 777-200 benchmark depending on the cooling system used. From this, 50% reduction is attributed to the airframe and 20% from the distributed electrical propulsion [20] [21]. This concept however requires very aggressive technology developments which introduces large risks and uncertainties in the design.

Because of the technological limitations of the N3-X concept, a concept was investigated that would be feasible in the nearer term: the *Single-aisle Turboelectric Aircraft with an Aft Boundary-Layer propulsor* (STARC-ABL) depicted in Figure 3.5. The airframe is similar to SUGAR Freeze and has a partially turboelectric propulsion system with two turbofans and is complemented by a single electrically driven aft-fan. The concept achieves a design mission fuel improvement of 12.2% when compared to the baseline configuration: a N+3 conventional configuration [92] [93].

Furthermore, a couple of electrified aircraft are studied by Bauhaus Luftfahrt (BHL). First, the *Concept validation study for fuselage wake filling propulsion* (CENTRELINE) is considered, see Figure 3.6. This hybrid electric aircraft has a turboelectric propulsion layout having an aft-fuselage boundary layer ingestion system [81] [63]. Secondly, Bauhaus Luftfahrt presents a fully electric regional passenger aircraft concept with a C-wing shaped airframe in order to achieve high aerodynamic efficiency: Ce-Liner, shown in Figure 3.7. The concept uses very advanced battery technology by the use of high temperature superconducting batteries with specific energy of 2000 Wh/kg [34] [40].

Another unconventional airframe shape is seen in the Airbus VoltAir in Figure 3.8. The aircraft uses a lower slenderness of the fuselage to enhance better aerodynamics and reduced weight. Additionally, it features natural laminar wings. Also this aircraft makes use of next generation batteries and high temperature superconducting technology in a fully electric propulsion system [83].

As part of the Clean Sky 2 program for Large Passenger Aircraft Innovative Aircraft Demonstrator Platform, two aircraft studies are shown. The *Novel Aircraft Configurations and scaled Flight Testing Instrumentation* (NOVAIR) concept was developed by a consortium of Delft University of Technology (TU Delft) and Netherlands Aerospace Center (NLR) and can be seen in Figure 3.9. The design studies a A320NEO aircraft with parallel hybrid electric propulsion, downscaling of the turbofan and the usage of more electric non-propulsive systems such as pneumatic and hydraulic components. The combination of battery boosting and electric taxiing, together with a 90% downscaling of the turbofan and the use of more electric components resulted in a 7% fuel reduction [97] [89]. Also the *Distributed fans Research Aircraft with electric Generators* (DRAGON) by ONERA was part of the Clean Sky 2 project and can be observed in Figure 3.10. It shows a tube-wing single-aisle passenger aircraft with a fully turboelectric propulsion design featuring a distributed propulsion system with large number of electric ducted fans along the wing span, powered by two turboshaft engines. This aircraft has a 8.5% reduction in fuel with respect to reference aircraft which are entering into service in 2035 [77].

Figure 3.2: SUGAR Volt/Freeze
(Boeing Image)

Figure 3.3: ECO-150
(ESAero Image)

Figure 3.4: N3-X
(NASA Image)

Figure 3.5: STARC-ABL
(NASA Image)

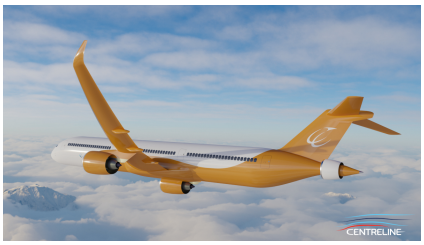

Figure 3.6: CENTRELINE
(Bauhaus Luftfahrt Image)

Figure 3.7: Ce-Liner
(Bauhaus Luftfahrt Image)

Figure 3.8: VoltAir
(Image from *Stückl et al.* [83])

Figure 3.9: NOVAIR
(Clean Aviation Image)

Figure 3.10: DRAGON
(ONERA Image)

The following Table 3.3 presents an overview of the electrified aircraft considered and provides data about the expected year of entry into service (EIS), Mach number, passenger capacity (PAX), propulsion system architectural layout, battery specific energy and mission range.

Table 3.3: Overview of electrified aircraft concepts

Conceptual Design	EIS	Mach	PAX	Propulsion system	Battery energy	Range	References
Boeing SUGAR Volt	2035	0.7	154	Parallel hybrid	750 Wh/kg	Economic: 900 nmi Design: 3500 nmi	[55] [10]
Boeing SUGAR Freeze	2040-2050	0.7	154	Partial turboelectric	n/a	Economic: 900 nmi Design: 3500 nmi	[9]
ESAero ECO-150	2035	0.8	150	Fully turboelectric	n/a	1650 nmi	[75] [76] [23]
NASA N3-X	2040-2045	0.84	300	Fully turboelectric	n/a	7500 nmi	[22] [21] [20]
NASA STARC-ABL	2035	0.8	154	Partial turboelectric	n/a	3500 nmi	[92] [93]
Bauhaus Luftfahrt CENTRELINE	2035	0.82	340	Fully turboelectric	n/a	6500 nmi	[81] [63]
Bauhaus Luftfahrt Ce-Liner	2035	0.75	189	Fully electric	2000 Wh/kg	900 nmi	[34] [40]
Airbus VoltAir	2035	/	68	Fully electric	750 Wh/kg	900 nmi	[83]
NOVAIR	2035	0.78	150	Parallel hybrid	500 Wh/kg	800 nmi	[97] [89]
ONERA DRAGON	2035	0.78	150	Fully Turboelectric	n/a	1200 nmi	[77] [47]

4

Hybrid Electric Aircraft design

This chapter will present the first research topic considered in this research: the design of hybrid electric aircraft, as seen in Figure 4.1. First, the relevance of this research topic is addressed in section 4.1. Secondly, a literature review on the methods to perform conceptual design of hybrid electric aircraft is presented by chronologically going over the most important advancements in section 4.2. Afterwards, the most promising methods will be reviewed more in depth in section 4.3 as they form an important basis of the future thesis work.

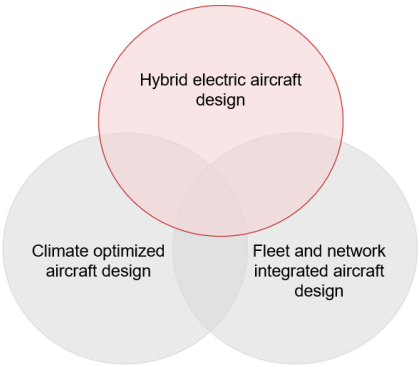

Figure 4.1: Research topic 1

4.1. Relevance of research topic

As already elaborately discussed in section 3.1, several climate targets have been put in place to reduce the environmental impact of the aviation sector. Many of these goals are quite ambitious and challenging. Large technological improvements have already been achieved from the evolutionary development of conventional propulsion technology, making them more efficient. Despite this, the prospective of efficiency improvements with evolutionary technological approaches is reaching an asymptote. Additionally, it is believed that the improvements alone will not be enough to meet the climate goals. Electrification of the propulsion systems is offering promising avenues in further reducing the climate impacts from aviation. Due to the progress in electrical component technologies and the possibility of configuring the electrical system and airframe for increased synergy, make the field of electrically driven propulsion and power systems very promising in providing the technological rupture required to meet the aggressive climate targets [65]. Currently, electrified aircraft for larger transport purposes, such as regional aircraft, are only in the conceptual design phase and such no single agreed-upon design method is set in stone. This brings the opportunity to investigate possible sizing methods and combine the most favorable aspects in one new methodology.

4.2. Literature review

Initially, the focus of designing electrified aircraft designs consisted of system level studies which assess the impact of unconventional propulsion systems on aircraft performance through a retrofit of existing aircraft, without actually sizing the aircraft itself. *Nam et al.* [57] [58] observed that little research is dedicated to exploring revolutionary aircraft concepts with unconventional propulsion systems and hence formulated a generalized power-based sizing method. This method is based on power-flow modeling and is able to perform point-performance calculations and mission analysis, resulting in the initial sizing and weight estimation of the aircraft. This method is not specifically developed for hybrid electric aircraft, but inspired many other researchers in the development of more advanced methods.

Later, pre-design methods were investigated for the design of hybrid electric aircraft. The formulations consist of first-order algebraic expressions and first principles for the modeling of the propulsion system and the aircraft. The study by *Perullo and Mavris* [62] presents a review of approaches to manage hybrid electric energy and and its pre-design methods for vehicle sizing. *Isikveren et al.* [41] established foundational equations to parametrically describe any duel-energy storage propulsion-power-system. Later, in 2018, *Isikveren* [39] polished his previous work and proposed a new graphical based method for the sizing of hybrid electric aircraft. For this, a simplified sizing algorithm was implemented in the pre-design phase with a so-called quadrant-based algorithmic nomograph, allowing maximum transparency for the designer.

Many sizing methods for hybrid electric aircraft make use of retrofitting into existing aircraft. *Pornet et al.* [66] had the objective to develop a methodology of integrating hybrid electric aircraft design in available sizing and performance programs by extending the traditional look-up tables. They investigated the use of conventional fuel besides batteries as an energy source by retrofitting a single-aisle commercial transport aircraft. Later, *Pornet* [64] derived sizing principles and design guidelines by investigating a retrofit of a transport aircraft with a parallel hybrid propulsion system and a clean-sheet design hybrid electric aircraft. This new conceptual design method, which can be used for sizing and performance assessment of hybrid electric aircraft, has an increased fidelity when compared to the previously mentioned pre-design methods.

In 2018, *Voskuijl et al.* [90] performed the analysis and design of a hybrid electric regional turboprop aircraft. For this, the supplied power split concept was introduced and a new modified Breguet range equation was derived for hybrid aircraft cruise flight. *Voskuijl et al.* however did not differentiate between the battery energy available and the installed battery energy capacity. As the latter determines the weight of the battery, this distinction is important to be considered. This adaptation was made by *De Vries et al.* [19] and a new range equation was derived. The equation is valid for aircraft with generic hybrid electric powertrain architectures and a constant power split.

As a continuation on the work performed by *Voskuijl et al.*, *Zamboni et al.* [96] generalized the hybrid electric propulsion system to highlight the control parameters needed to fully define the propulsive system and allowing a rapid exploration of the design space. They introduced power control parameters that are supplied by specific control laws.

Most recent methodologies exist for clean-sheet conceptual design of hybrid electric aircraft. *De Vries et al.* [18] developed a new conceptual design method at the Delft University of Technology (TU Delft) which sizes the wing, propulsion system and maximum take-off weight of aircraft featuring hybrid electric distributed propulsion by including the aero-propulsive interactions. The new sizing method is implemented in the in-house-developed conceptual design tool of the TU Delft: The Aircraft Design Initiator. Based on a set of top-level requirements, aircraft are preliminary sized through empirical weight estimations and linked to vortex lattice methods for wing aerodynamics. This research was performed under the European NOVAIR project, which is part of the Clean Sky 2 program targeting Large Passenger Aircraft, as explained in **??**. In parallel to the conceptual design assessment of *De Vries et al.*, another method was developed at Aachen University of Applied Sciences (FH Aachen) by *Finger et al.* [24]. This method however focuses on the design of general aviation (GA) aircraft including vertical take-off and landing (VTOL) capabilities. Both methods show great resemblance and were therefore compared and cross-validated [25][26]. In the validation study, both methods were used to design an existing 19-seat commuter aircraft as a base test case. Then this aircraft is resized under the consideration of a parallel, serial and fully electric propulsion systems. Both methods were initially not intended to size commuter aircraft, however in this way it was possible to verify that both

methods are not limited to the intended aircraft category (transport aircraft in *De Vries* and general aviation aircraft in *Finger*) and are universal enough to size hybrid electric aircraft in general.

4.3. Existing clean-sheet hybrid electric aircraft design methods

The methodologies of *De Vries et al.* [18] and *Finger et al.* [24] are part of more elaborate PhD thesis reports. Both thesis reports provide the design methodologies for clean-sheet hybrid electric aircraft design, including important equations. This literature is considered very important to the current research and for this reason both methods will be explained in more detail. They will serve as a basis to define the envisioned methodology for the design of a hybrid electric aircraft during the thesis work, which will be later elaborated upon in chapter 8.

The methodologies presented in the PhD reports of *De Vries* [17] and *Finger* [27] are exceptionally complementary. Both methods first perform a point-performance analysis through the use of power-loading diagrams. These diagrams depict the design constraints and such it is possible to determine the power-to-weight ratio (P/W) and wing loading (W/S) combinations in the feasible design space. Constraints are posed on the take-off distance, cruise speed, rate of climb and stall speed. After this, a mission analysis is worked out with a time-stepping approach and sequentially a mass estimation is performed.

The method developed by *De Vries* at the TU Delft, focuses on the preliminary sizing of hybrid electric transport aircraft with novel propulsion system layouts. This is done by including the aero-propulsive interaction effects that are present in distributed propulsion layouts, tip-mounted propulsion or boundary layer ingestion systems. To do so, the traditional sizing methods by *Raymer* [68], *Torenbeek* [87] and *Roskam* [71] are adjusted to account for both the hybrid electric powertrain and the aerodynamic effects of novel propulsion systems. In the point-performance analysis, the conventional thrust, lift and drag equations are expanded resulting in modified flight-performance constraint equations in the power-loading diagrams. Afterwards, a powertrain model is formulated which converts the aircraft-level power-loading diagram into a series of power-loading diagrams per component of the powertrain. A simplified analytical model is used to compute the power required for the different components of the powertrain for a given power-control strategy. Two power-control parameters are introduced to define the power shares of the system: the supplied power ratio (Φ) and the shaft power ratio (ϕ). For each performance constraint, a different power control parameter can be selected. After the power transmission analysis, a mission analysis is performed in a time-stepping manner to size the aircraft for its energy requirements. The mission profile is simplified and divided into phases such as climb, cruise, descent and loiter. Each phase is divided into segments. In one time step, the performance is assumed to be constant and thus from the battery power and fuel power, the required battery energy and fuel energy can be estimated considering the duration of the time step. Each subsequent time step, the aircraft weight is updated for the reduction in fuel weight. The total energy required to perform the prescribed mission is determined by integrating the energy consumption along the entire mission. In this approach, the designer has to specify the power-control strategy during each mission phase and the degree of hybridization of energy is a result of the mission analysis. The next step in the sizing process is the weight estimation, in which the resulting battery and fuel weights are included in a modified Class I weight estimation for hybrid electric aircraft. A new maximum take-off mass is calculated and the methodology is repeated until the take-off mass converges. The outcome of the methodology is the Class I mass breakdown, the power requirements and the wing surface area. A flowchart of the sizing process is seen in Figure 4.2 and is obtained from the comparison study [25], which altered the original flowchart as seen in the PhD thesis report [17].

The method developed by *Finger* at FH Aachen is very similar to that of the TU Delft and a flowchart can be seen in Figure 4.3 which was obtained from his PhD thesis report [27]. The two methods however show some important differences. The FH Aachen method was developed to size hybrid electric general aviation aircraft and focuses on the implantation of VTOL capabilities without considering any aero-propulsive effects. One of the largest differences can be seen in the constraint analysis using the power-loading diagrams. Contrarily to the TU Delft method, the method from FH Aachen uses one single aircraft-level power-loading diagram and assumes a constant power split for all constraints. In this method, the degree of hybridization of power is an input from the designer and is indicated by the hybrid electric design space which is the area below the design line in the constraint diagram. Opposed to the TU Delft method, the powertrain model is not generic and is dependent on the propulsion architecture type, however the design space representation is

less complex as it does not make use of multiple power-loading diagrams. Furthermore, there is a difference in the calculation of the operating empty mass. Both methods use modified Class I weight estimations, but the method from FH Aachen includes an additional Class II weight estimation that is based on geometric aircraft parameters. Also the definition of the operational empty mass is slightly different. Due to the fact that FH Aachen considers VTOL aircraft, which have significantly larger propulsion systems compared to conventional aircraft, the operational empty mass does not include the propulsion system itself. The TU Delft method on the other hand considers the conventional operating empty mass definition. Besides the ones mentioned, some other and smaller differences are observed in the assumptions and modeling approaches. For this, the reader is advised to read the comparison study on both methods in *Finger et al.* [25].

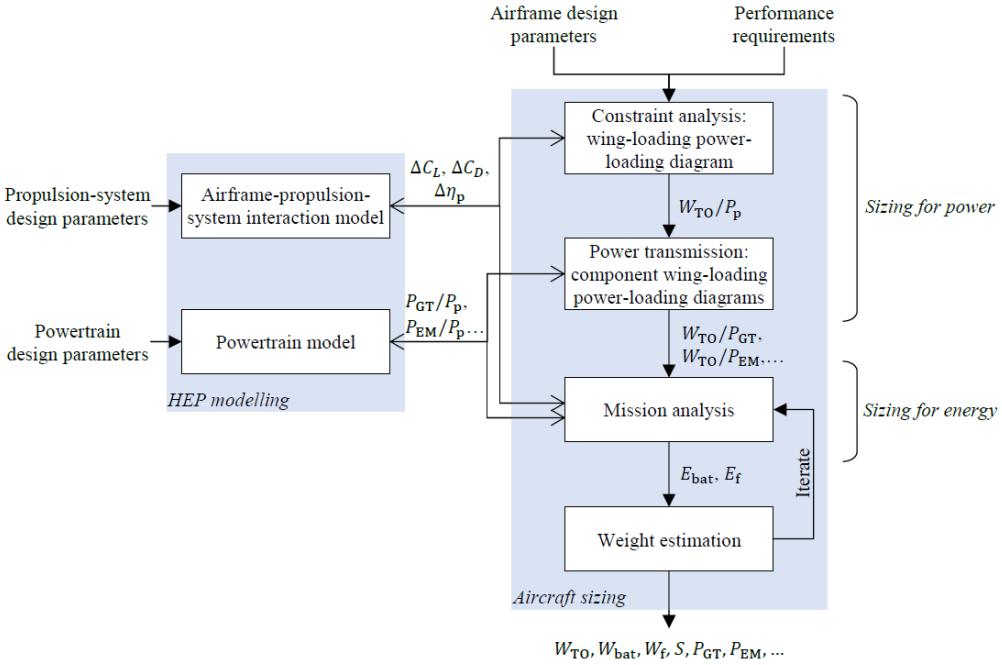

Figure 4.2: Flowchart of sizing process developed by *De Vries* at TU Delft [25]

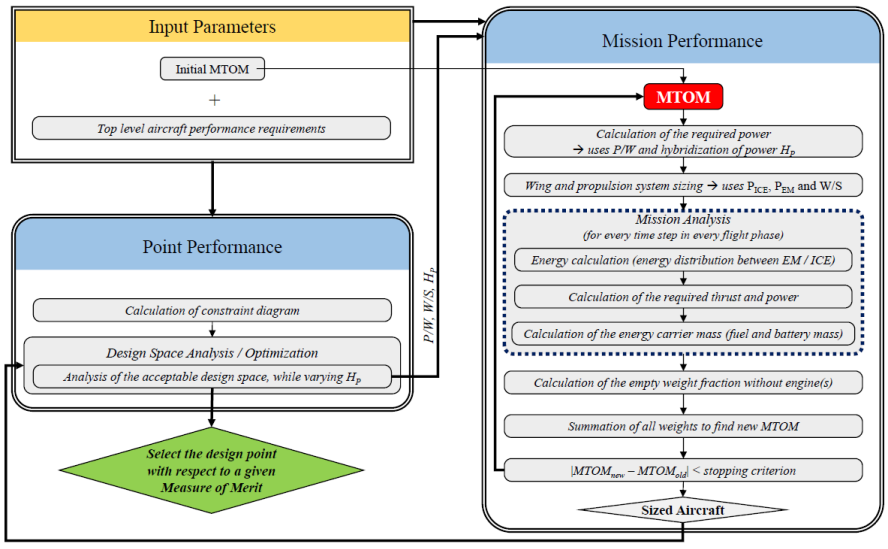

Figure 4.3: Flowchart of sizing process developed by *Finger* at FH Aachen [27]

5

Climate Optimized Aircraft Design

This chapter covers the second topic of this research: climate optimized aircraft design, again visualized by a Venn diagram in Figure 5.1. The chapter starts with an introduction regarding the relevance of the research topic in section 5.1. Then, a literature review is performed on climate integrated aircraft design strategies in section 5.2.

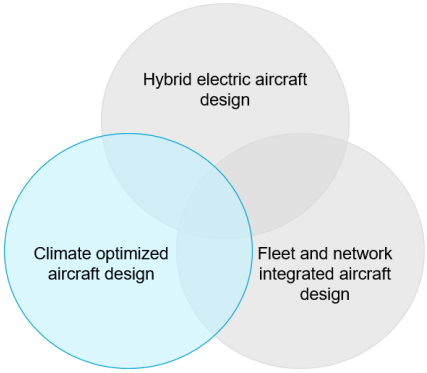

Figure 5.1: Research topic 2

5.1. Relevance of research topic

Conventional aircraft emit CO_2, H_2O, NO_x and soot particles due to the combustion of kerosene. Aircraft emissions causes a direct effect on climate and local air quality as the emissions impact the atmospheric composition. Global aviation accounts for about 2% of the greenhouse gas emissions and accounts for 3.5% on the effective radiative forcing [49]. Radiative forcing can be considered a concept which indicates the global mean temperature change. The emission species itself all have different impact on the global temperature. CO_2 is a greenhouse gas with a long atmospheric lifetime and has a positive (warming) impact on the effective radiative forcing. CO_2 emissions are a direct product of fuel combustion and are therefore dependent on the fuel consumption. Similarly, H_2O emissions are a direct product of fuel combustion and is a greenhouse gas with a positive impact on radiative forcing. The impact from NO_x emissions are twofold. First, NO_x increases the production of the greenhouse gas ozone (O_3) over short timescales and such causes a warming effect. Secondly, it also leads to the depletion of both ozone (O_3) and methane (CH_4) greenhouse gases over longer timescales, causing a cooling effect. The NO_x emissions itself are dependent on the thrust setting of the aircraft engine and maximum production occurs at full thrust settings. Lastly soot particles, which are impure carbon particles, are emitted due to incomplete combustion of kerosene. These particles together with H_2O gas trigger the formation of contrails, which can have both a warming or cooling effect depending on the contrail properties. Furthermore, the effects of NO_x and contrails on the radiative forcing vary significantly with flight altitude, while in term the cruise altitude also changes the fuel burn and hence also the effects of CO_2 and H_2O vary. In order to limit the climate impact from aviation, several studies have been performed to include the climate impact directly into the design of aircraft and aircraft operations.

5.2. Literature review

A large amount of research has been conducted to minimize the impact of aviation on climate. Most of them consider conventional kerosene-driven aircraft, however, some studies also investigate the effects when flying with hybrid electric aircraft.

Conventional aircraft

Several studies have been performed on aircraft operational measures to limit climate impact. Many focus on the change in flight altitude to reduce the climate impact of contrails. *Mannstein et al.* [54] estimate the effects of small changes in flight altitudes on the contrail and contrail cirrus formation. *Schumann et al.* [79] introduced the concept of climate optimized routing by considering the local climate impact of the different routes. The approach is illustrated by changing the flight level 2000 feet up or down.

Other studies suggest to avoid contrails by including both vertical and horizontal route deviations. *Gierens et al.* [29] provides an review of various strategies for contrail avoidance. *Sridhar et al.* [82] identified that the existing models did not take into account the effect of wind on the aircraft trajectory and therefore oversee the fuel savings potential of aircraft that fly in wind-optimal routes. Consequentially, this study develops a method to calculate a wind-optimal trajectory for cruising aircraft which at the same time circumvent airspace regions where persistent contrails are formed.

Although promising for reducing climate impact, most of these mitigation strategies cannot be implemented in the near future due to the technical challenges. Hence, *Niklaß et al.* [59] present an interim mitigation strategy considering climate restricted airspaces. Regions with climate costs larger than a certain threshold value are closed for air traffic operations. The restricted airspaces are defined through 3D climate change functions which characterize the environmental impact from an aircraft emission at a certain location.

Apart from studies on operational measures, research has been performed to directly limit the climate impact in the aircraft design. *Antoine and Kroo* [3] set up a framework which investigates the feasibility of using environmental performance as an optimization objective when conceptually designing an aircraft. In this study, designs were optimized according to a multi-objective optimization for minimum cost, minimum fuel consumption, minimum NO_x emissions and minimum noise. The climate impact is assessed by the CO_2 emissions over the entire mission and the NO_x emissions in the take-off and landing phases.

The NO_x emissions in take-off and landing phases are of great interest as restrictions are imposed by the ICAO. However, also the strong altitude dependencies of these emissions should be taken into account. Additionally, the effects due to contrails should be considered. For this, more advanced climate models and more comprehensive climate metrics have to be determined. The research by *Dallara and Kroo* [80] include more advanced models and climate impact is measured by the average temperature response metric. In this paper, aircraft are designed for reduced climate impact, which is different from aircraft designed for minimal fuel burn because of the importance of non-CO_2 emissions. In the study by *Koch* [48], the detailed AirClim model was employed in a comprehensive study within the German Aerospace Center (DLR) project CATS, in which options are investigated to reduce the climate impact from aviation by operational and technological measures. The detailed description of the approach and the results are provided by *Koch* [48], a summary of the project results is presented by *Dahlmann et al.* [15].

Studies by *Koch* and *Dallara and Kroo* are further extended by including more engine design variables such as the overall pressure ratio and turbine entry temperature by *Proesmans and Vos* [67]. The study performs a multi-disciplinary design optimization for a medium-range turbofan aircraft for different objectives: minimum fuel mass (FM), minimum direct operating cost (DOC) and minimal global-warming impact measured by the average temperature response (ATR) climate metric over a time horizon of 100 years. Two scenarios are considered: one where the number of airplanes in the global fleet remains constant and one where the overall transport productivity of the fleet remains constant. The thesis work performed by *Thijssen* [86] builds upon the work of *Proesmans and Vos.* In this work, propeller aircraft were implemented and the same optimization was performed. Interestingly, it was obtained that the FM and ATR objectives are aligned. Due to the low cruise altitudes the climate impact is fully attributed to the CO_2 emissions and short-lived emissions, which are also directly dependent on the fuel consumption.

Hybrid electric aircraft

All of the above studies assess climate impact in the design of conventional kerosene-driven aircraft. Some studies have been performed on the environmental impact assessment of hybrid electric aircraft as well. *Van Bogaert* [88] investigated the potential fuel burn reduction of a parallel hybrid electric regional aircraft with technology of the year 2035. The hybrid electric aircraft fuel consumption was compared to a reference aircraft based upon the ATR 72-600.

Hoelzen et al. [33] identified a research gap in the lack of investigation of the influence of battery power and battery energy density on the environmental performance of aircraft. Next to the tank-to-wheel emissions generally considered in environmental assessment, he included well-to-tank emissions. The environmental impact is determined through a sensitively study on the total CO_2 emissions. A similar study is performed by *Wroblewski and Ansell* [94] in which the life cycle CO_2 emissions of conventional and hybrid electric aircraft are analyzed for various missions with different degrees of hybridization and battery specific energy densities of the hybrid electric propulsive system. Furthermore, *Ribeiro et al.* [70] performed an environmental study to explore the impacts of the most promising lithium-based batteries from raw material extraction to end of life for integration in hybrid electric aircraft.

Previous studies focus on the CO_2 emission reduction potentials of hybrid electric aircraft compared to conventional aircraft, but do not take into account the important effects of non-CO_2 emissions on climate. The study from *Scholz et al.* [78] includes emissions of other pollutants (CH_4, H_2O and NO_x) through the climate metric sustained global temperature with a time horizon of 100 years. For a fair and complete analysis, the emissions of both the aircraft combustion and electricity production are taken into account . Moreover, the study evaluates the climate impact of incorporating a given hybrid electric aircraft concept on a fleet-wide scale.

None of the studies above on hybrid electric aircraft include contrails in the climate assessment. *Yin et al.* [95] studied the effects on the formation of contrails when flying with a parallel hybrid electric aircraft. The conventional Schmidt-Appleman criteria, which indicate the conditions of atmospheric water vapor pressure and environmental temperature to form persistent contrails, are adapted to globally estimate the potential contrail coverage when flying with hybrid electric aircraft.

6

Fleet-and-Network Integrated Aircraft Design

This chapter deals with the last research topic investigated in this literature study, which is the integration of aircraft design into an airline fleet-and-network model as seen in Figure 6.1. First, the relevance of the research topic is addressed in section 6.1. Secondly, a literature study is presented in section 6.2.

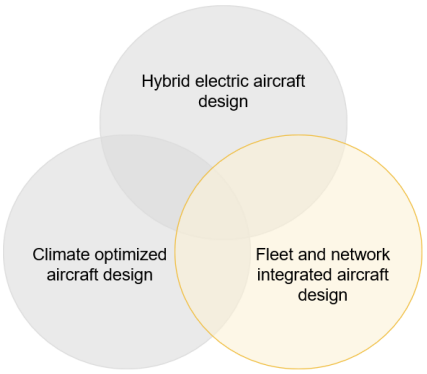

Figure 6.1: Research topic 3

6.1. Relevance of research topic

The environmental impact of air transportation is not only affected by efficient technologies and innovative aircraft designs, but also by the way these aircraft are used in the airline operations. Traditionally, the design of a new aircraft and the operational network are aspects determined independently of each other. Aircraft designers on one end, design a vehicle that satisfies the operational requirements, such as required mission range and capacity. Airline operators on the other hand, often assume the vehicle characteristics to be fixed by the design and determine the best allocation of the available aircraft in the fleet. There is a need for a tighter coupling between the operational planning by the airline operator and the design of new aircraft in order to allow for more efficient resource utilization and reduced climate impact. This can be achieved by considering fleet-and-network integrated vehicle design.

6.2. Literature review

Integrating the design of new aircraft in a fleet-and-network model is an interesting topic to ensure better resource allocation and reduction of climate impact. A lot of research has been performed considering kerosene powered aircraft. The author has found only one paper which (partly) covers network-optimized hybrid electric design.

Conventional aircraft

When coupling the design of aircraft in the context of a transportation network, the problem can be considered as a System-of-Systems (SOS). There is not a single and persistent definition for a SOS, but for this purpose the definition by *Crossley et al.* is listed as: *"The SOS describes a concept in which many independent, self-contained systems are brought together to satisfy a global need or needs"* [14]. Within a SOS, there is a mix of existing and yet-to-be-designed systems in which the latter must be designed with the goals of improving the SOS global performance.

Crossley at al. [14] investigated the SOS approach by considering a simplified problem of an airline trying to study how a yet-to-be-designer aircraft impacts the fleet operating costs. When considering variable resource allocation in the design optimization, the resulting statement is a mixed-integer, non-linear programming (MINLP) problem. These problems are hard to solve, but two approaches were applied and showed promising results. First, a response surface approach is used to model the airline design portion. Secondly, a decomposition approach is used, following the idea of multidisciplinary optimization. The problem is split into an aircraft allocation domain, which makes use of integer programming, and an aircraft design domain, making use of non-linear programming.

In 2007, *Taylor and Weck* [84] presented for the first time the benefits of concurrently defining and optimizing vehicle design into an integrated air transportation network. This was established by using a linear programming solver in the perturbation step of a simulated annealing algorithm. In this algorithm, the global optimum of a given function in a discrete and large search space is found in a probabilistic manner. The benefits of this new approach are shown through an example of an overnight package delivery air transportation system in the US.

The paper by *Mane et al.* [53], expands on the work performed by *Crossely et al.* [14]. They considered the concurrent aircraft design and resource allocation with a deterministic demand and only one coupling variable between the allocation and aircraft design problems via sequential decomposition. It was found that when the problem size increases, the decomposition approach can find solutions while traditional MINLP approaches could not and such this paper shows the scalablity of the coupled problem. This work was extended in multiple papers by *Mane et al.* by incorporating uncertain passenger demand by considering the uncertainty of on-demand fractional aircraft ownership operations [50] [51] [52].

Govindaraju and Crossley [30] investigated the effect of including a profit-motivated allocation for the concurrent aircraft design and fleet allocation. In this approach, the airline profit is maximised rather than an aircraft-specific objective which indirectly improves the fleet objective. Similarly, *Davendralingam and Crossley* [16] investigated the impact of aircraft design choices on the expected profit in a profit-motivated fleet allocation problem.

So far, maximizing profit has been the leading objective for aircraft designers. Nonetheless, with the increased concern on climate impact, the environmental performance of aircraft designs is becoming a new focus point. *Bower and Kroo* [8] performed a multi-objective aircraft optimization of a single-aisle conceptual aircraft considering economic and environmental performance. The objectives are to minimize the operating costs, CO_2 emissions and NO_x emissions of a fleet over the route network. *Govindaraju et al.* [31] also performed a multi-objective optimization for concurrent aircraft design and fleet assignment and examined the trade-offs between the reduction of fleet-level fuel consumption and some defined fleet-level performance metrics.

Alongside of the previously mentioned papers, research has been performed by *Jansen and Perez* on the coupled optimization of aircraft design and fleet allocation. A series of successive papers is presented, each extending on previous work. The first one covers the optimization of an aircraft family design and fleet assignment for minimum operating cost and fuel burn for a fixed deterministic trip demand in *Jansen et al.* [43]. In 2013, uncertain passenger demand was considered in *Jansen and Perez* [44]. Afterwards, the complexity of the problem was increased by including route networks in North America and Europe and comparing the trade-offs between different markets in *Jansen and Perez* [45]. Lastly, instead of optimizing a single aircraft for single markets independently, the paper in *Jansen and Perez* [46] presents the coupled optimization of a family of aircraft with the network allocation while considering operations in multiple markets.

In 2018, *Roy at al.* [73] found some shortcomings to the decomposition framework for which a significant amount of work has already been performed. They found that the subspace decomposition approach is not able to capture the synergy between the various subspaces and investigated an alternative approach for implementing this. Follow up efforts are performed by *Hwang and Martins* [35] [36] and *Roy and Crossley* [72]. Furthermore, more recent work of *Fregnani et al.* [28] [56] presents another new approach. The details of these studies will not be considered in this literature review as they mostly contain in-depth changes to the multidisciplinary design optimization approaches, which will not be part of the thesis work.

Hybrid electric aircraft

The author has found one article that considers the network-optimized design of a hybrid electric aircraft which was studied by *Weit et al.* [91]. In this study, a hybrid electric aircraft is designed by optimizing the hybridization ratio in order to maximize the aircraft direct operating profit. This is done by coupling three models: a network model, a vehicle model and an economics model. The network model considers the routes within the network of the airline Cape Air and basic mission requirements are gathered, such as mission profile, cruise altitude and range. In the vehicle sizing model, the Pilatus PC-12 is used as a baseline aircraft and the propulsion system is modified to a hybrid electric architecture. The outer shape, empty weight and maximum take-off weight of the original aircraft are kept fixed and such the power requirements for each phase of the mission are directly obtained from the PC-12 aircraft. Lastly, the profit is calculated in the economics module which employs a parametric cost build up as described by *Roskam* [71], modified to account for hybrid electric propulsion systems.

7

Research gaps, questions and objective

In this chapter, the literature described in previous chapters is critically studied to identify the research gaps present in current research. These research gaps are listed in section 7.1. After this, the research questions are provided in section 7.2. Lastly, in section 7.3, the research objective is stated.

7.1. Research gaps

In order to come up with the research questions and the research objective of the thesis work, the current gaps within the covered research domains should be investigated. As previously mentioned and depicted in Figure 2.1, three main topics were considered: hybrid electric aircraft design, climate optimized aircraft design and fleet-and-network integrated aircraft design. For each of these topics, relevant literature was studied and a literature review is presented. For the isolated topics, a lot of literature could be found, however, the main challenge was in finding research in the overlapping research areas. From this, two clear research gaps were identified:

- **Gap 1**: There is a research gap in the overlap between hybrid electric aircraft design and climate optimized aircraft design. First, when considering the current hybrid electric aircraft design methodologies, it can be observed that investigations were made on the influence of varying the design point for a chosen figure of merit such as maximum take-off weight, operational cost or energy efficiency. However, none of the methods directly include the effect of climate in the design of the hybrid electric aircraft. Secondly, considering literature found on the subject of climate optimized aircraft design, it can be seen that investigations were performed on the climate impact of hybrid electric aircraft. But also here, there is no direct coupling between climate and the design of the hybrid electric aircraft itself.

- **Gap 2**: There is a research gap in the overlap between hybrid electric aircraft design and fleet-and-network integrated design. Much effort has been made to couple the design of aircraft directly into a fleet-and-network model. However, this is mostly done for conventional kerosene-driven aircraft. One article was found that coupled the design of a hybrid electric aircraft for a given network, however this article did not design the aircraft itself but made use of a baseline conventional aircraft adapted for a hybrid electric propulsion system. So also here, the direct integration of clean-sheet hybrid electric aircraft design into a fleet-and-network model is missing.

Both gaps are visualized by the cross mark (X) in the Venn diagram as shown in Figure 7.1. In the diagram, there is one more area to be discussed: the overlap of the two research gaps marked with a question mark (?) in the figure. This area actually determines the research topic of the thesis work, which will investigate a combination of the currently missing research. For this area, research questions and a research objective are assembled.

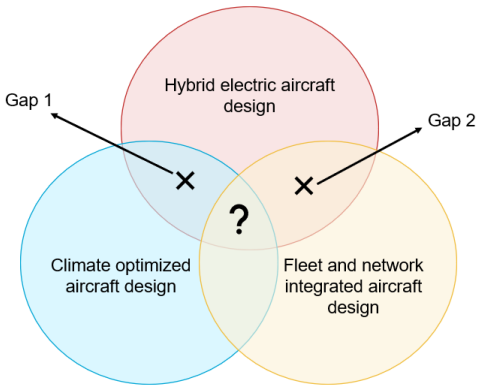

Figure 7.1: Research gaps

7.2. Research questions

The main research question to be solved during the thesis work is stated as follows:

> "*What is the optimal design point for a hybrid electric aircraft when integrating aircraft design in a fleet-and-network model and considering minimal climate impact?*"

The research question is split into sub questions and those are again split in smaller questions. The lower level questions will together provide the answer to the higher level questions.

1. What is the optimal design point for hybrid electric aircraft when considering optimization for climate by minimizing the CO_2 emissions?
   (a) What are the degrees of freedom when designing hybrid electric aircraft?
   (b) What is the relation between battery energy required and the CO_2 emissions from electricity production?
   (c) What is the optimal design point for minimal CO_2 emissions from burning kerosene and production of electricity?
2. How should the aircraft design tool be coupled with the fleet-and-network optimization tool?
   (a) What are typical inputs to a fleet-and-network optimization tool?
   (b) What are typical outputs of the fleet-and-network optimization tool?
   (c) What changes need to be made to connect a fleet-and-network optimization tool to aircraft design?
3. What is the effect of changing the aircraft design on the environmental and economical network performance?
   (a) What is the effect of changing the climate-optimized design point to a conventional design point on the network CO_2 and profit?
   (b) What is the effect of changing a top-level aircraft requirement on the network CO_2 and profit?
   (c) How will the output of the fleet-and-network optimization model change the aircraft design?

7.3. Research objective

The research objective describes the goal of the thesis project. This statement indicates what is to be achieved and how the author wants to achieve this goal.

> *This research aims to develop a methodology for the design of a climate optimized hybrid electric regional aircraft fleet by means of integrating aircraft design in a fleet-and-network model while considering the climate-optimal design point"*

8

Approach

In this chapter, an approach is presented to answer the research questions. This is done by splitting the work into two major tasks, which are similar to the research gaps identified. First, an approach is presented to design a hybrid electric aircraft for minimal climate impact in section 8.1. Secondly, a methodology is presented for the integration of hybrid aircraft design in the airline fleet-and-network model in section 8.2. The chapter will end with providing the thesis project planning in section 8.3.

8.1. Hybrid electric aircraft design for minimal climate impact

In order to conduct the preliminary sizing of the hybrid electric aircraft, the methodologies presented by *De Vries* [17] and *Finger* [27] were thoroughly studied. An adapted method is presented here which differs slightly from the existing methods. The adaptations focus on two main things: reduction of computational cost and integration of a climate figure of merit. The existing methods are quite computationally expensive, as it takes about 20 minutes to design a hybrid electric aircraft. In this study, the goal is to explore the design space for minimal climate impact and to directly integrate the design tool in an airline fleet-and-network model. For this, the computational time had to be reduced. Secondly, additional calculations should be made in order to include climate optimization in the design method.

Considering the design of the hybrid electric aircraft, the focus will be on those with a parallel hybrid architecture type, as seen in number 2 of Figure 3.1. The propulsive power is generated by a propeller. The power is provided by a gas turbine, which combusts kerosene fuel, and an electric motor, which is powered by a battery. This hybrid electric propulsion type is considered for three main reasons. First, a fully electric aircraft cannot be considered due the limited mission range. Secondly, the series hybrid electric propulsion architecture has a high weight due to the large electric motor. Lastly, the parallel hybrid electric architecture has a relatively low complexity.

For integrating the climate impact directly into the design of the hybrid electric aircraft, the aircraft will be optimized for a chosen climate metric. As already explained in the literature study on climate optimized aircraft design section 5.2, a climate metric can be used to identify the effect of various emission species on the climate. A suitable metric is for example the Average Temperature Response (ATR), which takes into account both long-lived and short-lived emissions. Modeling this effect requires a detailed mission analysis, which is not suited for this research. For this reason, the results from the study of *Thijssen* [86] were used to guide towards a suitable climate metric. The study shows that for low altitude operations, the climate impact is governed by the CO_2 emissions and short-lived emissions dependent on fuel burn. Thus, it was decided to optimize the aircraft for minimum CO_2 emissions. However, not only the CO_2 emissions of combustion will be taken into account, but also those coming from the production of energy as previously studied by *Scholz et al.* [78]. This will give a better indication on how much hybrid electric aircraft are actually contributing to a lower climate impact.

An initial extended design structure matrix (XDSM) was set-up in Figure 8.1 to visualize the climate optimization and the hybrid electric aircraft design set-up. The aircraft design module is governed by the Aircraft

Synthesizer. The inputs are the the aircraft parameters and performance requirements, shown in the diagram as REQ. The synthesizer consists of seven disciplines: Class I Weight Estimation, Power-Loading Diagram, Aircraft Geometry, Aerodynamic Module, Propulsion Weight Calculation, Class II Weight Estimation and Energy analysis. These disciplines will be explained further in this section. The Aircraft Synthesizer will design the aircraft by looping through the different disciplines until the value of maximum take-off weight (W_{TO}) converges. Furthermore, an optimization for climate will be executed. Traditionally, the design point in the power-loading diagram is selected for minimum power-over-weight ratio (P/W) and maximum wing loading (W/S) as this gives a good indication on the minimal operating cost of the aircraft. However, in this analysis the effect of changing the design point on a climate figure of merit will be investigated. Therefore, the wing loading and power split value will be changed in order to minimize the climate impact by minimizing the value of CO_2 emissions from both the combustion of kerosene and the production of electricity.

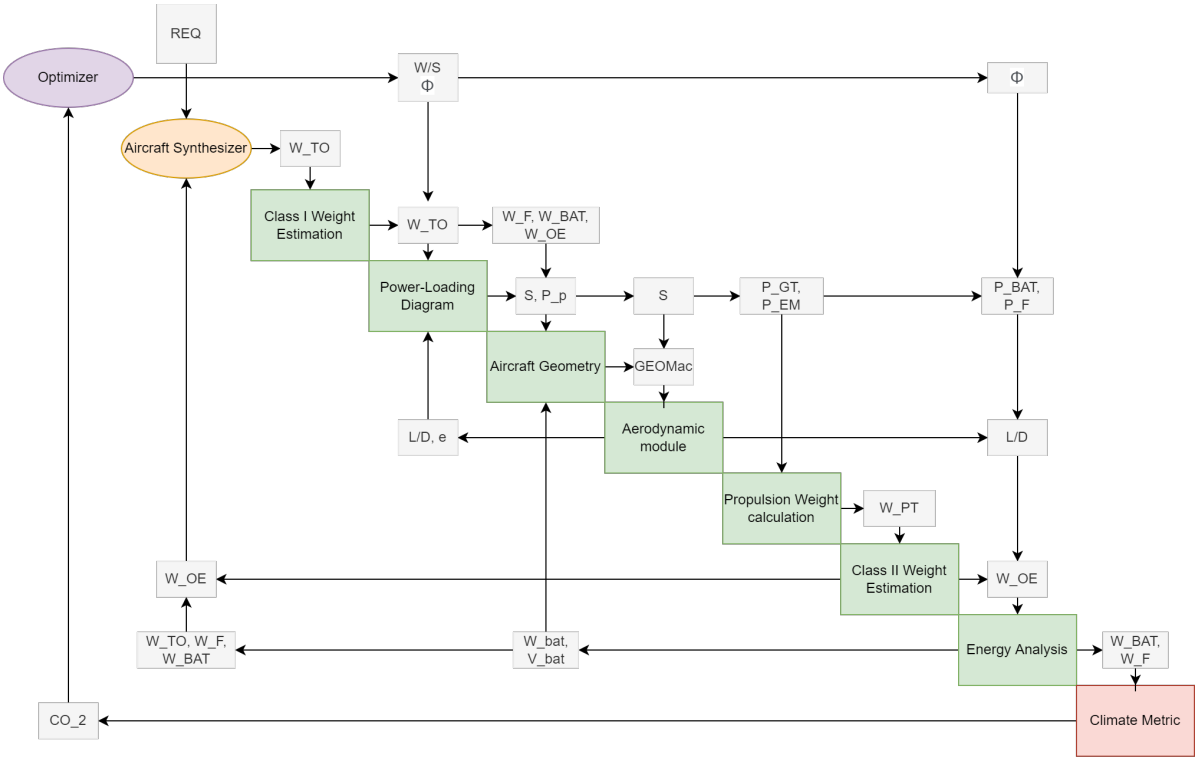

Figure 8.1: Hybrid electric aircraft sizing and optimization approach

Class I Weight Estimation

In order to initialize the sizing process of the aircraft, an initial Class I weight estimation will be performed to provide the values of maximum take-off weight, operational empty weight, fuel weight and battery weight to the subsequent disciplines. It should be noted that this Class I weight estimation will only run once to provide the initial guess values, however the values will later be updated by a more accurate Class II weight estimation.

Power-Loading Diagram

The constraint analysis consists of setting up the aircraft power-loading diagram for different aircraft performance constraints, as also done in traditional conventional aircraft Class I sizing methods. The diagram depicts the weight-over-power (W/P) ratio versus the wing loading (W/S). From the power-loading diagram in the constraint analysis, the feasible design space can be determined. The constraints considered for the analysis are:

- Stall speed constraint
- Take-off distance constraint
- Cruise speed constraint

- Climb rate constraint
- Climb rate constraint with one engine inoperative (OEI)

When looking at hybrid electric aircraft, the power-loading diagrams can be split up in multiple power-loading diagrams for each component in the powertrain. In order to do so, a powertrain matrix is used to deduce the power requirements of the different powertrain components. This methodology is presented in the PhD thesis of *De Vries* [17], for the use of a serial/parallel partial hybrid electric powertrain architecture (number 6) as shown in architectural descriptions in Figure 3.1. The powertrain matrix can be seen in Equation 8.1 where the signs of the efficiencies are selected such that the power flows in the direction of the full arrow heads in the architecture description of Figure 3.1. The matrix has the constant powertrain component efficiencies (η) and the aircraft propulsive power (P_p) as an input, of which the latter can be obtained from the aircraft level power-loading diagram.

$$\begin{bmatrix} -\eta_{GT} & 1 & 0 & 0 & 0 & 0 & 0 & 0 & 0 & 0 \\ 0 & -\eta_{GB} & 1 & 1 & 0 & 0 & 0 & 0 & 0 & 0 \\ 0 & 0 & 0 & -\eta_{P1} & 0 & 0 & 0 & 0 & 1 & 0 \\ 0 & 0 & -\eta_{EM1} & 0 & 1 & 0 & 0 & 0 & 0 & 0 \\ 0 & 0 & 0 & 0 & -\eta_{PMAD} & -\eta_{PMAD} & 1 & 0 & 0 & 0 \\ 0 & 0 & 0 & 0 & 0 & 0 & -\eta_{EM2} & 1 & 0 & 0 \\ 0 & 0 & 0 & 0 & 0 & 0 & 0 & -\eta_{P2} & 0 & 1 \\ \Phi & 0 & 0 & 0 & 0 & (\Phi-1) & 0 & 0 & 0 & 0 \\ 0 & 0 & 0 & \phi & 0 & 0 & 0 & (\phi-1) & 0 & 0 \\ 0 & 0 & 0 & 0 & 0 & 0 & 0 & 0 & 1 & 1 \end{bmatrix} \begin{bmatrix} P_f \\ P_{gt} \\ P_{gb} \\ P_{s1} \\ P_{e1} \\ P_{bat} \\ P_{e2} \\ P_{s2} \\ P_{p1} \\ P_{p2} \end{bmatrix} = \begin{bmatrix} 0 \\ 0 \\ 0 \\ 0 \\ 0 \\ 0 \\ 0 \\ 0 \\ 0 \\ Pp \end{bmatrix} \tag{8.1}$$

Additionally, the designer has to define three power control parameters. The first one is the supplied power ratio (Φ), originally defined by *Isikveren et al.* [41] and shown in Equation 8.2. This ratio determines the amount of power drawn from the electrical energy source, in this case the batteries, with respect to the total amount of power drawn from all energy sources, in this case the batteries and fuel. This ratio is similar to the definition of the degree of hybridization of power (H_p) as discussed in **??**, with the difference that H_p specifies the power split at the node (e.g. gearbox for parallel hybrid architecture), while Φ specifies the power split at the energy sources.

$$\Phi = \frac{P_{bat}}{P_{bat} + P_f} \tag{8.2}$$

A second parameter is the shaft power ratio (ϕ) shown in Equation 8.3. This ratio presents the amount of shaft power produced by the secondary electrical machines with respect to the total shaft power.

$$\phi = \frac{P_{s2}}{P_{s2} + P_{s1}} \tag{8.3}$$

Lastly, the designer has to specify the gas-turbine throttle (ξ_{GT}) as shown in Equation 8.4. This parameter represents the power produced by the gas turbine with respect to the maximum power it can produce.

$$\xi_{GT} = \frac{P_{GT}}{P_{GT_{max}}} \tag{8.4}$$

In this study, the focus will be on parallel hybrid electric aircraft architecture and the power flow paths are changed such that both the battery and turbine provide power to the primary propulsive system. Furthermore, the analysis is changed to first determine the power-loading diagram using the relative powers (W/P_i) instead of the absolute values (P_i). The matrix is now changed to the one shown in Equation 8.5.

$$\begin{bmatrix} -\frac{1}{\eta_{GT}} & 1 & 0 & 0 & 0 & 0 & 0 \\ 0 & -\frac{1}{\eta_{GB}} & -\frac{1}{\eta_{GB}} & 1 & 0 & 0 & 0 \\ 0 & 0 & 0 & -\frac{1}{\eta_{P1}} & 0 & 0 & 1 \\ 0 & 0 & -1 & 0 & \frac{1}{\eta_{EM1}} & 0 & 0 \\ 0 & 0 & 0 & 0 & 1 & -\frac{1}{\eta_{PMAD}} & 0 \\ \frac{1}{\Phi} & 0 & 0 & 0 & 0 & \frac{1}{(\Phi-1)} & 0 \\ 0 & 0 & 0 & 0 & 0 & 0 & 1 \end{bmatrix} \begin{bmatrix} W/P_f \\ W/P_{gt} \\ W/P_{gb} \\ W/P_{s1} \\ W/P_{e1} \\ W/P_{bat} \\ W/P_{p1} \end{bmatrix} = \begin{bmatrix} 0 \\ 0 \\ 0 \\ 0 \\ 0 \\ 0 \\ W/P_p \end{bmatrix} \tag{8.5}$$

The power matrix is applied to all constraint lines in the aircraft power-loading diagram in order to draw the constraint lines for the component-specified power-loading diagrams. Thus, for each constraint a different set of inputs can be provided. In this study, the power split will be constant for one constraint, but different from the other constraints. For the stall speed constraint, a power split of zero is used, as no electrical power system is used. For the take-off and rate of climb constraints, a constant (non-zero) value for power split will be chosen. The power split for the cruise phase is a variable, and will be varied in order to investigate the effect of power split on the design. Furthermore, the power-loading diagram from the gas turbine is corrected for the input throttle settings. Throttle settings will be selected for each constraint as well.

Now that the component power-loading diagrams are obtained, one can select a design point (combination of W/S and Φ). With the initial W_{TO} the absolute values of power of the respective powertrain components are calculated.

Aircraft Geometry

An initial aircraft geometry layout is generated which conceptually sizes the fuselage, wings and stabilizers of the hybrid electric aircraft. The sizing equations are obtained from the conventional aircraft sizing methods as given by *Torenbeek* [87] and *Raymer* [68]. An adaptation to the fuselage size will be made to account for the additional volume of the aircraft battery.

Aerodynamic Analysis

From the aircraft geometry, the aerodynamic values of drag coefficient (C_D) and Oswald efficiency factor (e) can be updated according to the method from *Obert* [60]. To get an estimation of the drag of the entire aircraft, the geometry is divided into elements and the sum of the drag of each element is taken.

Propulsion Weight Calculation

In the Propulsion Weight module, the weight of the hybrid electric powertrain (W_{PT}) is determined. A detailed weight estimation will be performed, which sums up the weights of the different powertrain components. The weight of the gas turbine and electric motor can be calculated from the power requirements and assuming a specific power value. For the other components, Class II estimations or statistical data can be used.

Class II Weight Estimation

In the Class II analysis, the operational empty weight is calculated, as this value is later used in the energy analysis. To do so, traditional Class II weight estimation methods are followed to obtain the weight of the different aircraft structural components. For this study, the operational empty weight of hybrid electric aircraft is determined in a similar way as that of conventional aircraft, with the exception of the powertrain weight. It is assumed that the weight of the powertrain of hybrid electric aircraft is more heavy than that of conventional kerosene-driven aircraft and is therefore considered separately. Therefore, the operational empty weight (W_{OE}) is the sum of the operational empty weight of conventional aircraft minus the contribution of the conventional powertrain weight (W'_{OE}) plus the hybrid electric powertrain weight (W_{PT}) which was calculated in the previous discipline. The relations are shown in Equation 8.6.

$$\begin{aligned} W_{OE} &= W'_{OE} + W_{PT} \\ W'_{OE} &= W_{OE_{conv}} - W_{PT_{conv}} \end{aligned} \tag{8.6}$$

Energy Analysis

The energy analysis is simplified with respect to the approaches given by *De Vries* and *Finger* in order to reduce the computational cost. Instead of a time-stepping approach which divides the mission into segments, a modified Breguet range equation will be used to calculate the energy required in the cruise phase. To determine the energy required for the other mission phases (take-off and climb and descent), the power split ratio and conventional fuel fraction methods will be used.

For hybrid electric aircraft, a modified range equation has been derived by *De Vries et al.* [19] as seen in Equation 8.7. This equation relates the range (R) to the total energy of the cruise phase of the mission ($E_{0_{tot}}$). This equation assumes a constant power split (Φ) and constant aircraft parameters: aircraft efficiencies (η_i), battery- and fuel-specific energies (e_b, e_f), lift-to-drag ratio (L/D), operational empty weight (W_{OE}) and payload weight (W_{PL}). For a given range, the total energy of the cruise phase is calculated. This total energy is split over the two energy sources (battery and fuel) through the power split ratio as seen in Equation 8.8.

$$R = \eta_3 \frac{e_f}{g} \left(\frac{L}{D}\right) \left(\eta_1 + \eta_2 \frac{\Phi}{1-\Phi}\right) ln \left[\frac{W_{OE} + W_{PL} + \frac{g}{e_f} E_{0_{tot}} \left(\phi + \frac{e_{bat}}{e_f}(1-\Phi)\right)}{W_{OE} + W_{PL} + \frac{g}{e_{bat}} \Phi E_{0_{tot}}} \right] \tag{8.7}$$

$$\begin{aligned} E_{0_{bat}} &= \Phi E_{0_{tot}} \\ E_{0_f} &= (1-\Phi) E_{0_{tot}} \end{aligned} \tag{8.8}$$

From the mission analysis, the fuel weight (W_f) is obtained directly. The battery weight (W_{bat}), on the other hand, still has to be calculated. To do so, the battery should be sized for both the energy requirement and the power requirement. From the mission analysis, the total energy required from the battery was determined. When assuming a battery specific energy value, the battery weight can be obtained. To this value, a 20% margin is added to limit the state of charge of the battery in order to avoid reducing the battery cycle life. To size the battery for power, the required battery power is obtained from the powertrain model analysis. When assuming a battery specific power value at pack level, the weight of the battery can be calculated. The highest value of the two will eventually determine the battery weight.

For this calculated fuel and battery weight, the maximum take-off weight can be re-calculated from Equation 8.9, where W_{OE} is the operational empty weight previously obtained from the Class II weight estimation and W_{PL} is the weight of the payload which is an aircraft design input. With this new maximum take-off weight, the design loop is entered again and the values of maximum take-off weight, operational empty weight, fuel weight and battery weight are updated.

$$W_{TO} = W_{OE} + W_{PL} + W_f + W_{bat} \tag{8.9}$$

Aircraft Design Model

The above mentioned approach is somewhat similar to the preliminary sizing of conventional aircraft. A conceptual aircraft design tool exists at the Faculty of Aerospace Engineering in the Flight Performance and Propulsion (FPP) department, developed by *Proesmans*. This tool is able to size conventional kerosene-driven aircraft and hydrogen driven aircraft. The goal is to implement this proposed methodology into the existing tool. For this, attention should be payed to the existing sizing models and check which parts can directly be used or which modules need adaptations in order to account for hybrid electric propulsion systems. Furthermore, in this research only parallel hybrid propulsion systems will be considered, but the tool should be coded such that it can easily be extended for other propulsion architectures or innovative integrated designs, such as distributed propulsion.

8.2. Integration of the Aircraft Design Tool with the Fleet-and-Network Model

After implementing the methodology for the design of hybrid electric aircraft for minimal climate impact in the Aircraft Design Model, it can be used to size aircraft and integrate the tool within Fleet-and-Network Model. For the Fleet-and-Network Model, an existing optimization scheme will be used which is designed by *Santos* at the Air Transport And Operations (ATO) department of the Faculty of Aerospace Engineering.

This tool requires a set of input aircraft by the means of an aircraft database and will determine the optimum allocation of aircraft and network for a chosen objective.

As described in the literature review on fleet-and-network integrated design (**??**), the integration results in a mixed-integer non-linear programming (MINLP) problem which are very hard to solve. In this research an iterative approach will be used to integrate aircraft designs and airline network planning. The intended approach is depicted in a flowchart in Figure 8.2. The approach will make use of two models: the Aircraft Design Model and the Fleet-and-Network model.

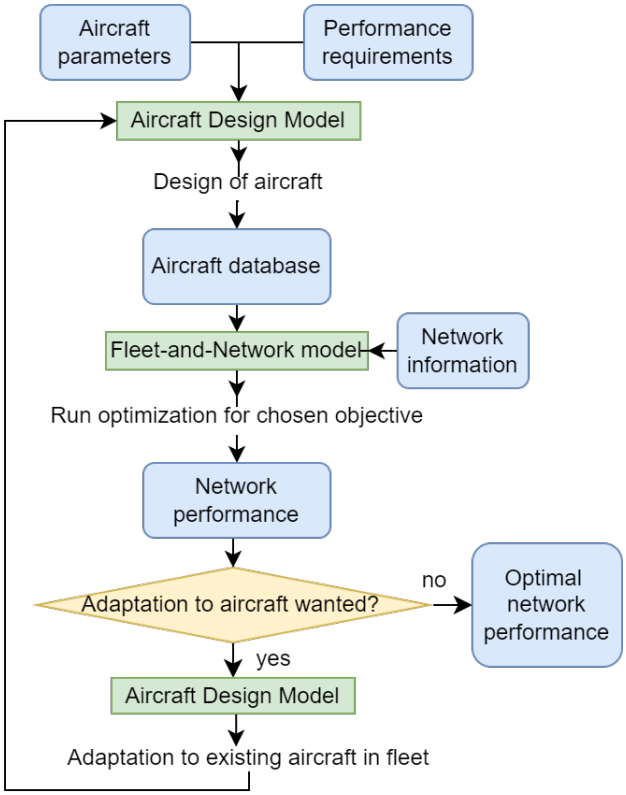

Figure 8.2: Aircraft design integration approach

Aircraft Design Model

First, a set of initial aircraft should be designed. For this, different aircraft parameters and performance requirements need to be set by the designer (or the airliner). With these inputs, the hybrid electric aircraft can be designed according to the methodology presented before and gathered in an aircraft database. Relevant aircraft performance characteristics are calculated which are needed for the integration with the Fleet-and-Network Model.

Fleet-and-Network Model

The Aircraft Design Model will be integrated in the Fleet-and-Network Model. An aircraft database and airline network information will be fed to the Fleet-and-Network model. The model will determine the network and fleet choice to optimize a chosen objective. In this research, two objectives will be considered. First, the profit of the airline can be maximized. Secondly, it is possible to minimize the CO_2 emissions. It should be noted that currently the CO_2 emissions are modeled in a simplified fashion. Therefore, the CO_2 estimation will be updated for more accurate outcomes. After running the Fleet-and-Network model, adaptations can be made to the existing aircraft in the database. Currently, two options can be defined for changing the existing aircraft. First, one can keep all top level performance requirements constant and simply adjust the design point. This will result in a change in the mass breakdown, power requirements and wing surface area. The different fuel mass will in its term change the amount CO_2 emissions from burning kerosene. The new battery mass will change the amount of CO_2 emissions coming from the electricity production. Due to this, also the airline

profit is different in case a CO_2 tax is applied. The adaptations to the aircraft design can also be more radical by changing the top level requirements of the aircraft such as altering the range and payload. The changes made to the aircraft designs are added to the existing aircraft database and one can observe the effect on the network and fleet performance. It is still to be determined how the network performance output will dictate a change in aircraft design in order to close the loop.

8.3. Thesis Planning

A thesis time planning has been made by means of a Gantt Chart and is depicted on the next page. The chart is split in four parts: (1) Literature study, (2) Thesis work, (3) General milestones and (4) Holidays. First, the planning for the literature study is presented, which lasts for 9 weeks rather than the conventional 8 weeks to account for the holidays during this time period. During this period, also the Research Methodologies course is followed and accounted for in the planning. Secondly, after the summer holidays, the actual thesis work will start and will last for about 6 months. During this work, two phases can be distinguished, which are similar as presented in the approach in chapter 8: (1) Hybrid electric aircraft design for minimal climate impact and (2) Integration of aircraft design tool with fleet-and-network model. In the first phase, the existing aircraft sizing tool will be studied and the hybrid electric aircraft sizing methodology is implemented. This method is then verified. A suggestion is to verify the sizing code with the cross-validation study of *De Vries* and *Finger* [26], as this paper clearly shows the selected inputs. Afterwards, the climate optimization is to be implemented. When the aircraft sizing model is finished, the second phase of the project starts. Also here, this phase starts with studying the existing code and making the necessary adaptations to this code. Then, the actual integration of both models is performed and the best method should be determined in which a feedback loop is created between aircraft design and network performance. The effects of different designs on the network performance should be studied and the desired changes to the aircraft design should be determined from the network performance outputs. To test the integration of the models, a case study and sensitivity study should be carried out. In the general milestones part, the key review points are depicted. These are the thesis kick-off, midterm meeting and green light meeting.

teamgantt
Created with Free Edition

Thesis Planning	start	end
Literature study	**25/04/22**	**05/08/22**
Kick off meeting	25/04	25/04
Information Literacy course	26/04	26/04
Research Methodologies course	28/04	29/04
Review of concepts	02/05	06/05
Review of design methodologies	09/05	13/05
Review of fleet integration	16/05	20/05
Identify research gap	23/05	25/05
Define research objectives	30/05	03/06
Define thesis approach	06/06	10/06
Iterate	13/06	17/06
Write project plan	13/06	23/06
Hand in project plan	24/06	24/06
Write literature study	06/06	23/06
Hand in literature study	24/06	24/06
Prepare literature presentation	03/08	04/08
Literature study presentation	05/08	05/08
Thesis work	**27/06/22**	**19/01/23**
Set up github and start up	27/06	01/07
Study existing sizing code	25/07	12/08
Implement hybrid electric aircraft siz...	15/08	02/09
Verification of hybrid electric sizing c...	05/09	16/09
Implement climate optimization	19/09	30/09
Study existing fleet and network mo...	03/10	14/10
Make changes to existing fleet and n...	17/10	28/10
Integrate sizing module and fleet and...	31/10	18/11
Case study	21/11	02/12
Sensitivity study	05/12	16/12
Buffer time 1/2	19/12	23/12
Buffer time 2/2	09/01	19/01
General milestones	**25/04/22**	**28/02/23**
Thesis kick-off	25/04	25/04
Write project plan	13/06	23/06
Hand in Project Plan	24/06	24/06
Write literature study	06/06	23/06
Hand in Literature Study	24/06	24/06
Prepare midterm meeting	23/11	24/11
Midterm meeting	25/11	25/11
Write draft thesis 1/2	05/12	23/12
Write draft thesis 2/2	09/01	19/01
Hand in thesis draft	20/01	20/01
Prepare greenlight meeting	23/01	25/01
Greenlight meeting	26/01	26/01
Review greenlight meeting	30/01	03/02
Request examination	27/01	27/01
Implement thesis feedback	06/02	15/02
Hand in thesis	17/02	17/02
Prepare defence presentation	20/02	24/02
Thesis defence	28/02	28/02
Holidays	**27/04/22**	**06/01/23**
Kingsday	27/04	27/04
Liberation day	05/05	05/05
Ascension day	26/05	27/05
Pentecost	05/06	06/06
Summer holiday	04/07	22/07
Christmas holiday	26/12	06/01

9

Conclusion

This paper presents the literature study performed in advance of the thesis work. The goal was to study the existing literature, define the research gaps in current research and come up with a research objective for the thesis work. In this work, the integration of hybrid electric aircraft in a fleet-and-network model will be investigated in order to limit aviation climate impact. For this purpose, three research topics have been studied. First, hybrid electric aircraft design methods are looked at and conceptual clean-sheet hybrid electric aircraft design approaches were found in recent literature. Secondly, climate optimized aircraft design studies were reviewed. A multidisciplinary design optimization can be implemented to minimize a climate objective. The latest studies make use of advanced climate models and comprehensive climate metrics which take into account the location and lifetime of the emitted aircraft species. This research often focuses on conventional kerosene-driven aircraft. From this, a first research gap was identified. There is no direct coupling of climate impact reduction in clean-sheet hybrid electric aircraft design. The last research topic considered is the integration of aircraft design into a fleet-and-network model. In this research area, a lot of studies were performed on integrating conventional aircraft design in the airline network planning to ensure optimal usage of resources and such reduce the climate impact. A second research gap was identified when considering hybrid electric aircraft. Also here, there is no direct integration of hybrid electric aircraft design in the airline fleet-and-network allocation. From the identified research gaps, the objective of the thesis work can be identified. The objective of the project is to develop a methodology for the design of a climate optimized hybrid electric regional aircraft fleet. To achieve this, aircraft design will be integrate in a fleet-and-network optimization model while considering the climate optimal design point of a hybrid electric aircraft. Hybrid electric aircraft are sized according to adapted Class I and Class II sizing methods and a simplified mission analysis. The energy required for a certain mission is approximated using a modified Breguet range equation to minimize the computational cost of the sizing procedure. The current project will focus on a parallel hybrid electric architecture. The sizing modules will be used in a multidisciplinary design optimization in which a chosen climate metric is minimized. For this purpose, CO_2 emissions from burning kerosene and CO_2 emissions from the production of electricity will be used as a climate metric. Direct integration of aircraft design in a network model leads to a mixed-integer non-linear programming (MINLP) problem which are difficult to solve. This project will make use of in iterative approach in order to avoid this MINLP statement. The fleet-and-network model requires a set of aircraft stored in an aircraft database and relevant network information. The fleet and network choice is determined by running the fleet-and-network optimization model for a chosen objective. The possible objectives are maximization of airline profit or minimization of fleet CO_2 emissions. Adaptations to the aircraft in the aircraft database can be made and the effect on network performance can be studied. These adaptations can consist of changing the aircraft design point from a climate optimized design to conventional aircraft design point and thereby keeping all aircraft top level performance requirements constants. Or else, one can change the aircraft top level requirements such as aircraft capacity or range. It is still to be determined how the network performance outcome will force a change in aircraft design. The outcomes of this study can be used by aircraft manufacturers to develop hybrid electric aircraft suitable for regional airline operations and therefore stimulate the implementation of electrified aircraft to limit aviation climate impact.

III

Supporting work

1

Hybrid-Electric Aircraft Design Module

1.1. Power-Loading Diagrams

An aircraft is sized by several loading requirements e.g. stall speed requirement, cruise speed requirement, take-off length requirement, climb rate requirement or climb gradient requirement. All requirements, except from the climb rate requirement, are obtained from preliminary sizing methods, such as outlined by *Raymer* [68]. The method used to determine the power-loading values for the climb rate requirement is obtained from *De Vries* [17] and implemented to allow verification and validation of the hybrid-electric sizing modules. Preliminary sizing methods often assume a constant climb rate velocity, while the method outlined in *De Vries* makes use of a varying climb rate velocity with a constant margin with respect to stall speed. The derivation of the relation between wing-loading and power-loading for the climb rate constraint is shown in Equation 1.1.

$$
\begin{aligned}
V_s &= \sqrt{\frac{\frac{W}{S}}{\frac{1}{2}\rho C_{L_{max}}}} \\
V &= 1.2 V_s \\
q_\infty &= \frac{1}{2}\rho V^2 \\
C_{L_{airf}} &= \frac{\frac{W}{S}\sqrt{1-(\frac{c}{V})^2}}{q_\infty} \\
\frac{T}{W} &= \frac{q_\infty}{\frac{W}{S}}\left(C_{D_0} + \frac{C_{L_{airf}}^2}{\pi A e}\right) + \frac{c}{V} \\
\frac{W}{P} &= \frac{1}{V\frac{T}{W}}
\end{aligned}
\tag{1.1}
$$

The hybrid-electric powertrain matrix presented by *De Vries* [17] is valid for hybrid-propulsion system architectures in a series/parallel partial hybrid configuration as shown in the schematic of Figure 1.1. The study presented in this thesis makes use of a simple parallel-hybrid architecture, which is in fact a limit case of the series/parallel partial hybrid configuration as it does not employ secondary powertrain components. The powertrain matrix provides the results for the power paths between the components of the powertrain. To obtain the power required by each component, the input power paths are summed. It is assumed that both battery and gas turbine are providing power to the propulsion system, resulting in the power paths as shown in Figure 1.2. The component powers are defined as seen in Equation 1.2. It should be noted that for the gas turbine, the output power flow (P_{gt}) is used instead of the input one (P_f), this because all weight correlations for gas turbines are based on the shaft power of the gas turbine and not the fuel power required.

$$
\begin{aligned}
P_{GT} &= P_{gt} \\
P_{GB} &= P_{gt} + P_{gb} \\
P_{EM1} &= P_{e1} \\
P_{EM2} &= P_{e2} = 0 \\
P_{P1} &= P_{s1} \\
P_{P2} &= P_{s2} = 0 \\
P_{PMAD} &= P_{bat} \\
P_{BAT} &= P_{bat}
\end{aligned}
\tag{1.2}
$$

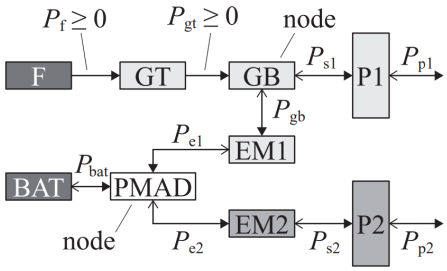

Figure 1.1: Series/parallel hybrid electric powertrain architecture and power-flow paths from *De Vries* [17]

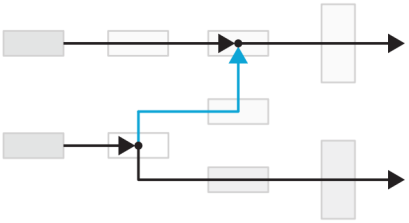

Figure 1.2: Power-flow paths for architecture where battery and gas turbine are providing power to propeller from *De Vries* [17]

In this thesis, the degree of electrification of the propulsion system is characterized by the supplied power split value (Φ). This value is similar to the definition of degree of hybridization of power (H_P) often used in literature. The difference is that H_P specifies the power split at the node (gearbox), while the Φ specifies the power split at the energy source (battery and fuel). The degree of hybridization of power for parallel hybrid-electric architectures can be related to the supplied power split value using the relation given by *De Vries* [17] and shown in Equation 1.3.

$$
\Phi = \frac{1}{1 - \frac{\eta_{gb}}{\eta_{gt}} \frac{(1-H_P)}{H_P}} \tag{1.3}
$$

1.2. Aircraft Geometry

The conceptual aircraft geometry is sized with the sizing equations outlined in *Torenbeek* [87] and the turboprop dimensions are sized by the equations in *Thijssen* [86]. The hybrid-electric aircraft geometry therefore does not differ from conventional aircraft, however the volumetric constraints are considered for placing the battery. The available wing tank volume is calculated using the formula from *Torenbeek* [87]. The equation is shown in Equation 1.4 and depends on the wing area S, wing span b, thickness-to-chord ratio at the wing root/tip $(t/c)_{r/t}$ and the taper ratio λ.

$$
V_t = 0.54 \frac{S^2}{b} (t/c)_r \frac{1 + \lambda \sqrt{\frac{(t/c)_r}{(t/c)_t}} + \lambda^2 \frac{(t/c)_r}{(t/c)_t}}{(1+\lambda)^2} \tag{1.4}
$$

The battery is stored in the wing, together with the fuel if Equation 1.5 is satisfied. A factor 1.1 was added to provide additional room for the cables, a factor 1.2 was added to account for the fact that the battery volume is a solid block which cannot occupy the wing tank volume properly.

$$
V_f + V_{bat} \cdot 1.2 \cdot 1.1 \leq V_t \tag{1.5}
$$

If the battery cannot fit in the wing, it will be positioned in the fuselage compartment underneath the floor. The height of this compartment is obtained from the conceptual cabin cross-section sizing. The width and height of the battery are determined such that it fits underneath the floor and has the largest cross-sectional area, shown by the colored squares in Figure 1.3. The battery volume is then simply the frontal area

times 80% of the fuselage cabin length. The battery is located in the fuselage compartment if Equation 1.6 is satisfied, which again accounts for a 1.1 factor to provide additional room for cables.

$$V_{bat} \cdot 1.1 \leq V_{fuselage\_compartment} \tag{1.6}$$

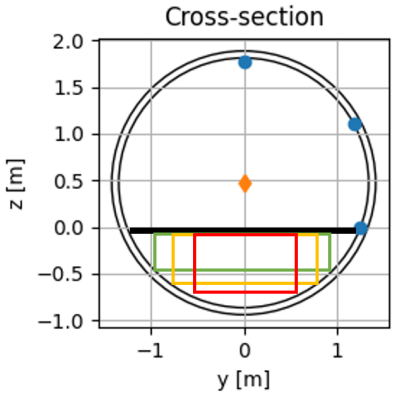

Figure 1.3: Battery location in fuselage compartment. Blue points: aisle height, cabin seat height, floor location; Colored squares: possible battery width and height combinations

If the battery cannot fit in the wing or in the fuselage compartment under the floor, the hybrid-electric aircraft design is considered infeasible.

1.3. Hybrid Powertrain Weight Estimation

Calculating the hybrid-electric powertrain weight is done by summing the following powertrain component masses: electric motor EM, gas turbine GT and propeller P. The component masses are not obtained from classical Class II weight predictions but estimated from the component required power and specific power values. In the approach, the electric motor (EM) and power management and distribution box ($PMAD$) are combined and due to the lack of information on cooling systems and cables, a 30% weight penalty is included in the equivalent specific power of the electric motor. The electric motor weight is then obtained from the required electric motor take-off power (P_{EM} $[W]$) and equivalent specific power ($SP_{EM,eq}$ $[W/kg]$). The equivalent specific power is calculated from state-of-the art specific powers of electric motor and converters and the assumed weight penalty as seen in Equation 1.7.

$$SP_{EM,eq} = \left[\left(\frac{1}{SP_{EM}} + \frac{1}{SP_{convert}} \right) \cdot 1.3 \right]^{-1} \tag{1.7}$$

Also the gas turbine (GT) and gearbox (GB) are combined for the weight estimation. Opposed to the electric motor, the gas turbine specific power is calculated rather than obtained from state-of-the art research. The gas turbine specific power is determined by calculating the weight of the gas turbine with a Class II weight estimation and the power required by the gas turbine for a conventional kerosene aircraft. The Class II weight estimation shown in *Teeuwen* [85] is used, where the total gas turbine mass consists of the engine mass, fuel system mass and propulsion system mass. The propulsion system mass itself consists of the engine control mass, starting system mass and propeller control mass (Equation 1.8).

$$\begin{aligned} m_{GT} &= m_{eng} + m_{fs} + m_{prop} \\ m_{prop} &= m_{ec} + m_{ess} + m_{pc} \end{aligned} \tag{1.8}$$

Laslty, the propeller mass is added to the hybrid powertrain weight using Equation 1.9 from *Teeuwen* [85], where d_P is the propeller diameter, P_{TO} is the take-off power and B is number of propeller blades.

$$m_P = 1.1(d_P P_{TO} \sqrt{B})^{0.52} \tag{1.9}$$

1.4. Energy Analysis

The energy analysis is used to determine the fuel and battery mass required to perform the design mission. This module makes use of a modified hybrid-electric range equation derived by *De Vries et al.* [19] to estimate the energy required for cruise. The energy required during the other mission phases is obtained from the conventional fuel fractions, combustion and electrical efficiencies and the supplied power split values. For each segment, the propulsive energy required to perform the mission segment (E_p $[Wh]$) is calculated from the conventional fuel fractions using Equation 1.10. The fuel mass required by a conventional aircraft during this mission phase ($m_{f,conv}$ $[kg]$) is multiplied with the combustion efficiency (η_{comb} [%]) and the specific energy of the fuel (e_f $[Wh/kg]$). For a hybrid-electric aircraft with a parallel architecture, this energy is provided by both the fuel and the battery and are related to the combustion efficiencies (η_{comb}), the electrical efficiencies (η_{el}), and power split (Φ) according to Equation 1.11. The combustion and electrical efficiencies are defined in terms of the component branch efficiencies of *De Vries* [19]: η_1, η_2, η_3. The equation can be rewritten to obtain the total energy required during the mission phase and can be seen in Equation 1.12.

$$E_p = m_{f,conv} \cdot \eta_{comb} \cdot e_f \tag{1.10}$$

$$\begin{aligned} E_p &= E_f \cdot \eta_{comb} + E_{bat} \cdot \eta_{el} \\ \Leftrightarrow E_p &= E_{tot} \cdot (1-\Phi) \cdot \eta_{comb} + E_{tot} \cdot \phi \cdot \eta_{el} \end{aligned} \tag{1.11}$$

$$E_{tot} = \frac{E_p}{\eta_3 \cdot \eta_1 \cdot (1-\Phi) + \eta_3 \cdot \eta_2 \cdot \Phi} \tag{1.12}$$

The energy analysis is significantly simplified with respect to generic time-stepping mission analysis, where the aircraft states are known at all times in the mission. The current energy analysis is a modified fuel fraction method and therefore does not take into account the effects of aircraft operating conditions (such as altitude and velocity) on the fuel and battery mass estimations. A couple of corrections were implemented to include the most important effects of flight velocity and altitude.

1. First, a propeller efficiency correction is applied according to the relation with Mach number outlined in *Torenbeek* [87] and shown in graph in Figure 1.4. The propeller efficiency line is fitted with a 4th order polynomial as seen in Equation 1.13.

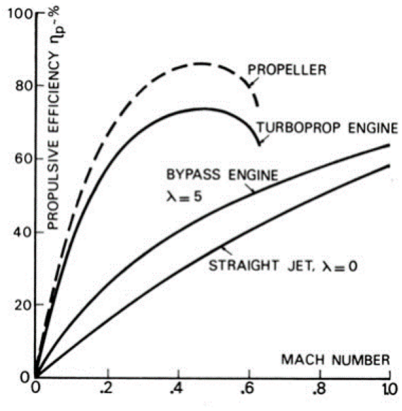

Fig. 4-18. Propulsive efficiency of subsonic turbo-engines

Figure 1.4: Torenbeek propeller correction with Mach [87].

$$\eta_P = -1941M^4 + 2814M^3 - 1741M^2 + 576M + 3 \tag{1.13}$$

2. A second correction is applied on the gas turbine efficiency as gas turbine efficiency is influenced by the operating altitude. Because the hybrid-electric design module does not have a detailed turboprop parameter performance analysis, an approximation of this effects is implemented as follows: the gas turbine efficiency deteriorates by 1% for every 10 degrees rise in temperature [1]. Flying at a higher altitude will therefore have a beneficial effect on the gas turbine efficiency.

3. Lastly, a correction is applied on the fuel fraction to determine the fuel and battery energy required for climb and descent. Initially, the method did not take into account the effect of having to climb to higher altitudes, as the fuel fraction was simply constant for the phase and independent on altitude or velocity. The fuel fraction during climb and descent is therefore scaled according to the potential energy and kinetic energy (Equation 1.14).

$$E_{pot} = m \cdot g \cdot h$$
$$E_{kin} = \frac{1}{2} m \cdot V^2 \tag{1.14}$$

1.5. Verification/Validation

Verifying and validating the the hybrid-electric aircraft design module was done in a two-step procedure. First a conventional kerosene Dash 8 Q400 aircraft was designed. Because the energy analysis is based on the conventional fuel fraction method, the fuel fractions were matched with the data as given by the Q400 Fuel Efficiency Manual [6]. The resulting calculated fuel fractions are summarized in Table 1.1 for each mission phase. The cruise mission fuel fraction is determined using the range equation and therefore not provided in the table.

Secondly, a hybrid-electric Dornier 228 aircraft was designed with the same inputs as *Finger et al.* [25]. For this, adjustments needed to be made to the aerodynamic data as the reference paper makes use of a two-term drag polar, while the existing aerodynamics module makes use of a symmetric drag polar. The values of zero-lift drag coefficient (C_{D_0}) and Oswald efficiency factor (e) were determined such that the drag polars match at most of the lift coefficients. The result can be seen in Figure 1.5 with a C_{D_0} value of 0.025 and e of 0.8. With this approach, it is not possible to match the drag value at low lift coefficients (<0.25), however the lift-coefficients of the verification study did not reach this limit.

Table 1.1: Calculated Fuel Fractions for Dash 8 Q400,

Phase	**Fuel mass [6]**	**Calculated Fuel Fraction**
Take-off	42 kg	0.9986
Climb	324 kg	0.9891
Cruise	1335 kg	From range equation
Descent	318 kg	0.9886

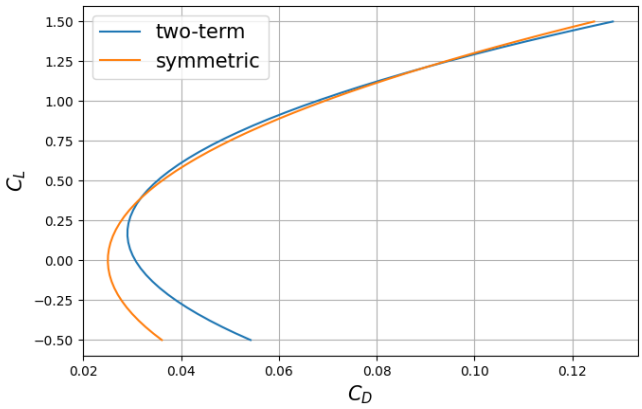

Figure 1.5: Drag polar matching of two-term drag polar from *Finger* [25] and symmetric drag polar.

[1] https://www.powerengineeringint.com/renewables/taking-the-heat/

2

Fleet-and-Network Allocation Module

2.1. Mission modelling

It has been mentioned that the approach presented in this thesis has a different way of modelling the climb and descent phases, when compared to previous work performed by *Zuijderwijk* [98]. This results in a notable difference in assumed fuel and battery energy required to perform a mission. In the thesis presented here, aircraft performance is measured by a value of $fuel/energy\_km$ which solely consists of the fuel or energy required during the cruise phase. Additionally, the aircraft is characterized by fuel and energy required to perform a stop. In this thesis, this includes the fuel and energy required for a take-off - climb - descent - landing cycle: $fuel/energy\_climb\_descent$. A schematic is shown in Figure 2.1 . The study in *Zuijderwijk* [98] on the other hand, combines the climb and descent phase with the cruise phase to measure the value of $fuel/energy\_km$. The fuel and energy required to perform a stop is then obtained from performing a landing and take-off cycle: $fuel/energy\_LTO$. Also this is shown schematically, in Figure 2.2.

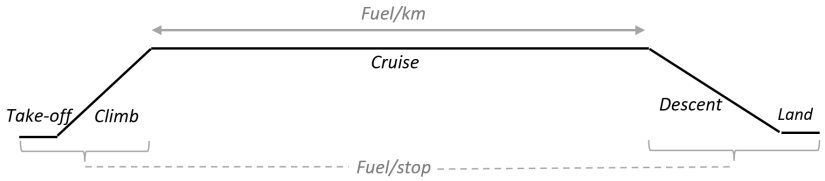

Figure 2.1: Fuel and battery modelling for climb and descent cycle

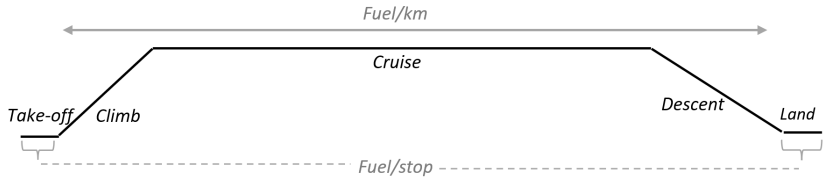

Figure 2.2: Fuel and battery modelling for climb and descent cycle in *Zuijderwijk* [98]

Moreover, the total mission range is modelled as the sum of the cruise range and the horizontal distance during climb and descent phases. The cruise range is defined by the designer. The climb and descent distances are obtained by assuming a constant climb and descent angle. For the distance covered during the climb phase, a constant climb gradient was assumed of 9%, as the Airport Planning Manual of the Q400 [7] lists a maximum climb gradient of 9.2% at maximum climb power. This corresponds to a climb angle of 5.1 degrees. The distance travelled during climb is therefore depending on the cruise altitude and can be calculated using Equation 2.1. It was observed that this assumed climb gradient is somewhat large for general regional turboprop aircraft, so it is advised that in future work more research is performed to estimate the climb gradient or calculate the climb gradient for each aircraft separately. The horizontal distance covered during the descent phase is obtained from the rule of thumb for descent: the 3-to-1 formula. This means that

it takes 3 NM to descend 1000 feet, which corresponds to a glide angle of about 3 degrees. Also this distance is depending on the cruise altitude and can be determined from Equation 2.2.

$$R_c = \frac{h}{0.09} \tag{2.1}$$

$$R_d = \frac{h \cdot 3NM}{1000ft} = \frac{h \cdot 5600}{300} \tag{2.2}$$

An aircraft flying from an origin airport a to a destination airport b can do this by either a direct flight or by having an additional stop at another airport c. Due to this additional stop, the achievable cruise range of the 2-stop mission (R_{c_2}) will be lower than the cruise range for a 1-stop mission (R_{c_1}). This in term also causes a difference in the total range for both missions (R_{t_1} and R_{t_2}). To calculate the equivalent cruise range and total range of a 2-stop mission, the derivation in Equation 2.3 is used, where $m_{c/d}$ is the fuel mass or battery energy required during the climb-and-descent cycle and m_{km} is the fuel mass or battery energy required per kilometer in cruise. When an aircraft design is optimized for minimizing the climate impact, this equivalent total range is important to consider. The fuel mass and battery energy per climb-and-descent cycle ($m_{c/d}$) and the fuel mass and battery energy per kilometer (m_{km}) will be changed during the climate-optimization. The climate-optimized aircraft should still be able to perform the same missions as the non-optimized alternative, posing an important constraint on the optimization problem.

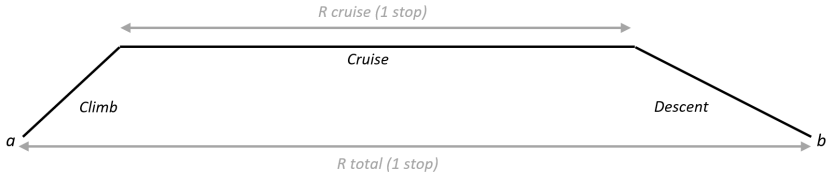

Figure 2.3: Cruise and total range for 1-stop mission

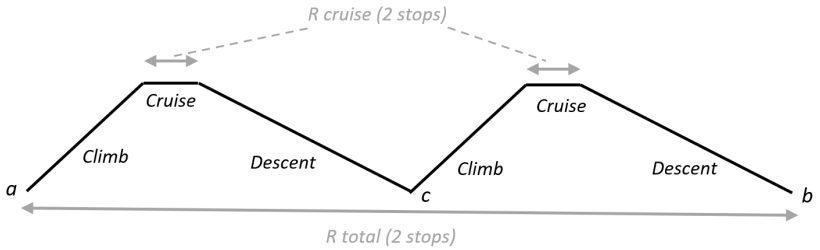

Figure 2.4: Cruise and total range for 2-stop mission

$$\begin{aligned} m_{c/d} + R_{c_1} \cdot m_{km} &= 2 \cdot m_{c/d} + R_{c_2} \cdot m_{km} \\ \Leftrightarrow R_{c_2} &= \frac{R_{c_1} \cdot m_{km} - m_{c/d}}{m_{km}} \\ \Leftrightarrow R_{t_2} &= 2 \cdot (R_c + R_d) + R_{c_2} \\ \Leftrightarrow R_{t_2} &= 2 \cdot (R_c + R_d) + \left(\frac{R_{c1} \cdot m_{km} - m_{c/d}}{m_{km}} \right) \end{aligned} \tag{2.3}$$

2.2. Fleet diversity constraint

The fleet-and-network model receives a database of aircraft and aircraft configurations which can be operated in the airline network. Each off-design configuration is implemented discretely, where passengers are traded in steps of 10. The fleet-and-network mode therefore does not distinguish between on-design aircraft configurations and off-design aircraft configurations when allocating aircraft to routes. A maximum fleet diversity constraint was implemented which limits the maximum amount of aircraft types in the fleet, but not the amount of aircraft configurations. The maximum fleet diversity constraint was implemented in a creative way and explained through the example in Figure 2.5. For the example, there are 3 different aircraft types in the database, each with its on-design aircraft configuration and a set of off-design aircraft configurations. Assume the first aircraft, aircraft 0, to have off-design configurations with indexes 1,2,3,4; assume the second aircraft, aircraft 5, to have off-design configurations 6, 7; and assume the third aircraft, aircraft 8, with off-design configurations 9,10,11,12,13,14. Each aircraft type is characterized by an index *'idx'*. Each aircraft configuration of an aircraft type is characterized by index *'i'* (see line 1 of Figure 2.5). The fleet-and-network model will determine the amount needed of each aircraft configuration (see line 2). The sum of the amount of aircraft configurations for each aircraft type is determined (see line 3) and translated into a binary number (see line 4). The total sum of aircraft types in binary form should be less or equal than the given maximum fleet diversity constraint (see line 5).

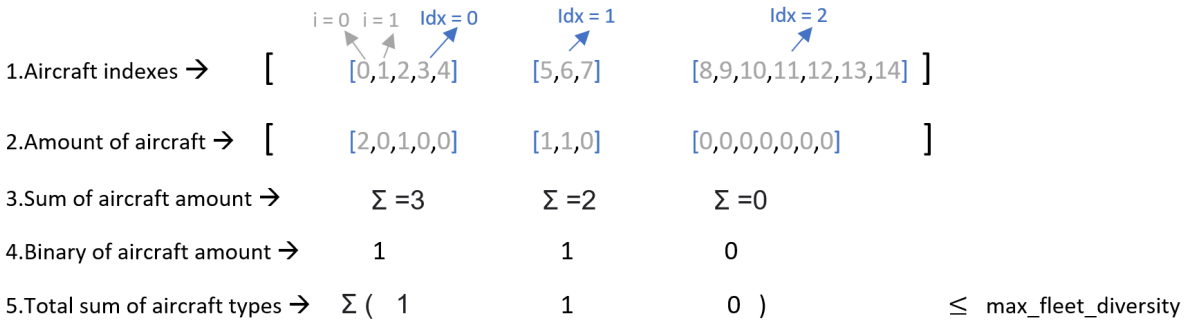

Figure 2.5: Fleet Diversity constraint

Bibliography

[1] NASA Aeronautics. Nasa aeronautics: Strategic implementation plan: 2019 update, 2019.

[2] Airbus. Global market forecast, 2021. URL https://www.airbus.com/en/products-services/commercial-aircraft/market/global-market-forecast.

[3] Nicolas E Antoine and Ilan M Kroo. Framework for aircraft conceptual design and environmental performance studies. *AIAA journal*, 43(10):2100–2109, 2005.

[4] Boeing. Boeing raises forecast for new airplane demand, 2017. URL https://boeing.mediaroom.com/2017-06-20-Boeing-Raises-Forecast-for-New-Airplane-Demand.

[5] Boeing. Commercial market outlook 2021-2040, 2021. URL https://www.boeing.com/commercial/market/commercial-market-outlook.

[6] Bombardier. Fuel efficiency manual q400 nextgen. Technical report, 2013.

[7] Bombardier. Airport planning manual. Technical report, 2014.

[8] Geoffrey Bower and Ilan Kroo. Multi-objective aircraft optimization for minimum cost and emissions over specific route networks. In *The 26th Congress of ICAS and 8th AIAA ATIO*, page 8905, 2008.

[9] Marty K Bradley and Christopher K Droney. Subsonic ultra green aircraft research phase ii: N+ 4 advanced concept development. Technical report, 2012.

[10] Marty K Bradley and Christopher K Droney. Subsonic ultra green aircraft research: phase ii–volume ii–hybrid electric design exploration. *NASA CR-218704*, 2015.

[11] Benjamin J Brelje and Joaquim RRA Martins. Electric, hybrid, and turboelectric fixed-wing aircraft: A review of concepts, models, and design approaches. *Progress in Aerospace Sciences*, 104:1–19, 2019.

[12] European Commission, Directorate-General for Mobility, Transport, Directorate-General for Research, and Innovation. *Flightpath 2050 : Europes vision for aviation : maintaining global leadership and serving societys needs*. Publications Office, 2011. doi: doi/10.2777/50266.

[13] Bain & Company. Air travel forecast: When will airlines recover from covid-19?, 2022. URL https://www.bain.com/insights/air-travel-forecast-when-will-airlines-recover-from-\covid-19-interactive/.

[14] William Crossley, Muharrem Mane, and A Nusawardhana. Variable resource allocation using multidisciplinary optimization: Initial investigations for system of systems. In *10th AIAA/ISSMO multidisciplinary analysis and optimization conference*, page 4605, 2004.

[15] Katrin Dahlmann, Alexander Koch, Florian Linke, Benjamin Lührs, Volker Grewe, Tom Otten, Doreen Seider, Volker Gollnick, and Ulrich Schumann. Climate-compatible air transport systemclimate impact mitigation potential for actual and future aircraft. *Aerospace*, 3(4):38, 2016.

[16] Navindran Davendralingam and William Crossley. Robust approach for concurrent aircraft design and airline network design. *Journal of Aircraft*, 51(6):1773–1783, 2014.

[17] R de Vries. Hybrid-electric aircraft with over-the-wing distributed propulsion: Aerodynamic performance and conceptual design. 2022.

[18] Reynard De Vries, Malcom Brown, and Roelof Vos. Preliminary sizing method for hybrid-electric distributed-propulsion aircraft. *Journal of Aircraft*, 56(6):2172–2188, 2019.

[19] Reynard De Vries, Maurice FM Hoogreef, and Roelof Vos. Range equation for hybrid-electric aircraft with constant power split. *Journal of Aircraft*, 57(3):552–557, 2020.

[20] James Felder, Hyun Kim, and Gerald Brown. Turboelectric distributed propulsion engine cycle analysis for hybrid-wing-body aircraft. In *47th AIAA aerospace sciences meeting including the new horizons forum and aerospace exposition*, page 1132, 2009.

[21] James Felder, Michael Tong, and Julio Chu. Sensitivity of mission energy consumption to turboelectric distributed propulsion design assumptions on the n3-x hybrid wing body aircraft. In *48th AIAA/ASME/SAE/ASEE Joint Propulsion Conference & Exhibit*, page 3701, 2012.

[22] James L. Felder, Gerald V. Brown, Hyun DaeKim, and Julio Chu. Turboelectric distributed propulsion in a hybrid wing body aircraft. 2011.

[23] Felder, James L. Nasa electric propulsion system studies. URL https://ntrs.nasa.gov/citations/20160009274.

[24] D Felix Finger, Cees Bil, and Carsten Braun. Initial sizing methodology for hybrid-electric general aviation aircraft. *Journal of Aircraft*, 57(2):245–255, 2020.

[25] D Felix Finger, Reynard de Vries, Roelof Vos, Carsten Braun, and Cees Bil. A comparison of hybrid-electric aircraft sizing methods. In *AIAA Scitech 2020 Forum*, page 1006, 2020.

[26] D Felix Finger, Reynard de Vries, Roelof Vos, Carsten Braun, and Cees Bil. Cross-validation of hybrid-electric aircraft sizing methods. *Journal of Aircraft*, pages 1–19, 2022.

[27] Dominik Felix Finger. *Methodology for multidisciplinary aircraft design under consideration of hybrid-electric propulsion technology*. PhD thesis, RMIT University, 2020.

[28] Jose A Fregnani, Bento S Mattos, and Jose A Hernandes. An innovative approach for integrated airline network and aircraft family optimization. In *AIAA Aviation 2019 Forum*, page 2865, 2019.

[29] Klaus Martin Gierens, Ling Lim, and Kostas Eleftheratos. A review of various strategies for contrail avoidance. *Open Atmospheric Science Journal*, 2:1–7, 2008.

[30] Parithi Govindaraju and William A Crossley. Profit motivated airline fleet allocation and concurrent aircraft design for multiple airlines. In *2013 Aviation Technology, Integration, and Operations Conference*, page 4391, 2013.

[31] Parithi Govindaraju, Navindran Davendralingam, and William A Crossley. A concurrent aircraft design and fleet assignment approach to mitigate environmental impact through fuel burn reduction under operational uncertainty. *Journal of Aerospace Operations*, 4(4):163–184, 2017.

[32] British Aviation Group. Airbus global market forecast 2019-2038, 2019. URL https://www.britishaviationgroup.co.uk/news/airbus-global-market-forecast-2019-2038/.

[33] Julian Hoelzen, Yaolong Liu, Boris Bensmann, Christopher Winnefeld, Ali Elham, Jens Friedrichs, and Richard Hanke-Rauschenbach. Conceptual design of operation strategies for hybrid electric aircraft. *Energies*, 11(1):217, 2018.

[34] Mirko Hornung, Askin T Isikveren, Mara Cole, and Andreas Sizmann. Ce-liner-case study for emobility in air transportation. In *2013 Aviation Technology, Integration, and Operations Conference*, page 4302, 2013.

[35] John Hwang and Joaquim RRA Martins. Allocation-mission-design optimization of next-generation aircraft using a parallel computational framework. In *57th AIAA/ASCE/AHS/ASC Structures, Structural Dynamics, and Materials Conference*, page 1662, 2016.

[36] John T Hwang and Joaquim RRA Martins. Parallel allocation-mission optimization of a 128-route network. In *16th AIAA/ISSMO Multidisciplinary Analysis and Optimization Conference*, page 2321, 2015.

[37] IATA. Iata economics chart of the week, 2020. URL https://www.iata.org/en/iata-repository/publications/economic-reports/Five-years-to-return-to-the-pre-pandemic-level-of-passenger-demand/.

[38] International Air Transport Association (IATA). Aircraft technology roadmap to 2050. 2019.

[39] Askin T Isikveren. Method of quadrant-based algorithmic nomographs for hybrid/electric aircraft predesign. *Journal of Aircraft*, 55(1):396–405, 2018.

[40] Askin T Isikveren, Arne Seitz, Patrick C Vratny, Clément Pornet, Kay O Plötner, and Mirko Hornung. Conceptual studies of universally-electric systems architectures suitable for transport aircraft. In *Deutscher Luft-und Raumfahrt Kongress*. DLRK Berlin, Germany, 2012.

[41] Askin T Isikveren, Sascha Kaiser, Clément Pornet, and Patrick C Vratny. Pre-design strategies and sizing techniques for dual-energy aircraft. *Aircraft Engineering and Aerospace Technology: An International Journal*, 2014.

[42] SS Jagtap. Systems evaluation of subsonic hybrid-electric propulsion concepts for nasa n+ 3 goals and conceptual aircraft sizing. *International Journal of Automotive and Mechanical Engineering*, 16(4):7259–7286, 2019.

[43] Peter Jansen and Ruben Perez. Coupled optimization of aircraft family design and fleet assignment for minimum cost and fuel burn. In *12th AIAA Aviation Technology, Integration, and Operations (ATIO) Conference and 14th AIAA/ISSMO Multidisciplinary Analysis and Optimization Conference*, page 5495, 2012.

[44] Peter W Jansen and Ruben E Perez. Coupled optimization of aircraft design and fleet allocation with uncertain passenger demand. In *2013 Aviation Technology, Integration, and Operations Conference*, page 4392, 2013.

[45] Peter W Jansen and Ruben E Perez. Robust coupled optimization of aircraft design and fleet allocation for multiple markets. In *AIAA/3AF Aircraft Noise and Emissions Reduction Symposium*, page 2735, 2014.

[46] Peter W Jansen and Ruben E Perez. Coupled optimization of aircraft families and fleet allocation for multiple markets. *Journal of Aircraft*, 53(5):1485–1504, 2016.

[47] Elitza Karadotcheva, Sang N Nguyen, Emile S Greenhalgh, Milo SP Shaffer, Anthony RJ Kucernak, and Peter Linde. Structural power performance targets for future electric aircraft. *Energies*, 14(19):6006, 2021.

[48] Alexander Koch. *Climate impact mitigation potential given by flight profile and aircraft optimization*. PhD thesis, DLR, 2013.

[49] David S Lee, DW Fahey, Agnieszka Skowron, MR Allen, Ulrike Burkhardt, Q Chen, SJ Doherty, S Freeman, PM Forster, J Fuglestvedt, et al. The contribution of global aviation to anthropogenic climate forcing for 2000 to 2018. *Atmospheric Environment*, 244:117834, 2021.

[50] Muharrem Mane and William Crossley. Concurrent aircraft design and resource allocation under uncertainty for on-demand air transportation. In *The 26th Congress of ICAS and 8th AIAA ATIO*, page 8903, 2008.

[51] Muharrem Mane and William Crossley. Concurrent aircraft design and trip assignment under uncertainty: Fractional operations. In *9th AIAA Aviation Technology, Integration, and Operations Conference (ATIO) and Aircraft Noise and Emissions Reduction Symposium (ANERS)*, page 7007, 2009.

[52] Muharrem Mane and William A Crossley. Allocation and design of aircraft for on-demand air transportation with uncertain operations. *Journal of aircraft*, 49(1):141–150, 2012.

[53] Muharrem Mane, William A Crossley, and Nusawardhana. System-of-systems inspired aircraft sizing and airline resource allocation via decomposition. *Journal of aircraft*, 44(4):1222–1235, 2007.

[54] Hermann Mannstein, Peter Spichtinger, and Klaus Gierens. A note on how to avoid contrail cirrus. *Transportation Research Part D: Transport and Environment*, 10(5):421–426, 2005.

[55] K Bradley Marty and K Droney Christopher. Subsonic ultra green aircraft research: Phase i final report. *Boeing Research and Technology, CA, Tech. Rep. NASA/CR–2011-216847*, 2011.

[56] Bento Mattos, José Hernandes, and José Alexandre Fregnani. Airline network-airplane integrated optimization considering manufacturer's program cost. 09 2021.

[57] Taewoo Nam, Danielle Soban, and Dimitri Mavris. A generalized aircraft sizing method and application to electric aircraft. In *3rd International Energy Conversion Engineering Conference*, page 5574, 2005.

[58] Taewoo Nam, Danielle Soban, and Dimitri Mavris. Power based sizing method for aircraft consuming unconventional energy. In *43rd AIAA Aerospace Sciences Meeting and Exhibit*, page 818, 2005.

[59] Malte Niklaß, Benjamin Lührs, Volker Grewe, Katrin Dahlmann, Tanja Luchkova, Florian Linke, and Volker Gollnick. Potential to reduce the climate impact of aviation by climate restricted airspaces. *Transport Policy*, 83:102–110, 2019.

[60] E Obert. Drag polars of nineteen jet transport aircraft at mach numbers m= 0.40-0.60 (unpublished). Technical report, Technical report, 2013.

[61] International Civil Aviation Organization. Resolutions - assembly 40th session, 10 2019.

[62] Christopher Perullo and Dimitri Mavris. A review of hybrid-electric energy management and its inclusion in vehicle sizing. *Aircraft Engineering and Aerospace Technology: An International Journal*, 2014.

[63] F Peter, A Habermann, M Lüdemann, K Plötner, F Troeltsch, A Seitz, Julian Bijewitz, and MTU Aero Engines AG. *Definition of the CENTRELINE reference aircraft and power plant systems*. Deutsche Gesellschaft für Luft-und Raumfahrt-Lilienthal-Oberth eV, 2021.

[64] Clément Pornet. *Conceptual design methods for sizing and performance of hybrid-electric transport aircraft*. PhD thesis, Technische Universität München, 2018.

[65] Clément Pornet and Askin T Isikveren. Conceptual design of hybrid-electric transport aircraft. *Progress in Aerospace Sciences*, 79:114–135, 2015.

[66] Clément Pornet, Corin Gologan, Patrick C Vratny, Arne Seitz, Oliver Schmitz, Askin T Isikveren, and Mirko Hornung. Methodology for sizing and performance assessment of hybrid energy aircraft. *Journal of Aircraft*, 52(1):341–352, 2015.

[67] Pieter-Jan Proesmans and Roelof Vos. Airplane design optimization for minimal global warming impact. In *AIAA Scitech 2021 Forum*, page 1297, 2021.

[68] Daniel Raymer. *Aircraft design: a conceptual approach*. American Institute of Aeronautics and Astronautics, Inc., 2012.

[69] Manuel A Rendón, Carlos D Sánchez R, Josselyn Gallo M, Alexandre H Anzai, et al. Aircraft hybrid-electric propulsion: Development trends, challenges and opportunities. *Journal of Control, Automation and Electrical Systems*, 32(5):1244–1268, 2021.

[70] João Ribeiro, Frederico Afonso, Inês Ribeiro, Bruna Ferreira, Hugo Policarpo, Paulo Peças, and Fernando Lau. Environmental assessment of hybrid-electric propulsion in conceptual aircraft design. *Journal of Cleaner Production*, 247:119477, 2020.

[71] Jan Roskam. *Airplane design*. DARcorporation, 1985.

[72] Satadru Roy and William A Crossley. An ego-like optimization framework for simultaneous aircraft design and airline allocation. In *57th AIAA/ASCE/AHS/ASC Structures, Structural Dynamics, and Materials Conference*, page 1659, 2016.

[73] Satadru Roy, William A Crossley, Kenneth T Moore, Justin S Gray, and Joaquim RRA Martins. Next generation aircraft design considering airline operations and economics. In *2018 AIAA/ASCE/AHS/ASC Structures, Structural Dynamics, and Materials Conference*, page 1647, 2018.

[74] Smruti Sahoo, Xin Zhao, and Konstantinos Kyprianidis. A review of concepts, benefits, and challenges for future electrical propulsion-based aircraft. *Aerospace*, 7(4):44, 2020.

[75] Benjamin T Schiltgen and Jeffrey Freeman. Aeropropulsive interaction and thermal system integration within the eco-150: A turboelectric distributed propulsion airliner with conventional electric machines. In *16th AIAA Aviation Technology, Integration, and Operations Conference*, page 4064, 2016.

[76] Benjamin T Schiltgen and Jeffrey Freeman. Eco-150-300 design and performance: a tube-and-wing distributed electric propulsion airliner. In *AIAA Scitech 2019 Forum*, page 1808, 2019.

[77] Peter Schmollgruber, Olivier Atinault, Italo Cafarelli, Carsten Döll, Christophe François, Jean Hermetz, Romain Liaboeuf, Bernard Paluch, and Michael Ridel. Multidisciplinary exploration of dragon: an onera hybrid electric distributed propulsion concept. In *AIAA Scitech 2019 Forum*, page 1585, 2019.

[78] Anna E Scholz, Johannes Michelmann, and Mirko Hornung. Design, operational and environmental assessment of a hybrid-electric aircraft. In *AIAA Scitech 2021 Forum*, page 0259, 2021.

[79] Ulrich Schumann, Kaspar Graf, and Hermann Mannstein. Potential to reduce the climate impact of aviation by flight level changes. In *3rd AIAA atmospheric space environments conference*, page 3376, 2011.

[80] Emily Schwartz Dallara and Ilan M Kroo. Aircraft design for reduced climate impact. In *49th AIAA Aerospace Sciences Meeting including the New Horizons Forum and Aerospace Exposition. Orlando, Florida*, 2011.

[81] Arne Seitz, Fabian Peter, Julian Bijewitz, Anaïs Habermann, Zdobyslaw Goraj, Mariusz Kowalski, A Castillo Pardo, Cesare Hall, Frank Meller, Rasmus Merkler, et al. Concept validation study for fuselage wake-filling propulsion integration. In *31st Congress of the International Council of the Aeronautical Sciences*, pages 09–14. ICAS, 2018.

[82] Banavar Sridhar, Neil Y Chen, Hok K Ng, and Florian Linke. Design of aircraft trajectories based on trade-offs between emission sources. 2011.

[83] Stefan Stückl, Jan van Toor, and Hans Lobentanzer. Voltair-the all electric propulsion concept platform–a vision for atmospheric friendly flight. In *28th International Congress of the Aeronautical Sciences (ICAS)*, 2012.

[84] Christine Taylor and Olivier L De Weck. Coupled vehicle design and network flow optimization for air transportation systems. *Journal of Aircraft*, 44(5):1479–1486, 2007.

[85] Yorick Teeuwen. Propeller design for conceptual turboprop aircraft. 2017.

[86] Roel Thijssen. Propeller aircraft design optimization for reduced climate impact. 2022.

[87] Egbert Torenbeek. *Synthesis of subsonic airplane design: an introduction to the preliminary design of subsonic general aviation and transport aircraft, with emphasis on layout, aerodynamic design, propulsion and performance*. Springer Science & Business Media, 2013.

[88] Joris Van Bogaert. Assessment of potential fuel saving benefits of hybrid-electric regional aircraft. 2015.

[89] Jos Vankan and Wim Lammen. Parallel hybrid electric propulsion architecture for single aisle aircraft-powertrain investigation. In *MATEC Web of Conferences*, volume 304, page 03008. EDP Sciences, 2019.

[90] Mark Voskuijl, Joris Van Bogaert, and Arvind G Rao. Analysis and design of hybrid electric regional turboprop aircraft. *CEAS Aeronautical Journal*, 9(1):15–25, 2018.

[91] Colby J Weit, Cedric Y Justin, and Dimitri N Mavris. Network-optimized design of a notional hybrid electric airplane for thin-haul operations. In *AIAA Aviation 2019 Forum*, page 3002, 2019.

[92] Jason Welstead and James L Felder. Conceptual design of a single-aisle turboelectric commercial transport with fuselage boundary layer ingestion. In *54th AIAA aerospace sciences meeting*, page 1027, 2016.

[93] Jason Welstead, Jim Felder, Mark Guynn, Bill Haller, Mike Tong, Scott Jones, Irian Ordaz, Jesse Quinlan, and Brian Mason. Overview of the nasa starc-abl (rev. b) advanced concept. In *One Boeing NASA Electric Aircraft Workshop*, number NF1676L-26767, 2017.

[94] Gabrielle E Wroblewski and Phillip J Ansell. Mission analysis and emissions for conventional and hybrid-electric commercial transport aircraft. *Journal of Aircraft*, 56(3):1200–1213, 2019.

[95] Feijia Yin, Volker Grewe, and Klaus Gierens. Impact of hybrid-electric aircraft on contrail coverage. *Aerospace*, 7(10):147, 2020.

[96] Jacopo Zamboni, Roelof Vos, Mathias Emeneth, and Alexander Schneegans. A method for the conceptual design of hybrid electric aircraft. In *AIAA Scitech 2019 Forum*, page 1587, 2019.

[97] Thomas Zill, Michael Iwanizki, Peter Schmollgruber, Sebastien Defoort, Carsten Döll, Maurice Hoogreef, and W Lammen. An overview of the conceptual design studies of hybrid electric propulsion air vehicles in the frame of clean sky 2 large passenger aircraft. In *Aerospace Europe Conference*, 2020.

[98] Noa Zuijderwijk. Study to the adaptation of electrified aircraft by regional airliner. 2022.